INTERNATIONAL MOLYBDENUM ASSOCIATION
THE VOICE OF THE MOLYBDENUM INDUSTRY

Molybdenum alloying – more than hardenability

Proceedings of the 2018 Molybdenum and Steel Symposium Nov. 28–29, 2018 Shanghai, China

www.imoa.info

Table of contents

Adv. Manuf.
https://doi.org/10.1007/s40436-019-00261-6

Guest editorial: Molybdenum alloying: more than hardenability

Hardy Mohrbacher[1,2]

Received: 28 May 2019 / Revised: 30 May 2019 / Accepted: 31 May 2019

Molybdenum is a transitional metal in the periodic table of elements where it ranks in position 42 in the 5th period and group V1 B. Having a high melting point of 2 623 °C, molybdenum belongs to the so-called refractory metals. Accordingly, as pure metal it finds many applications where high temperatures are encountered during operation, for example in furnaces. However, nearly 80% of all molybdenum produced every year by the world's mining industry is used as addition to iron and steel alloys. Carbon and alloy steels account for 40% of molybdenum use, followed by stainless steels (23%), tool steels and castings (both around 8%).

The widespread use of molybdenum as alloying element is due to its unique metallurgical effects. Molybdenum is commonly known for enhancing hardenability of iron and steel alloys. Furthermore, it forms carbides when a sufficient amount of carbon is present in the alloy. Both effects enable the production of strong and wear resistant alloys. It therefore, traditionally, is a constituent of many heat treatable steels and tool steels. Respective research efforts have been reported as early as the 1930s. More widespread use of molybdenum in the steel industry appeared in the 1960s when Climax Molybdenum Company initiated a substantial and remarkable market development program exploring new potential applications. These applications typically demanded higher strength of the final product yet also sufficient toughness, resistance against softening at elevated temperatures of operation or corrosion resistance. Increasingly, manufacturing and fabricating of parts, components, installations and equipment came into focus requiring particular attention to forming and welding behavior of steel products. This led to the evolution of high strength low alloy (HSLA) steels, which became a workhorse material for the oil & gas industry in the early 1970s and had pertained ever since at further increasing strength levels. Similar types of HSLA steels soon conquered the constructional arena and somewhat later the automotive industry. The motivation for the use of these steels has always been similar: to enhance efficiency, improve performance in operation and facilitate manufacturing. Molybdenum is a key alloying element in bridging these often mutually contradictory requirements.

With the upgrading of steelmaking facilities in the industrialized countries starting in the later 1970s, the use of molybdenum in some of the mainstream alloys became obsolete. The advent of thermo-mechanical rolling and accelerated cooling could provide sufficient hardenability to achieve medium strength levels using rather lean-alloyed steel. Today, as a general rule, it can be stated that molybdenum becomes relevant in steels with a yield strength of 500 MPa or more. Exceptions in lower strength levels may apply when particularly heavy gages need to be produced. On the other hand, thin gages would require molybdenum alloying only at an even higher strength level. Fortunately, the trend in steel development is proceeding towards much higher strength grades. Many applications in mechanical engineering nowadays, demand material having a yield strength of at least 700 MPa and carmakers routinely use steel grades of over 1 000 MPa strength for a large share of the vehicle structure. Accordingly, the challenges with regard to manufacturing and fabrication are increasing further.

Molybdenum alloying has clearly regained its relevance in this modern steel age. It is not being displaced anymore

✉ Hardy Mohrbacher
hm@niobelcon.net

[1] NiobelCon bvba, Schilde, Belgium

[2] Department of MTM, KU Leuven, Leuven, Belgium

Published online: 14 June 2019

from alloys by more capable metallurgical processes. On the contrary, often molybdenum alloying actually enables using the full potential of most modern steelmaking equipment. It also enhances efficiency of secondary treatments, thus contributing to sustainability and cost reduction. Furthermore, molybdenum alloying facilitates the use of established manufacturing processes when producing components from such advanced steel grades. Last but not least, the performance of ultra-high strength steels under operational conditions requires increased attention. The demand for sufficient toughness at high strength level has been around for decades and continues to be of high importance. A new challenge, at ultra-high strength level, is the resistance of steel to hydrogen embrittlement. Hydrogen can accumulate in steel during steel processing, fabrication processes such as welding or surface treatments or during operation by corrosion phenomena and can cause the steel to crack. Another challenge is to retain the very high strength of steel at high temperatures, be it during operation or during intermediate processing such as heat treatment or welding. In all these cases molybdenum alloying offers proven, viable solutions to the challenges.

In the casting industry, a similar evolution towards higher performing materials has been developing. In contrast to the steel industry, the possibilities of upgrading material properties by thermo-mechanical processing, using lean alloy concepts, are rather limited in the foundry industry. In other words, alloying continues to play a relatively more important role in this sector. Not surprisingly molybdenum alloying is prominent in cast iron and steel products, again for promoting strength, toughness, heat resistance and wear resistance.

The Chinese metallurgical industry is by far the largest in the world for both steel production and castings. In each sector China accounts for approximately half of the annual world production. Major investments in state-of-the-art metallurgical processing equipment have been made since the beginning of the millennium. Over less than two decades, Chinese steelmakers have succeeded in developing leading edge products, and have made increasing use of the potential offered by their modern equipment. China is also one of the three major molybdenum mining hubs in the world. Considering its annual molybdenum output, the country is largely self-sufficient in molybdenum supplies to the metallurgical industry. Hence, molybdenum alloying should be a natural choice when producing high performance iron and steel alloys.

The amount of molybdenum added to an alloy spans from as little as 0.1% in HSLA steels to around 9% in tool steels. The question of how much molybdenum should be added in a specific application is usually answered by considering a balance of performance gain on the one hand and cost optimization on the other hand. Comprehensive research is needed to unravel the full benefits of molybdenum alloying for justifying the alloy cost. Ideally this argumentation includes a holistic consideration of processing, manufacturing and end use. However, a small amount of molybdenum typically goes a long way in increasing strength of steels and irons while keeping their toughness intact. Using a higher strength steel allows the engineer to reduce the gage for a given application, leading to a lighter structure, but also to significant savings in the amount of steel required. In that sense, adding as little as 0.1%–0.2% of molybdenum to a steel to increase its strength can save tonnes of steel, making the application more sustainable. The International Molybdenum Association (IMOA), being the voice of the global molybdenum industry, is fully dedicated to molybdenum market development amongst many other services offered to its members. IMOA has been consolidating molybdenum-related knowledge and know-how gained over the decades and is making it available to the metallurgical industry with the clear intention of finding the most sustainable solution.

In order to facilitate knowledge exchange with the Chinese metallurgical industry and to fertilize new alloy development, an International Symposium on Applications of Molybdenum in the Iron and Steel Industry was organized in Shanghai in November 2018. The event was co-organized and hosted by the Center of Advanced Solidification Technology (CAST) at Shanghai University. More than 100 Chinese and international experts participated in this symposium presenting and discussing the many beneficial facets that molybdenum alloying offers. This was the second event of its kind in China after a first symposium held in Beijing in the year 2010, that time in cooperation with the Central Iron & Steel Research Institute (CISRI). The following four papers provide a summary of the presented and discussed information in the major application areas flat carbon steels, engineering steels and castings as well as an overview of the Chinese molybdenum industry.

Adv. Manuf.
https://doi.org/10.1007/s40436-019-00285-y

Molybdenum alloying in high-performance flat-rolled steel grades

Pello Uranga[1] · Cheng-Jia Shang[2] · Takehide Senuma[3] · Jer-Ren Yang[4] · Ai-Min Guo[5] · Hardy Mohrbacher[6,7]

Received: 28 May 2019 / Revised: 29 November 2019 / Accepted: 2 December 2019

Abstract Considerable progress in developing flat-rolled steel grades has been made by the Chinese steel industry over the recent two decades. The increasing demand for high-performance products to be used in infrastructural projects as well as in production of consumer and capital goods has been driving this development until today. The installation of state-of-the-art steel making and rolling facilities has provided the possibility of processing the most advanced steel grades. The production of high-performance steel grades relies on specific alloying elements of which molybdenum is one of the most powerful. China is nearly self-sufficient in molybdenum supplies. This paper highlights the potential and advantages of molybdenum alloying over the entire range of flat-rolled steel products. Specific aspects of steel property improvement with respect to particular applications are indicated.

✉ Hardy Mohrbacher
hm@niobelcon.net

[1] CEIT and TECNUN, University of Navarra, San Sebastian, Spain

[2] Collaborative Innovation Center of Steel Technology, University of Science and Technology Beijing, Beijing 100083, People's Republic of China

[3] Graduate School for Nature Science, Okayama University, Okayama, Japan

[4] Institute of Materials Science and Engineering, Taiwan University, Taipei, Taiwan, People's Republic of China

[5] CITIC Metal, Beijing 100027, People's Republic of China

[6] Department of Materials Engineering, KU Leuven, 3001 Leuven, Belgium

[7] NiobelCon bvba, 2970 Schilde, Belgium

Keywords HSLA steel · Quench & tempering · Direct quenching · Press hardening · Quenching & partitioning · Precipitation

1 Introduction

Flat carbon steel is one of the most versatile materials used in a large number of industrial applications. The gages of products in this steel family range from 0.5 mm to over 100 mm. Typical products manufactured from flat steels are vehicles, pipelines, pressure vessels, machines, construction equipment, bridges, offshore platforms, ships, or containers. Most of these items involve a combination of cutting, forming and joining operations during the manufacturing process. These fabrication techniques imply particular requirements towards the steel [1, 2]. The quest for increased strength has always been a driving force for steel development over the last five decades. Higher strength allows making structures lighter by maintaining the same load bearing capacity at reduced material gage. Consequently, sustainability and efficiency in terms of raw material consumption, manufacturing time, transport weight and emissions generated along the entire production chain are subjected to continuous improvement. However, increasing the strength of steel can be in conflict with forming and welding operations applied during manufacturing. With regard to the applications, energy absorption capacity, toughness, fatigue resistance and resistance against hydrogen embrittlement are key properties for steels of increased strength. Therefore, particular attention has to be attributed to the alloy concept and microstructural design of steel. The alloy concept dominantly affects the weldability, whereby reducing the carbon content or carbon equivalent (CE) clearly has a positive impact. Steel offers a

Published online: 09 January 2020

variety of microstructures, which majorly determine its properties. The combination of alloy and process design allows adjusting the microstructure. Regarding process design, thermo-mechanical controlled processing (TMCP) represents the baseline for making high strength steel and is widely used in strip as well as plate rolling. Various cooling strategies at the end of the rolling process or separate heat-treatments are further methods of influencing the microstructure and optimizing properties. For thin-gaged cold rolled products the final microstructure is adjusted by a continuous annealing process incorporating a suitable cooling strategy. Molybdenum as an alloying element has a wide spectrum of metallurgical effects. It can help achieving the desired strength level at reduced carbon equivalent, thus improving weldability. The various interactions of molybdenum during steel processing allow promoting particular microstructural features relevant for manufacturing and final properties. The present paper will give an overview on how molybdenum is used in combination with state-of-the-art processing technology for producing modern high strength steel. For particular products, the resulting benefits with regard to manufacturing processes will be highlighted.

2 Strengthening mechanisms and processing strategies for high-performance HSLA steel

The simplest way of raising a steel's strength is increasing its carbon content. However, this approach harms toughness, formability and weldability. Accordingly, since the early 1970's efforts are being done of reducing the carbon content in flat steels while enhancing strength by other mechanisms. Figure 1 identifies the possibilities for increasing strength in low-carbon steel. Besides of a modest effect caused by solid solution strengthening, typically provided by silicon and manganese alloying, grain refinement offers a significant potential for raising strength by 200–300 MPa. This is related to the well-known Hall-Petch effect [3]. It is particularly advantageous that grain refinement simultaneously lowers the ductile-to-brittle transition temperature (DBTT) [4]. Hence, grain refinement is the only strengthening mechanism being beneficial to strength and toughness. Therefore, grain-refined low-carbon steel should always be the baseline for any high strength steel development. The standard way of achieving grain refinement is provided by niobium microalloying in combination with TMCP rolling. The mass fraction of Nb is less than 0.1%. That approach reaches a limit at around 500 MPa yield strength. Steel grades of even higher strength need to involve additional mechanisms such as precipitation or dislocation strengthening. Ultra-fine particles, typically consisting of microalloy (Nb, Ti, or V) carbides and having a size of less than 10 nm, form during or after phase transformation from austenite to ferrite. The dispersed particles are acting as obstacles for dislocations and particularly enhance the yield stress. The precipitation mechanism requires a cooling-stop or coiling temperature in the range of 580–650 °C to obtain the best result. Depending on the amount of microalloy added, strength can be increased by up to 300 MPa. Accelerated cooling and relatively low cooling-stop or coiling temperature promote dislocation strengthening. This mechanism increases strength by about 150 MPa. The microstructure then gradually changes from polygonal ferrite to bainite. In addition to high dislocation density, a pronounced substructure of low angle boundaries, which also contributes to grain refinement, is characteristic for bainite [5]. It is

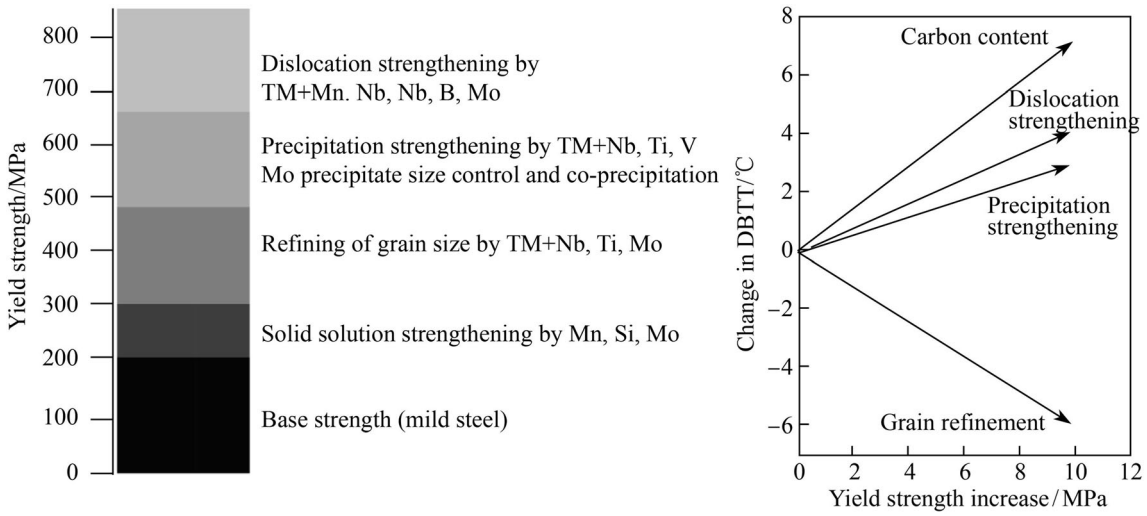

Fig. 1 Strengthening mechanisms in steel and effect on toughness (ductile-to-brittle transition temperature)

however obvious that the conditions for obtaining the maximum precipitation strengthening are not exactly matching those for dislocation strengthening. Therefore, advanced processing routes have to be established combining both effects to a high degree. By doing so, yield strength can reach in the order of 900 MPa at a carbon content of around 0.05%. Upper-shelf impact energy (Charpy) is typically above 300 J and DBTT can be as low as −140 °C. Generally, the more homogeneous the microstructure, the better is the toughness behavior. Avoiding significant scattering of grain sizes is prerequisite for obtaining the best performance in that respect. The presence of the second phase such as pearlite or martensite/austenite (MA) phase has a clearly detrimental effect on DBTT. Therefore, single phase microstructures are preferred when the best toughness is demanded.

Molybdenum alloying contributes to the production of such advanced steel grades in several ways. The alloyed amount of molybdenum is usually below 0.7% and more typically in the range of 0.1%–0.3%. Despite molybdenum being a carbide former, its alloy range and the low carbon content guarantee full solubility in these steels throughout the process [6]. Thus, the metallurgical effects of molybdenum appear as direct interactions with lattice defects or indirect interactions by way of synergies with other alloying elements. Molybdenum is an atom of significantly larger size than that of iron. It has the tendency of segregating to grain boundaries or binding with other lattice defects such as vacancies or dislocations [7–9]. It also lowers the activity of carbon [10, 11], thus slowing down processes that rely on carbon diffusion. Along the processing chain of flat rolled products molybdenum alloying: enhances the solubility of the micro-alloys Nb and Ti during slab reheating [10], supports recrystallization delay during austenite conditioning [12], retards precipitation of micro-alloys during austenite conditioning [13], delays phase transformation from fcc to bcc [14], promotes non-polygonal ferrite formation with high dislocation density [15], controls micro-alloy precipitation in bcc to ultra-fine size and dense particle distribution [16].

2.1 Strengthening by microstructural refinement and dislocations

Figure 2 demonstrates the effect of molybdenum in terms of recrystallization delay during austenite rolling compared to a standard C-Mn-Cr steel (see Fig. 2a). The addition of 0.25% Mo (mass fraction, the same below) produces already clearly pronounced austenite pancaking (see Fig. 2b). This effect is caused by molybdenum's solute drag on the austenite grain boundaries. Furthermore, molybdenum retards dynamic recovery due to its interaction with dislocations. By that, the formation of subgrains acting as nuclei for recrystallization is also retarded [17]. The combination of 0.25% Mo and 0.04% Nb results in even stronger pancaking (see Fig. 2c). Here, solute drag of both elements and additional pinning by NbC precipitates leads to an earlier and stronger recrystallization delay. Stronger pancaking produces a finer-grained microstructure after the transformation from austenite to ferrite. Besides austenite pancaking, the cooling conditions after hot rolling have a decisive impact on the microstructure of the final product. Molybdenum has also during this processing stage a significant effect on the microstructure. Figure 3 shows the microstructure of two model steels with Nb- and NbMo-alloying produced at coiling temperatures of 700 °C (high) and 500 °C (low). The microstructure after coiling at high temperature is polygonal ferritic. Compared to the Nb microalloyed base concept, the co-addition of molybdenum produces a finer-grained yet still polygonal ferritic microstructure. At low coiling temperature, the Nb-added steel reveals clearly refined, mostly polygonal ferrite showing a slightly increased amount of low-angle grain boundaries ($2° < \theta < 15°$). The addition of molybdenum, however, produces very fine-grained non-polygonal ferrite and a large amount of low-angle grain boundaries. The combination of very fine grain size and pronounced substructure provides an excellent combination of high strength and very low DBTT. The bainitic microstructure comprises a high dislocation density. Figure 4 identifies the individual contributions to strength. Grain refinement is the dominating effect. Low coiling temperature and the addition of molybdenum further promote the strength contribution by grain refinement. Molybdenum enhances the contributions from dislocation density and precipitation at lower coiling temperature whereas the formation of MA-phase is promoted at higher coiling temperature. The optimum coiling temperature for all mechanisms acting together appears to be 600 °C.

2.2 Strengthening by micro-alloy precipitation

The implementation of precipitation strengthening demands an intermediate cooling regime, providing suitable conditions for the diffusion-based process of forming microalloy carbide particles. Niobium and titanium are most suited for precipitation since their solubility in ferrite is extremely low. Thus, all solute microalloy still being present in austenite after finish rolling precipitates either during or after austenite-to-ferrite transformation, depending on the kinetics. Interphase precipitation occurs quasi-simultaneously with the phase transformation as was described in detail for Mo-Ti-alloyed steel by Yen et al. [18]. The development of interphase-precipitated carbides can be associated with the growth of an incoherent ferrite/austenite interface by the ledge mechanism (see Fig. 5)

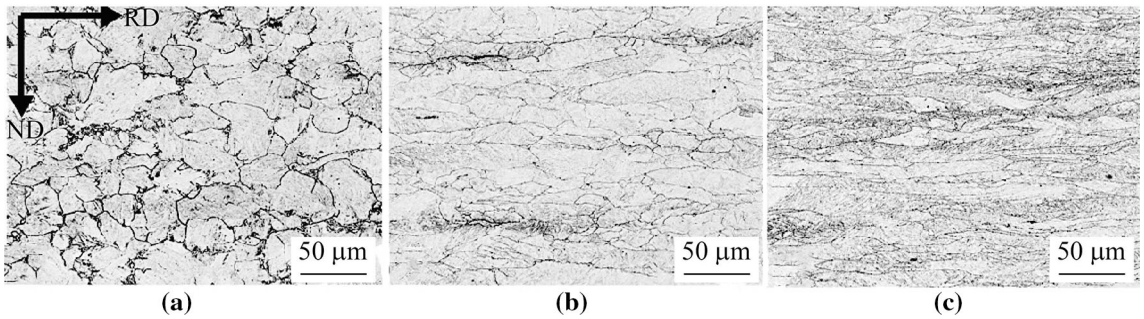

Fig. 2 Prior austenite grain structures in a C-Mn-Cr steel alloyed with mass fraction **a** 0%Mo, **b** 0.25%Mo, **c** 0.25%Mo+0.04%Nb, rolling reduction of 78%, finish rolling temperature of 900 °C

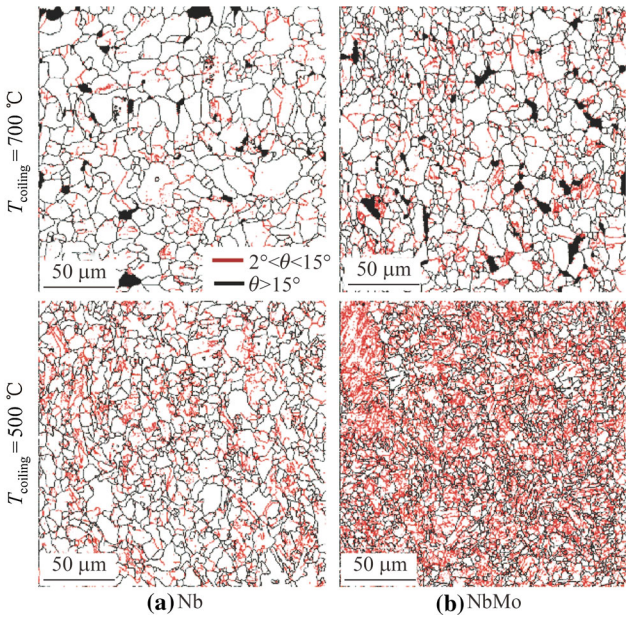

Fig. 3 Grain boundary mapping of 0.035%Nb and 0.035%Nb-0.2%Mo alloyed steel after simulated coiling (base alloy: 0.04%C-1.55%Mn-0.2%Si; black lines = high-angle grain boundaries, red lines = low-angle grain boundaries)

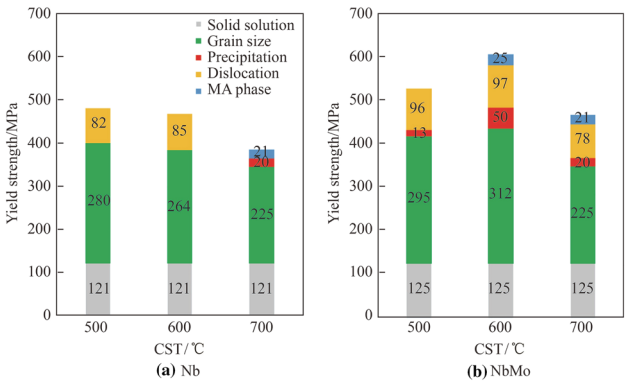

Fig. 4 Contributions to yield strength in function of coiling simulation temperature (CST) for Nb- and NbMo-alloy

making the particles to be aligned in rows. Inter-particle distance along the row and the distance between the rows determine the magnitude of strengthening. The inter-phase precipitation mechanism collapses when the speed of phase transformation is becoming too high, i.e., diffusion of carbon and microalloys is not fast enough to partition to the phase boundary. Molybdenum alloying facilitates inter-phase precipitation as it retards the transformation (see Fig. 6a) and reduces the phase boundary mobility. The micrographs in Fig. 6b clearly show inter-phase precipitation of TiC. The spacing of precipitate rows is the shortest, and the precipitate density along rows is the highest for a simulated coiling temperature of 650 °C.

In the case of low coiling temperature, phase transformation proceeds quickly and is likely finished before precipitation has initiated. Precipitation in this case can only occur spontaneously in the ferritic microstructure. Nucleation sites are provided by dislocation clusters present in this microstructure. In this situation molybdenum assists precipitation by providing a high dislocation density (see Fig. 2). Microalloy carbides have a cubic lattice with considerably larger lattice constant than ferrite. The precipitates nucleate with a Baker-Nutting orientation relationship $[100]_{MC}//[110]_{\alpha\text{-Fe}}$, $(100)_{MC}//(100)_{\alpha\text{-Fe}}$ reducing the lattice misfit to 2.2%, 6.8% and 10.1% for VC, TiC and NbC, respectively. The formation enthalpy for the carbides is − 44.2, − 78.1 and − 47.5 kJ/mol for VC, TiC and NbC, respectively. Considering the combination of solubility in ferrite, lattice mismatch and formation enthalpy, it appears that titanium carbide should be the most efficient for precipitation strengthening. Molybdenum has a formation enthalpy of + 16.5 kJ/mol. Thus, neither the precipitation of molybdenum as such nor the partial replacement of Ti by Mo in TiC is energetically favorable. However, the formation of a (Ti, Mo) mixed carbide in the early formation stage reduces the interfacial strain energy

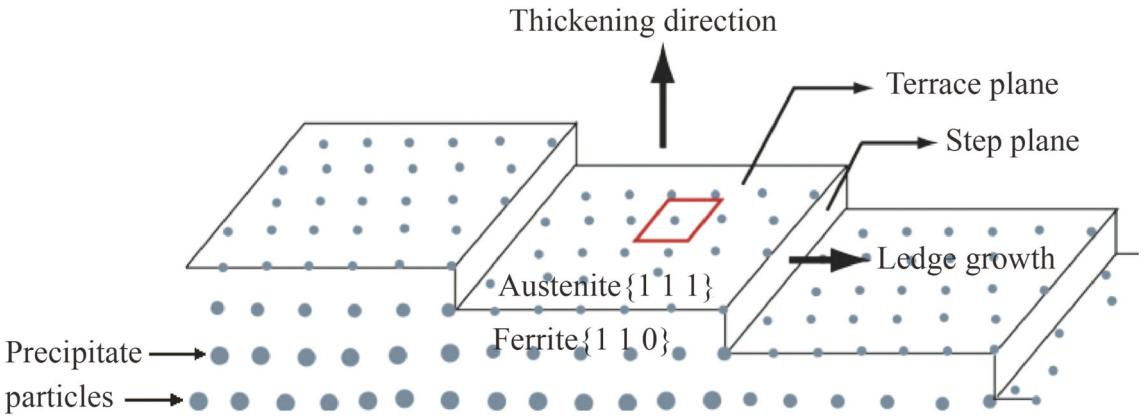

Fig. 5 Interphase precipitation by ledge mechanism during slow transformation from austenite to ferrite

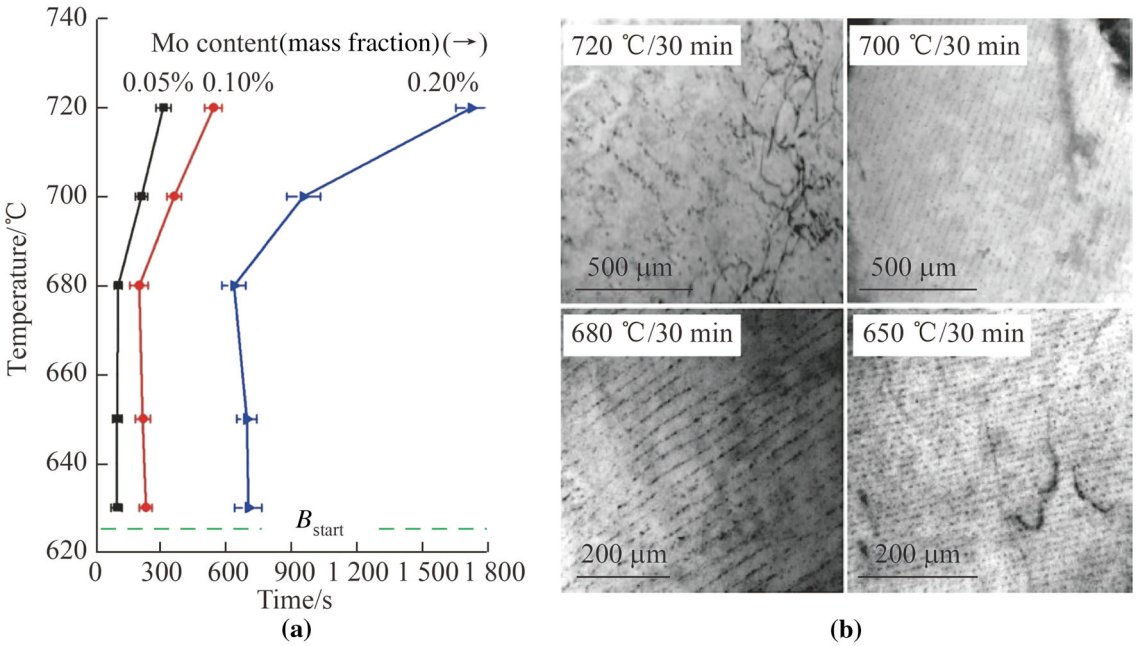

Fig. 6 Metallurgical effects after finishing of hot rolling enabling steel strengthening by interphase precipitation **a** delay effect of molybdenum on the austenite-to-ferrite transformation, **b** influences of coiling temperature on the precipitate particle distribution

between precipitate and ferrite matrix. Molybdenum can thus facilitate particle nucleation.

Figure 7 compares the influence of coiling temperature on three alloy concepts. Besides the mass fraction 0.04%Nb and 0.04%Nb-0.2%Mo alloys already discussed before, a 0.09%Ti-0.2%Mo alloy with the same base composition is included here. All three alloy concepts reveal their maximum strength at a coiling temperature of 600 °C (see Fig. 7a). Clearly, the TiMo alloy shows the highest strength level at any coiling temperature. Although the NbMo alloy has the smallest average grain size (see Fig. 7b), the larger strength in the TiMo is originating from precipitation. At a given coiling temperature, the various strengthening mechanisms are contributing to the total strength with different magnitudes. The best compromise is achieved in the current model alloys and thermo-mechanical treatment conditions at a simulated coiling temperature of 600 °C. The Nb-alloy shows only a small strengthening contribution by precipitation. The addition of molybdenum in the NbMo-alloy significantly promotes precipitation. The TiMo-alloy contains a higher amount of microalloy (0.09%Ti, mass fraction) than the NbMo-alloy (0.04%Nb, mass fraction). Therefore, the number of precipitates is larger leading to higher strengthening. The kinetics of Ti precipitation is also faster than that of Nb. Thus, precipitation can be considered being more complete in the TiMo-alloy within the isothermal holding period of 90 min applied here.

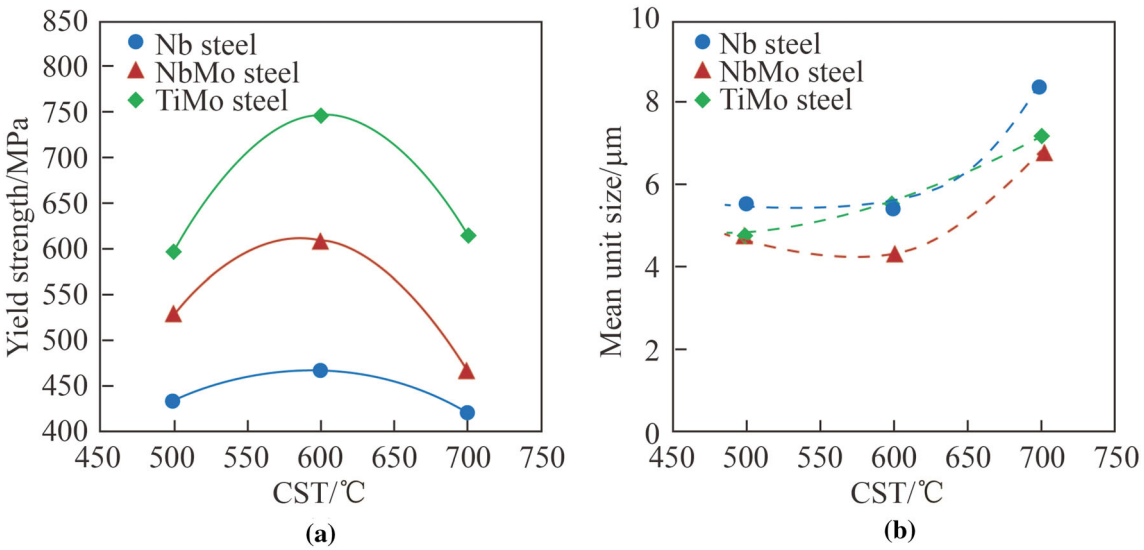

Fig. 7 Dependence of **a** yield strength and **b** grain size on CST and alloy concept

2.3 Two-step processing with secondary heat treatment

In real production of plate or strip steel, the material is continuously cooling from the CST, be it at slow rate. The actual slow-cooling rate is less for a coil than for a plate. Accordingly, the time period that the steel resides in the temperature range favorable to precipitation is shorter for plate than for coiled strip products. Therefore, it is quite difficult to obtain a large contribution of precipitation strengthening in plate products, especially when simultaneously fine grain size demands a low. This conflict can be solved by process modification. In the first step, bainitic microstructure with fine grain size and high dislocation density is produced by targeting a low cooling-stop temperature. In the second step, the fine-grained bainitic steel is re-heated to a temperature allowing efficient precipitation [19]. It is important in this process sequence that the initially produced bainitic structure with high dislocation density is not being removed by recovery or recrystallization during the subsequent annealing process. In this respect molybdenum acts as a stabilizing element retaining the pronounced sub-structure as well as high dislocation density generated in the initial process step. Figure 8 demonstrates this effect for the same TiMo-alloy as discussed before. In the initial process step the alloy is rolled and subsequently accelerated cooled (15 K/s) to 650 °C followed by continuous slow cooling (1 K/s) to room temperature. This process results in a bainitic microstructure with high dislocation density (see Figs. 8a, c) containing a share of MA-phase. The second processing step is fast induction heating to a peak temperature of 710 °C followed by slow cooling (1 K/s) back to room temperature. The induction heat treatment (HT) decomposes the MA-phase, yet neither reduces the grain boundary density (see Fig. 8b) nor the dislocation density (see Fig. 8d). However, the precipitate density is significantly increased by the induction heat treatment. The analysis of mechanisms contributing to strength (see Fig. 8e) indicates no precipitation strengthening after the initial process step. The induction heat treatment generates a strength gain of around 130 MPa by precipitation. The strength contribution by MA-phase present after the initial process stage disappears after heat treatment but is balanced by more contribution from grain refinement. This is beneficial to toughness and partially compensates for the detrimental effect caused by precipitation.

Compared to a strip product coiled under optimized conditions (see Fig. 7a), the strength of the heat-treated plate with identical alloy concept (see Fig. 8e) appears still inferior. The reason is the shorter residence of the steel in the temperature range favorable to precipitation. By decoupling the two processing stages it is possible to perform heat treatment of longer duration. That possibility is demonstrated using a 0.05%C-1.7%Mn-0.18%Cr-0.08%Nb (mass fraction) model alloy with Mo additions ranging from 0 to 0.3% [20]. The steels are fast cooled after rolling to a cooling-stop temperature of 450 °C and held for 10 min followed by air-cooling to room temperature. In the second stage, the steels are heated to 600 °C and held for up to 8 h. It is found that the presence of granular bainite in the microstructure is necessary for efficient precipitation. Granular bainite contains a high dislocation density and the dislocation line is the most advantageous nucleation site for heterogeneous precipitation of Nb carbides in a bcc matrix. Increasing molybdenum content enhances the share of

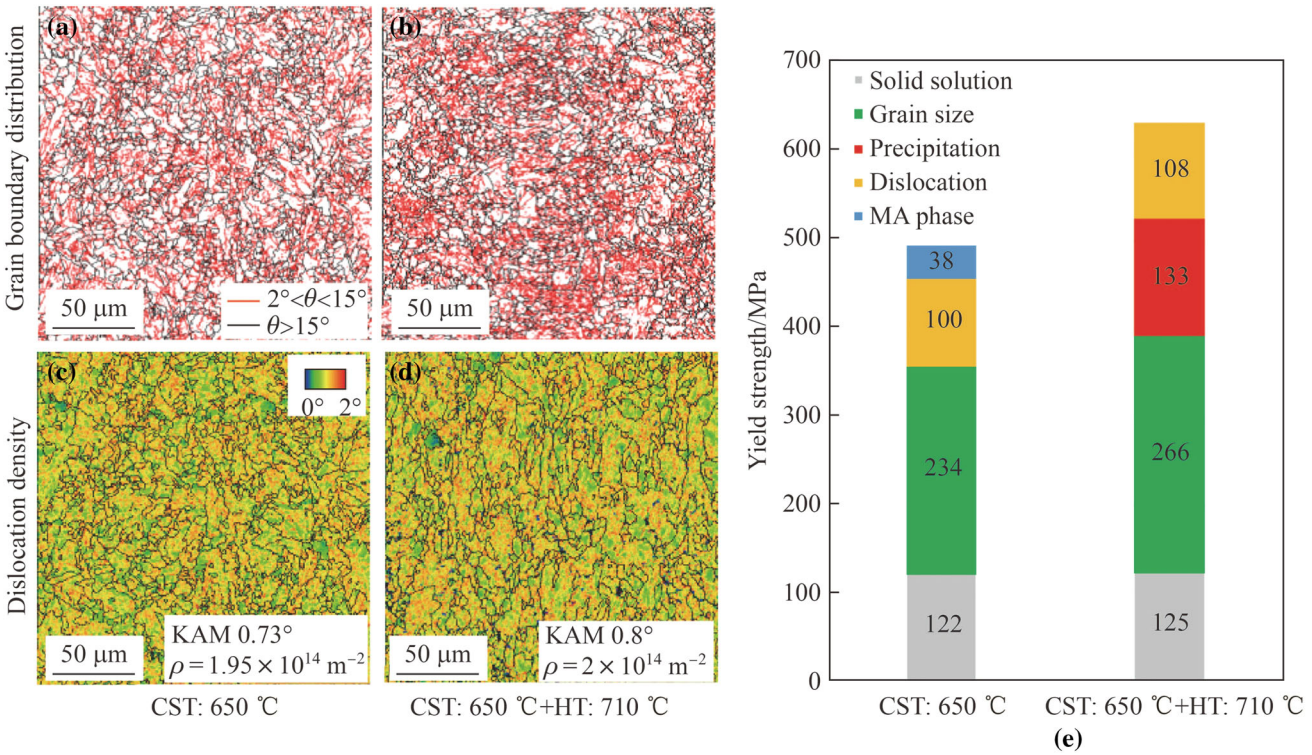

Fig. 8 Grain boundary distribution before **a** and after **b** heat treatment (HT) in a TiMo-alloy, dislocation density before **c** and after **d** heat treatment in a TiMo-alloy, **e** contributions to yield strength before and after heat treatment

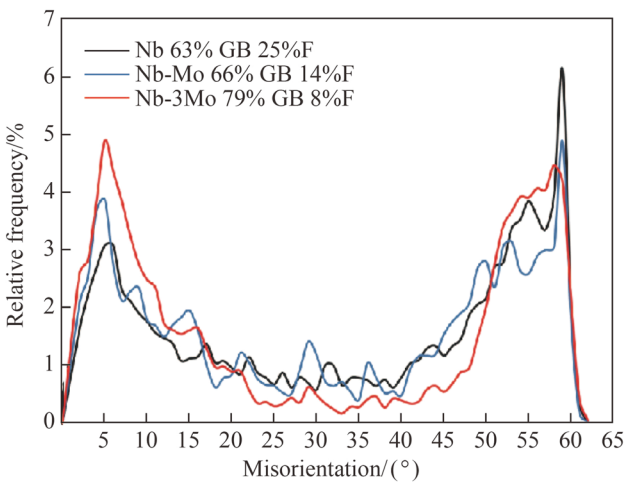

Fig. 9 Density distributions of grain boundary misorientation angle and amount of granular bainite (GB) and ferrite (F) in 0.05%C-0.2%Si-1.7%Mn-0.18%Cr-0.016%Ti-0.08%Nb (mass fraction) alloys added with 0.1% and 0.3%Mo (mass fraction) (CST = 450 °C)

granular bainite (see Fig. 9). The heat treatment at 600 °C results in a significant yield strength increase after a duration of 1 h (see Table 1). The precipitation effect is the largest for the Nb-0.1%Mo (mass fraction) alloy gaining 140 MPa in yield strength. After 8 h heat treatment, over-ageing leads to a small loss of strength. The Nb-0.3%Mo (mass traction) alloy has the highest overall strength since it contains the largest share of granular bainite. All three alloys quite well retain their strength even after 8 h exposure to high temperature. Elongation improves significantly which is a favorable result considering the achieved strength increase (see Table 1).

The practical implementation of a two-step process with initial fast cooling to obtain non-polygonal ferritic microstructure and secondary heat treatment to promote precipitation strengthening can be realized in several different ways (see Fig. 10). Using tempering furnaces for plate products or batch annealing (BA) for coiled products requires long annealing periods at temperatures below A_{c1}. For lower gages, online inductive heating has been already implemented by Japanese steelmaker JFE and is known under the term “heating online process” (HOP). In this quick heating process, a relatively high peak temperature allows achieving faster precipitation. Modern technologies such as compact strip processing (CSP), endless strip production (ESP) or ultra-thin cast strip (UCS) processing allow producing thin-gaged hot rolled strip. These products can be treated in the same way as traditional cold rolled steel using continuous annealing (CAL) or hot-dip galvanizing (HDG) lines. Typically, the residence time on peak annealing temperature is 60–120 s. Annealing temperatures closer to A_{c1} will result in more complete precipitation.

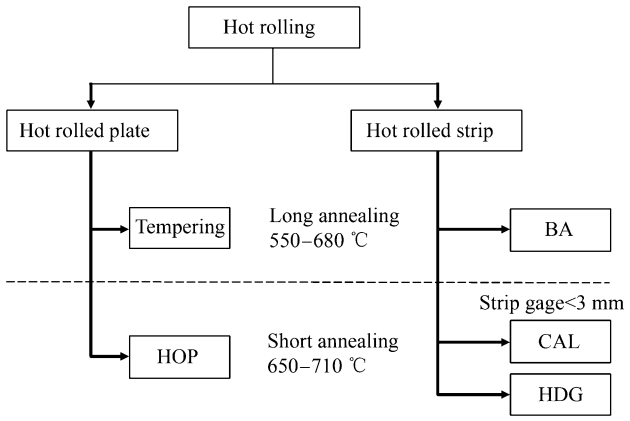

Fig. 10 Possibilities of two-step processing for combining microstructural strengthening and precipitation strengthening in hot rolled products

Table 1 Effects of heat treatment at 600 °C on mechanical properties of 0.05%C-0.2%Si-1.7%Mn-0.18%Cr-0.016%Ti-0.08%Nb (mass fraction) alloys added with 0.1% and 0.3%Mo (mass fraction) (CST = 450 °C)

Tempering time/h	Nb			Nb-Mo			Nb-3Mo		
	Y_S/MPa	T_S/MPa	E_l/%	Y_S/MPa	T_S/MPa	E_l/%	Y_S/MPa	T_S/MPa	E_l/%
0	512	630	22	479	683	21	575	679	19
1	594	652	29	619	678	27	672	718	27
8	586	638	30	605	655	27	651	702	27

Note: Y_S - Yield strength, T_S - Tensile strength, E_l - Elongation

2.4 Application examples of high-performance HSLA steels

China has been the first country installing large-scale pipeline systems applying X80 grade pipe steel [24]. This steel is mostly produced as hot-rolled strip for spiral welded pipe. However, hot-rolled plate is used for longitudinal welded pipe when particularly heavy wall gage is needed. Due to toughness requirements, a carbon content of 0.04%–0.06% and a homogeneous, fine-grained acicular ferritic microstructure is preferred [25]. Alloy concepts using 0.07%–0.1% Nb and 0.2%–0.3% Mo have been established as robust solution for hot-rolled strip production. Severe austenite pancaking followed by accelerated cooling to a low coiling temperature are key process characteristics. Initially, plate steel alloy designs did not use Mo-alloying due to the more efficient cooling after finish rolling. More recent modifications of plate steel X80 alloys, however, considered Mo additions of around 0.2%. This modification provides a better process robustness and also improves toughness properties especially when heavier gages of around 30 mm have to be produced. Recent pipe steel developments are targeting the strength levels of X90 and X100. A cost-effective approach to X-100 with a minimum of 6% uniform elongation to meet strain-based design requirements is using 0.08% Nb and 0.25% Mo base chemistry produced into a dual-phase microstructure of ferrite and a carbon rich second phase [26]. Such multi-phase processing requires holding in the inter-critical temperature regime before quenching and thus needs the superior capabilities of a modern hot rolling mill.

Light-weighting of frame and chassis structures for commercial vehicles including trailers has been a major driving force for developing hot strip grades with minimum yield strength of 700 MPa in the gage range of 5–10 mm [1, 2]. Recent developments in China introduced truck frame steel grades with 600 MPa yield strength and higher. The alloy design is based on low carbon content and Nb-Ti dual microalloying [27]. With this concept either polygonal ferritic or bainitic microstructure with precipitation strengthening can be produced depending on the run-out table conditions in the hot-strip mill. The presence of pearlite or other hard phases in the microstructure is rather avoided as these have a negative impact on the bendability. Furthermore, such hard particles also lead to edge damage after mechanical cutting and cause increased wear on cutting tools. Pearlite-free steels intrinsically feature good toughness and fatigue resistance due to fine grain size and low carbon content. For reaching 700 MPa yield strength most concepts are based on 0.06%C-1.8%Mn-0.06%Nb-Ti-Mo alloying. This concept exhibits a remarkable robustness against temperature variations on the run-out table of the hot-strip mill [1]. The resulting narrow scattering of strength is beneficial to forming operations in manufacturing, especially with respect to compensating spring-back occurring during forming of high strength steel. Good weldability is a result of reduced CE and particularly a low absolute carbon content. The CE (IIW) is typically in the range of 0.35–0.45 so that harden ability is rather low. The carbon content being typically clearly below 0.1 reduces peak hardness in particular, thus minimizing the risk of cold cracking.

Besides strength, many applications require other properties such as resistance against weathering or increased temperature. Substitution of traditional SPA-H steel (min(yield strength) = 355 MPa) by higher strength steel (yield strength > 550 MPa) enables weight reduction of 15%–20% in the construction of shipping containers or truck cargo boxes resulting in significantly lower fuel consumption. The reduced gage of such containers requires, however, a relatively better weathering resistance to guarantee sufficient lifetime. Typical alloying elements in weathering steels are Cr, Cu and Ni. Molybdenum additionally contributes to weathering resistance and simultaneously increases strength. A practical alloy

concept for 700 MPa weathering steel uses around 0.2% Mo added to a low-carbon Cr-Cu-Ni-Nb-Ti base alloy. The microstructure of finished steel ideally consists of acicular ferrite and granular bainite, while keeping the share of MA-phase on a low level for guaranteeing high toughness and good cold bending properties. Other weather resistant steel applications for bridges or transmission line towers requiring yield strength in the range of 460–550 MPa are produced as heavy plate or angles. Molybdenum addition in the range of 0.2%–0.4% to these products consisting of a Cr-Cu-Ni-Nb base alloy showed appreciable improvement of weathering resistance [28].

Engineering codes for the construction of high-rise buildings sometimes demand fire resistant steel to be used in vertical columns [29]. Such steels are intended to resist accelerated creep, or thermally activated deformation when exposed to high temperature for a relatively short time. It has been shown that additions 0.5% Mo and 0.02% Nb to a standard grade 50 steel increased the elevated temperature strength in a synergetic way. Molybdenum by itself reduces softening and enhances creep resistance at elevated temperature. It also prevents niobium precipitates from coarsening and thus helps maintaining that strengthening mechanism during elevated temperature exposure [30].

3 Alloy concepts and processing routes for martensitic steels

Increasingly many applications in manufacturing of machinery, agricultural, hoisting or transportation equipment as well as vehicle structures require material strength clearly above 800 MPa [21–23]. Such a strength level is difficult to achieve with the low-carbon HSLA steel approach described in Sect. 2 of this paper. Martensitic steel can readily fulfil demands for ultra-high strength and hardness. However, unless it is sufficiently tempered, martensite has lower ductility and toughness than ferritic or bainitic steels. When the strength is passing the threshold of roughly 1 000 MPa, steels also become increasingly sensitive to hydrogen embrittlement [31]. The presence of diffusible hydrogen in martensitic steel can severely lower fracture toughness or cause so-called “delayed cracking” which unexpectedly destroys an initially sound component [32]. Such critical issues require metallurgical optimization, which is related to the alloy concept and processing.

3.1 Process variants for producing martensitic steels

The lack of formability in martensitic steel has been elegantly solved by the automotive industry using a process called “press hardening” or “hot stamping” (see Fig. 11). Forming is done in the hot, thus, austenitic state and subsequent quenching by the water-cooled stamping die assures the transformation to martensite. The paint-baking

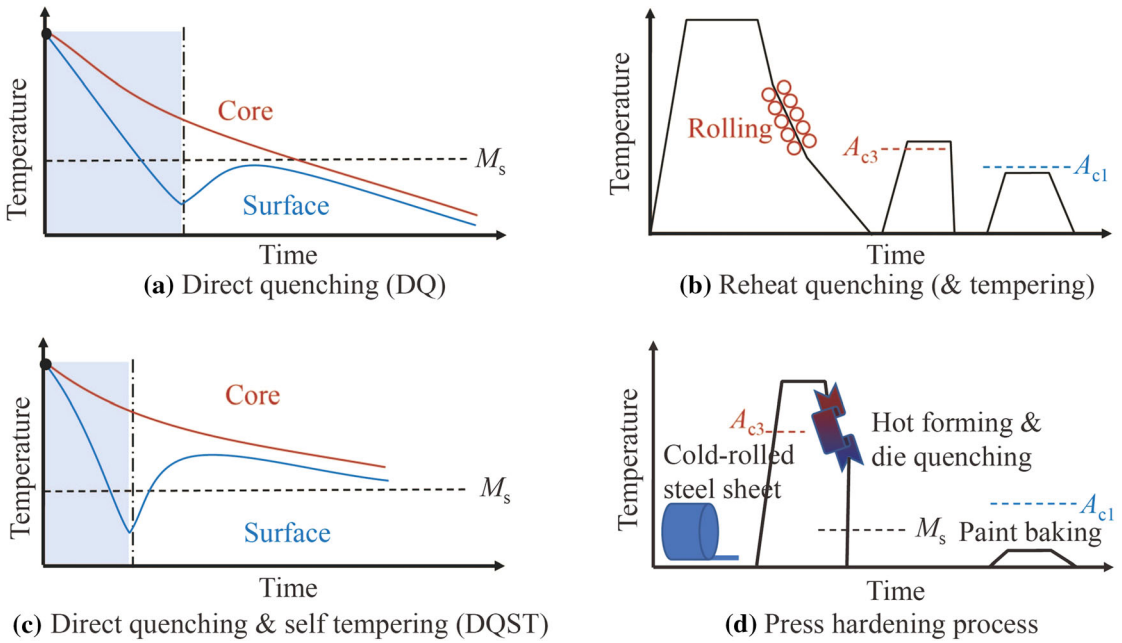

Fig. 11 Production principles for producing martensitic or tempered martensitic steel (M_s: martensite-start temperature, A_{c3}: end of austenite transformation, A_{c1}: start of austenite transformation)

process (170 °C for 20 min) at the end of car body manufacturing acts as a low-temperature tempering treatment to the press hardened components. The production of martensitic hot-rolled strip and plate is nowadays preferably practiced via direct quenching (DQ) from the rolling heat (see Fig. 11). This procedure makes the traditional re-austenitizing and quenching process obsolete, thus, reducing energy consumption, simplifying in-plant logistics and largely enhancing production capacity. The objective of DQ is to produce microstructures consisting predominantly of martensite and/or bainite by utilizing the highest possible cooling rates. Modern cooling facilities can easily apply cooling rates of 100 K/s. However, such high cooling rates apply only to thin-gauge plates and to the surface-near area of heavy gaged plates. The attainable cooling rate at the plate core is substantially lower and decreases with increasing plate thickness. Subsequent tempering is required for adjusting an adequate balance of tensile and toughness properties. By applying very short and intensive cooling, which is interrupted before the plate center is cooled below martensite-start temperature, the remaining heat will provide an in-line tempering effect. This process is termed quenching and self-tempering (QST). In the most favorable arrangement, the cooling facility is positioned directly behind the last stand of the rolling mill. Accordingly, the finish rolling temperature equals the cooling start temperature. It is also acceptable having a short transfer time (up to 30 s) without causing a detrimental effect on the mechanical properties after DQ [33].

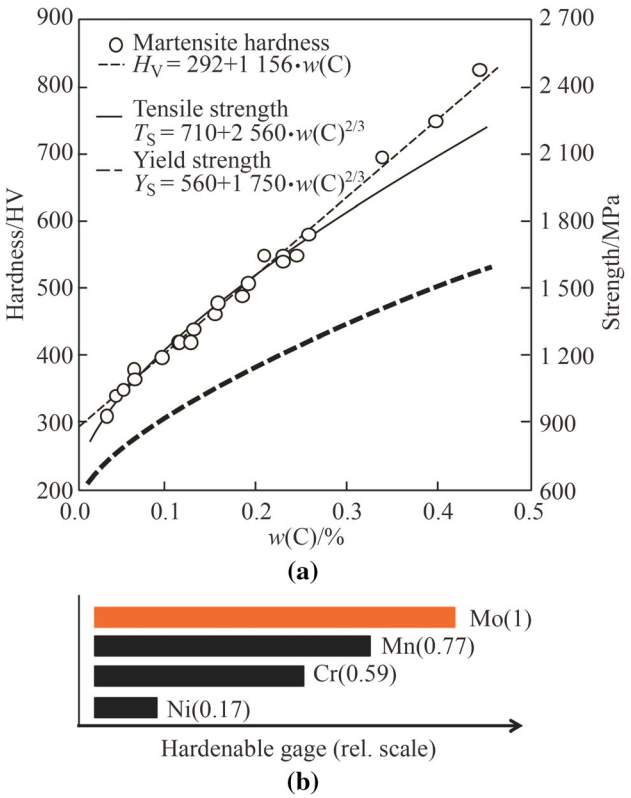

Fig. 12 Effects of alloying elements in martensitic steel **a** influences of carbon content on measured hardness (HV0.5) and comparison to calculated strength [34] in unalloyed carbon-manganese steel in as-quenched condition, **b** relative effect of alloying elements on hardening depth

3.2 Molybdenum alloying effects in martensitic steels

Considering alloy concepts, carbon is the dominating element providing strength to martensite (see Fig. 12a). A carbon content of only 0.08% results in tensile strength of around 1 100 MPa and yield strength of over 900 MPa. The highest tensile strength applied recently in car body components approaches 2 000 MPa. Such martensitic steel is alloyed with 0.34%C. Alloying elements boosting hardenability need to be used for achieving full martensitic strength, especially in products of heavier gage. For the same weight percentage added, molybdenum is the most powerful hardenability element compared to other typical alloys such as manganese, chromium, or nickel according to the ratio shown in Fig. 12b [35]. Micro-alloying of boron increases hardenability very effectively. Simple low-cost martensitic steels rely on a Mn-B alloy concept. However, this basic alloy concept cannot fulfil advanced requirements with regard to toughness and delayed cracking resistance.

Using molybdenum as alloying element to martensitic steel not only offers superior harden ability but brings about additional benefits such as microstructural refinement, tempering resistance, delayed cracking resistance, synergy effects with other alloying elements.

The martensitic microstructure develops within the prior austenite grains present before quenching [36]. Therefore, austenite conditioning has a direct influence on the final martensite properties such as strength and toughness [37, 38]. It was already demonstrated in Fig. 2 that molybdenum significantly contributed to austenite pancaking during finishing hot rolling. This effect is even stronger in combination with niobium microalloying. The pancaked microstructure is quenched into martensite directly after finish rolling when applying the DQ process. Accordingly, the martensitic sub-structure develops within pancaked prior austenite grains. On the contrary, for reheat quenching processes, the pancaked austenite transforms into a typically ferritic-pearlitic microstructure by conventional cooling. The latter is clearly finer in a Mo-Nb alloy as compared to a Nb-only alloy [38]. The finer ferrite-pearlite microstructure provides a faster re-austenitizing kinetics, thus accelerating the reheating process. Solute drag by molybdenum and precipitate pinning in niobium is co-alloyed concepts control the austenite grain size and

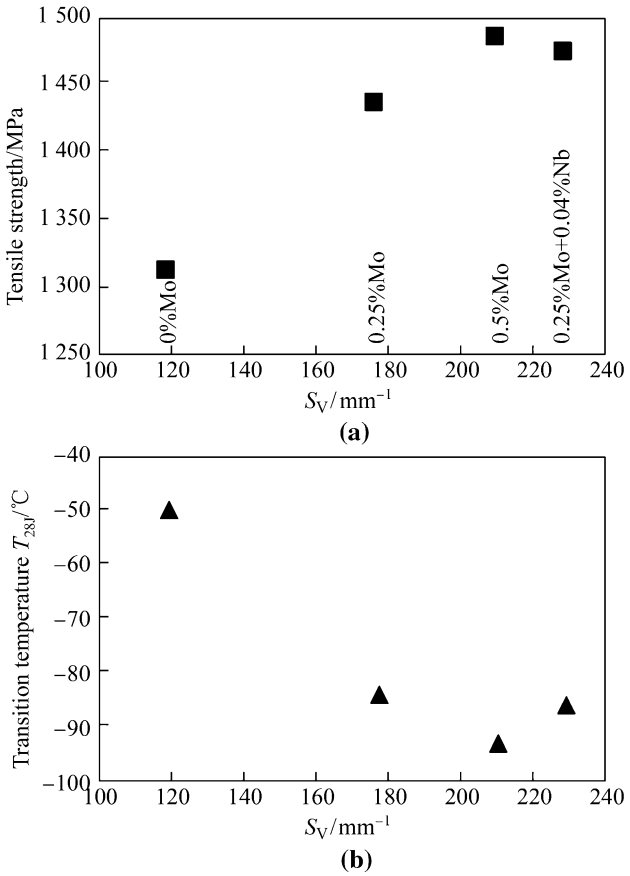

Fig. 13 Influence of molybdenum and molybdenum-niobium synergy on strength and toughness of directly quenched 0.16%C-Mn-Cr-Ni base alloy measured in transverse direction (FRT: 900 °C) (intensity of austenite pancaking expressed as $S_v = 0.429(1/d_{RD}) + 0.571\ (1/d_{TD}) + (1/d_{ND})$)

guarantee quenching into martensite from a more refined prior austenitic microstructure. It was shown that the martensite packet correlated with the austenite pancake thickness size for DQ steels [38]. Therefore, better strength and toughness properties can be expected with increasing molybdenum alloy content due to stronger austenite pancaking. Figure 13 demonstrates this effect using the ratio of grain boundary area to volume being a measure for the degree of austenite pancaking. With increasing molybdenum content in the range of 0–0.5% austenite pancaking becomes more pronounced and the tensile strength increases by almost 180 MPa. Simultaneously, the transition temperature (T_{28J}) decreases from −50 °C in the Mo-free steel to below −90 °C in the 0.5%Mo added steel. The combination of 0.25%Mo and 0.04%Nb results in even stronger austenite pancaking (S_V parameter), yet the improvement of properties appears to saturate on high level. Applying a high-temperature tempering treatment (600 °C for 30 min) to the same alloys necessarily leads to a gain of 40%–60% in elongation on the expense of

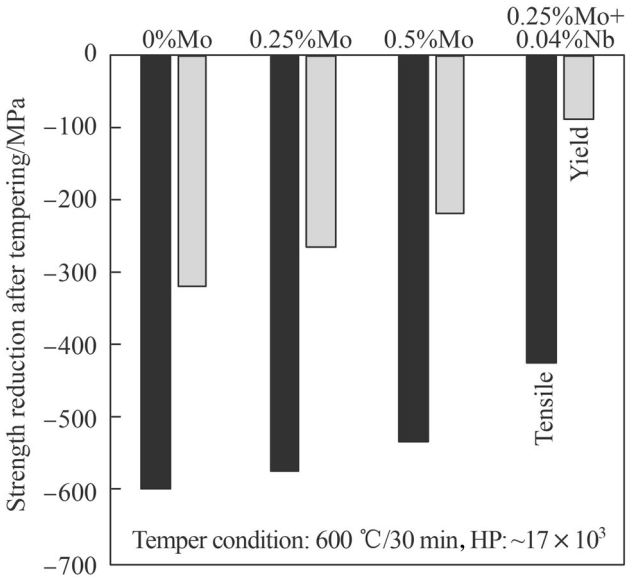

Fig. 14 Reduction of yield and tensile strength after tempering treatment of directly quenched 0.16%C-Mn-Cr-Ni base alloy (HP: Hollomon-Jaffe parameter)

strength (see Fig. 14). The temper-induced strength loss is particularly large in the Mo-free alloy. Increasing molybdenum addition reduces the strength loss. Particular high tempering resistance is found for the 0.25%Mo-0.04%Nb alloyed variant. It appears that niobium precipitates formed during the tempering treatment deliver around 180 MPa additional yield strength as compared to the 0.25%Mo alloy. Regarding the tensile strength the same effect applies but is with about 150 MPa somewhat smaller.

The sensitivity to hydrogen embrittlement is a consequence of three conditions acting together: microstructure, diffusible hydrogen and stress. Diffusible hydrogen present in a martensitic steel can originate from different sources such as steel making, intermediate treatments, welding or corrosion occurring during operational conditions. Pronounced hydrogen embrittlement is observed when the amount of diffusible hydrogen in the steel is high. In this case hydrogen aggregates at prior austenite grain boundaries present in the martensitic microstructure. Hydrogen lowers grain boundary cohesion so that in severe cases the material fails far below the actual yield strength with practically zero ductility. The resulting fracture pattern is showing intergranular cracking along the prior austenite grain boundaries. In less severe case of hydrogen embrittlement, the fracture pattern changes to the quasi-cleavage type. If the diffusible hydrogen content remains below a critical threshold value, ductile fracture occurs showing the typical dimple type pattern. The challenge towards alloy and process design is to appropriately modify the steel so that it can sustain the typical amount of hydrogen being picked up by the material during all phases of production

and over the component service life. The microstructural cornerstones of such a modification are [38]: (i) Refinement of the prior austenite grain size before final quenching to lower the hydrogen concentration per unit grain boundary area. (ii) Introduction of hydrogen trapping sites such as nano-sized precipitates to fix hydrogen or to at least reduce its diffusivity. (iii) Reinforcement of the grain boundary cohesion to counteract the deleterious effect of hydrogen.

Figure 15 highlights the prior austenite grain size effect on the time to delayed fracture in typical press-hardening steels. The grain size was in this case adjusted by the heating conditions before quenching and was thus not related to specific alloying. It is obvious, that martensitic steel in the 2 000 MPa class is much more sensitive to hydrogen-induced delayed cracking than steel in the 1 500 MPa class. Higher manganese addition is likewise detrimental to delayed cracking resistance. Therefore, emphasizing on manganese alloying for obtaining high hardenability is not a recommended option. Grain refinement, however, brings an improvement in all cases. Nevertheless, the delayed cracking resistance of standard 32MnB5 even with finest prior austenite grain size is too low for safe application in components.

The effect of Mo and Mo-Nb alloy additions to standard 32MnB5 is demonstrated in Fig. 16. The grain sizes in these modified alloys are in the range of 4–6 µm. Adding 0.15%Mo results already in a substantial increase in the time to delayed fracture and again a synergy between Mo and Nb becomes evident. The improvement is more pronounced at the higher molybdenum level of 0.5%. The synergy of 0.5%Mo and 0.05%Nb makes the 2 000 MPa steel approximately twice as resistant against delayed cracking as a conventional 1 500 MPa steel. Both, Mo and Nb contribute to grain refinement in the prior austenite microstructure. The larger part of the property gain obviously relates not to grain refinement but to stronger grain boundary cohesion. Molybdenum is known to provide that effect. The synergy with niobium relates to an enhanced amount of ultra-fine precipitates forming in the steel before quenching. These precipitates consisting basically of NbC can act as efficient hydrogen trap [39]. Analysis by transmission electron microscopy indeed revealed that the area density of ultra-fine niobium precipitates was boosted by the addition of 0.15%Mo (see Fig. 17), thus severely enhancing the number of hydrogen trapping sites. More intricate beneficial effects of molybdenum in retarding delayed fracture relate to: (i) reduction in the mobility of dislocations initiated from the crack tip, (ii) reduction of pile-up stress of dislocations at the grain boundary, (iii) vacancy trapping obstructing the formation of vacancy clusters and micro-voids.

These effects impede the underlying mechanisms of hydrogen-induced crack initiation and propagation, which will not be discussed in detail in the present context.

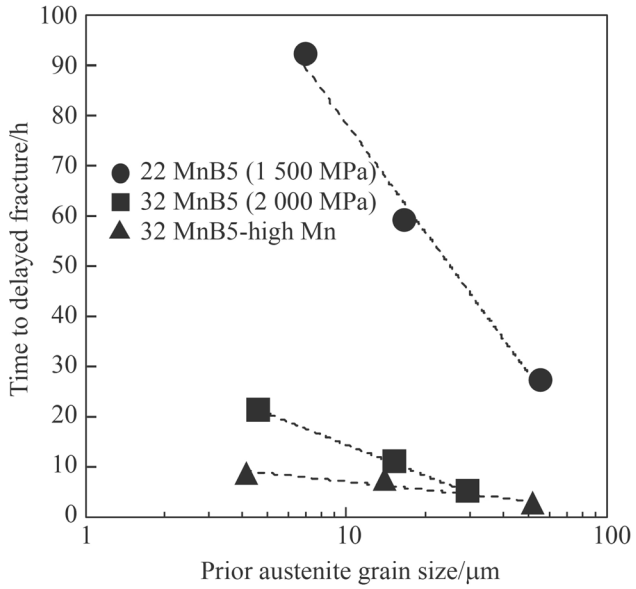

Fig. 15 Effects of prior austenite grain size on the time to delayed fracture in standard manganese-boron alloyed press hardened steels (standard Mn: 1.2%, high-Mn: 2.5%)

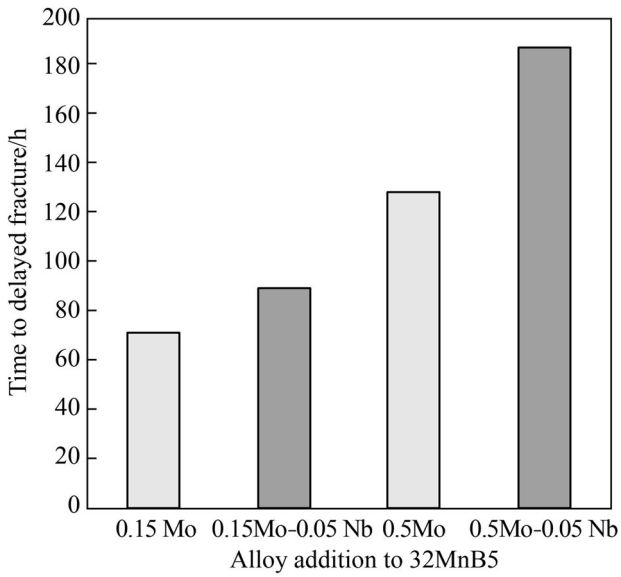

Fig. 16 Effects of molybdenum and niobium additions to standard 32MnB5 on the time to delayed fracture in press-hardened steels (Mn: 1.2%)

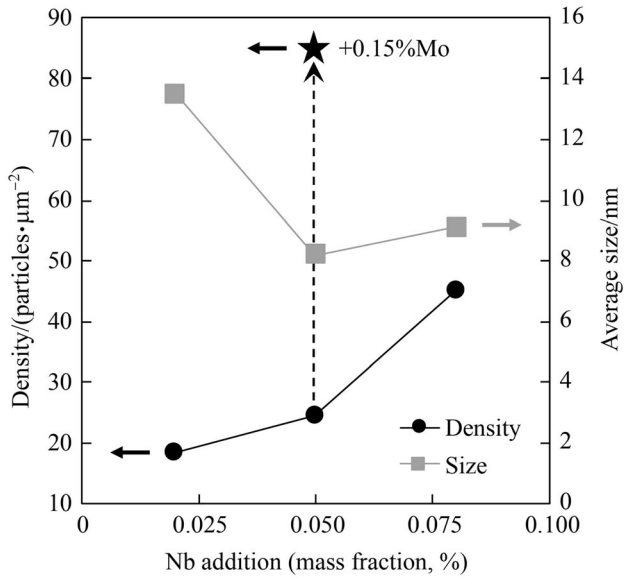

Fig. 17 Average size and area density of ultra-fine NbC precipitates in press hardened steel as analyzed by transmission electron microscopy (the effect of 0.15%Mo addition on the NbC particle density is indicated for a 0.05%Nb alloyed steel)

3.3 Application examples of martensitic steels

Martensitic steels are particularly interesting for application in hoisting equipment. Crane booms demand the lowest possible dead weight for lifting heavy loads with a long reach. For that purpose, steel grades with minimum yield strength of 960–1 300 MPa are nowadays being used. Taking a conventional grade 50 steel (355 MPa, yield strength) as a reference, substitution by a 960 MPa grade allows reducing the material gage and thus the component weight by more than 70%. Regarding a typical butt-welding situation with a V-shape bevel, the weld seam volume will be reduced by over 90% [1]. Accordingly, component handling and manufacturing become much more efficient. However, it must be mentioned that the weldability of ultra-high strength steels is more demanding in terms of filler material as well as skill level of the welder. Another important consideration relates to the heat-affected zone properties after welding [40]. The heat input by the welding process leads to peak temperatures of over 1 300 °C close to the fusion line and induces significant modification of the original microstructure. This results in soft zones having a yield strength lower than that of the base material as well as the fusion line. Such soft zones bear the risk of localized premature yielding under service load conditions. An appropriate alloy concept using molybdenum and niobium reduces or completely avoids heat-affected zone softening. This is related to the tempering resistance provided by these alloying elements as was demonstrated by Fig. 14. For that reason, molybdenum is added up to 0.7% in such steels while niobium is usually limited to 0.05%. The carbon equivalent (CE IIW) of such steels is typically in the range of 0.5–0.6, while the absolute carbon content remains below 0.2%. Components used for equipment in the mining and mineral processing industry typically require high resistance against wear. Correspondingly, the steel should have high hardness which is achieved by raising the carbon content. Toughness is not only needed due to likely high-impact loading under service conditions, but also to further improve wear resistance [41, 42]. Molybdenum alloying, often in combination with niobium, provides the required property spectrum of strength, hardness and toughness. The production of thin-gage martensitic steel has been steadily increasing over the last years due to the intensive use of press-hardened components in car bodies. Car models utilize 1 500 MPa press hardening steel (22MnB5) to an amount of up to 40% of the total body weight. For enabling further weight saving or crash resistance, steelmakers are developing press-hardening steel in the 2 000 MPa class (34MnB5). Qualification tests by carmakers confirmed that sufficient delayed cracking resistance required alloying of molybdenum. First 2 000 MPa class products in the market indeed rely on a combined molybdenum and niobium addition to standard 34MnB5 steel [43].

4 Alloy concepts and processing routes for multi-phase steels

HSLA steels offer a very good compromise between strength, toughness and weldability. However, some applications require higher elongation than that HSLA steel can provide at comparable strength level. Other applications need higher strength than that offered by HSLA steels yet having more ductility than martensitic steels. This product range of steels having tensile strengths from 600 MPa up to 1 200 MPa and high ductility is covered by so-called multi-phase steels. In this concept a particular combination of strong phases and ductile phases is adjusted by specific thermo-mechanical treatment.

4.1 Dual-phase steel design and applications

Microstructural design consists of a ductile matrix, typically ferrite, containing a dispersed second phase of usually martensite and/or bainite has been existing for several decades and is most prominently represented by the dual-phase steel family, which can reach tensile strength up to about 1 000 MPa. The vast majority of dual-phase steel production is cold-rolled to gages below 2 mm and used for car body components. Hot-rolled dual-phase steel in the gage range of 3–6 mm is being used almost exclusively for

manufacturing of vehicle wheels. More recently, however, heavier-gaged hot-rolled dual-phase steel gained interest in pipeline applications. While the current top grade for pipe manufacturing is X80, as discussed in Sect. 2, future projects investigate the feasibility of grade X90 or X100. Enhancing strength further based on the established X80 alloy platform would result in rather low elongation of higher strength steel and thus not allow the implementation of strain-based design concepts to pipeline construction. A dual-phase microstructure can solve this conflict providing sufficient elongation at X90–X100 strength level. The challenge for the steel producer is to rather precisely adjust the two microstructural phases, being ferrite and martensite, in terms of volume fraction, grain size and spatial distribution under the available processing conditions.

Molybdenum alloying plays a prominent role in achieving a dual-phase microstructure, especially in hot-rolled products such as strip and plate. Dual-phase steel production requires initial transformation of austenite into ferrite, enrichment of the remaining austenite with carbon and final fast-cooling converting the carbon enriched austenite into martensite. This process is schematically shown in Fig. 18 for hot strip production [44]. Strip speed, length of the run-out table and cooling conditions determine the acceptable processing window for forming a sufficient volume fraction of ferrite. Within this time frame, pearlite formation must be suppressed. A two-step cooling strategy is the preferred approach since it allows better control of the ferrite phase share while requiring lower alloy content. The metallurgical functionality of molybdenum is two-fold in this respect [45, 46]. Firstly, it moderately delays ferrite formation but strongly obstructs pearlite formation (see Fig. 19). In that respect molybdenum widens the time window for ferrite formation. Secondly, molybdenum obstructs the decay of the carbon-enriched austenite into bainite. In strip mills allowing two-step cooling strategy, the addition of around 0.15%Mo is sufficient for robust production of dual-phase steel. Flexibility of the cooling strategy is higher when producing dual-phase steel plate products, since the plate is at rest in the cooling device. The difficulty in this case relates more to the heavy gage of the product, making that the cooling rate at the plate surface is much higher than in the core. Molybdenum at a higher addition level can favorably mitigate the phase formation in this situation as well.

The production of X100 plate, for instance, can be realized by using 0.07%C-0.08%Nb-0.25%Mo base chemistry. After TMCP rolling, the plate is cooled to a temperature in the inter-critical region, i.e., between A_{r3} and A_{r1}, to allow ferrite formation and carbon partitioning followed by final quenching [26]. Polygonal ferrite grains decorate the periphery of former austenite pancakes while a finer-grained mixture of non-polygonal ferrite and martensite develops inside. This approach requires the advanced processing capabilities of a modern plate mill. The particularly fine-grained structure of Mo-Nb alloyed steel (see Fig. 20) thereby facilitates the partitioning of carbon by reducing the distance for carbon to diffuse from newly formed ferrite to remaining austenite grains.

The adjustment of a dual-phase microstructure in cold-rolled steel is nowadays primarily done by using the hot-dip galvanizing process. The integrated recrystallization annealing cycle prior to galvanizing is performed in the

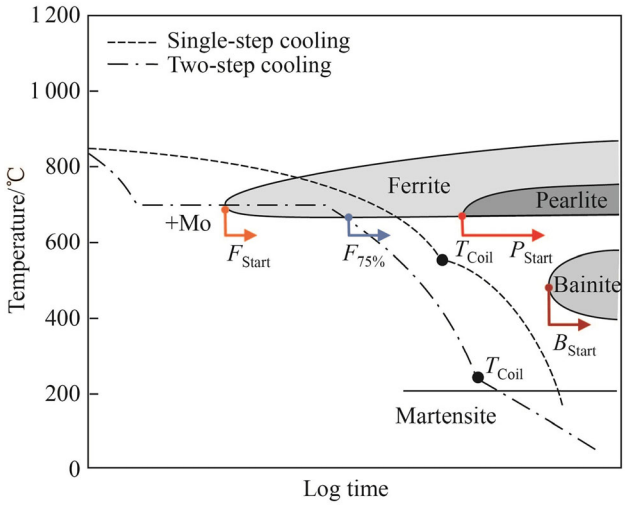

Fig. 18 Alloying and processing strategies for producing hot-rolled dual-phase steel with ferrite-martensite microstructure (the effects of molybdenum are schematically indicated)

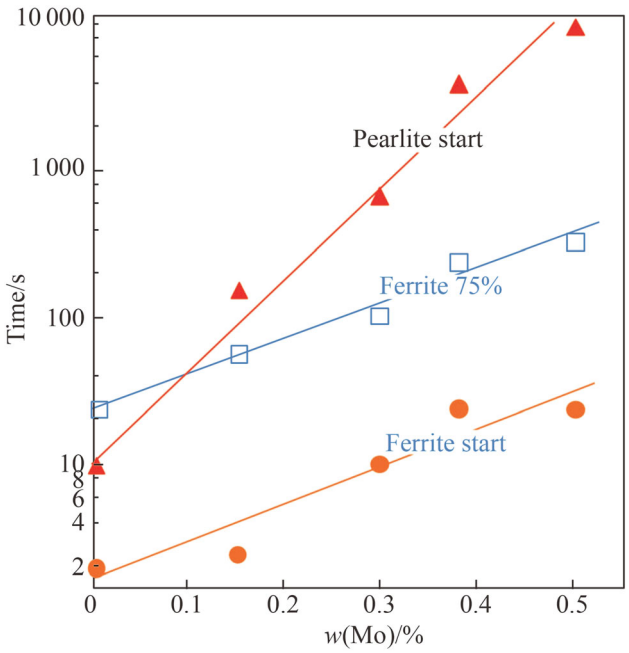

Fig. 19 Influences of molybdenum alloy content on the delay of ferrite and pearlite formation times

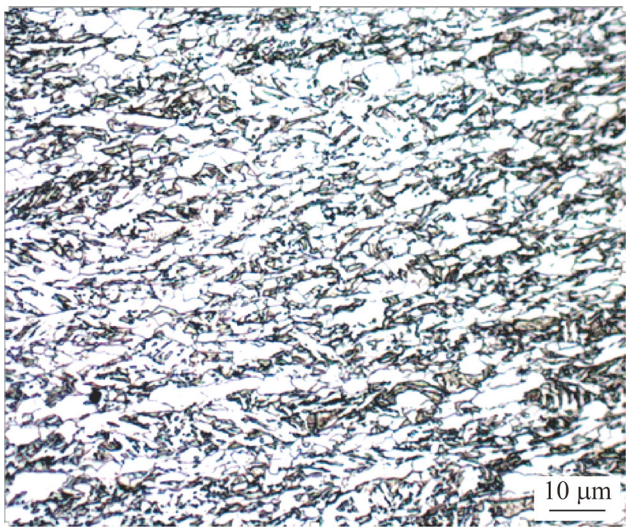

Fig. 20 Dual-phase microstructure of Mo-Nb alloyed X100 pipe steel

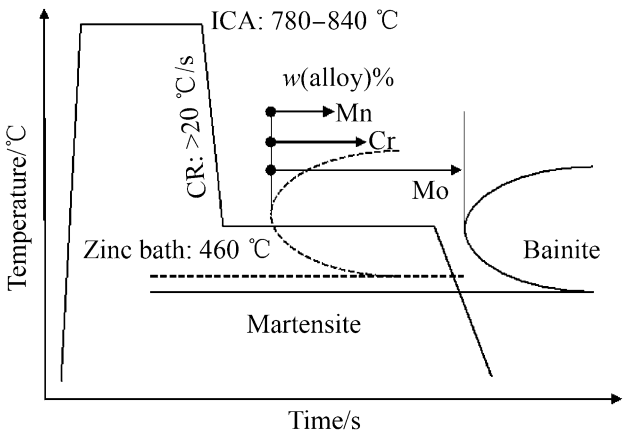

Fig. 21 Time-temperature characteristic of hot-dip galvanizing cycle and effect of alloying elements on suppressing bainite formation during isothermal holding in the zinc bath

inter-critical temperature range between A_{c1} and A_{c3}. A sufficient amount of new austenite is formed by dissolving the pearlite present in the original cold-rolled steel. After the inter-critical annealing stage, the steel strip is fast cooled to a temperature of around 460 °C before entering the liquid zinc bath followed by final cooling. It is thereby important that the meta-stable austenite does not transform into bainite during the passage through the liquid zinc bath. Again, the retardation of bainite formation by molybdenum alloying allows enhancing the robustness of this process (see Fig. 21). This bainite-retarding effect is relatively stronger for molybdenum as compared to manganese or chromium [47].

4.2 Multi-phase steel containing retained austenite

Increased ductility in ultra-high strength steel requires a microstructural design having strong phases such as martensite or bainite representing the majority phase and dispersed retained austenite islands being the minority phase [48]. The austenite phase provides ductility to the strong matrix and in-situ transforms into martensite upon applied deformation, known as the transformation-induced plasticity (TRIP) effect. The strain-induced martensite phase results in substantial work-hardening of the steel. A practical way of producing such steel is to quickly cool the austenitic microstructure, being present after either hot rolling or a prior annealing treatment, into the bainite forming temperature range followed by isothermal holding [49, 50]. This treatment, also known as austempering, allows formation of carbide-free bainite. The carbon is partitioned from the advancing bainite phase to the remaining austenite phase. Part of this austenite fraction is carbon-enriched high enough to remain meta-stable at room temperature. Sufficiently high additions of silicon and/or aluminum help suppressing the precipitation of cementite during bainite growth. However, both alloying elements are strong ferrite promotors. The unwanted formation of any ferrite phase fraction will significantly lower the strength of the steel. Molybdenum alloying effectively retards premature ferrite formation especially at lower quenching rates. During isothermal holding in the bainite temperature range molybdenum is retarding the phase transformation kinetics as well. Since carbon diffusion is already relatively slow in this temperature range, the retarded transformation kinetics provides more time for completing carbon partitioning. Molybdenum segregates to grain and lath boundaries attracting carbon atoms. The resulting high solute carbon concentration at the periphery

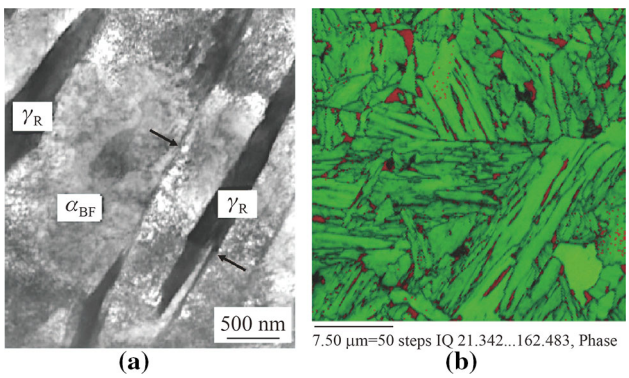

Fig. 22 Formation of retained austenite films **a** microstructure of a TRIP bainitic-ferrite steel (α_{BF}) showing retained austenite (γ_R) films along the bainitic sheaf boundaries (arrows) **b** identification of phases by electron back scatter diffraction (EBSD) analysis (green: bainitic-ferrite, red: retained austenite)

of such carbide-free bainite needles results in the formation of retained austenite films (see Fig. 22) [51].

Steel processed to a microstructure comprising a bainitic matrix containing retained austenite has been commercialized for automotive applications under the name TBF (TRIP Bainitic-Ferrite) steel. Due to the combination of ultra-high strength and good elongation TBF steel has high energy absorption capacity and is well-suited for crash-resistant components in the lateral structure of the car body.

Further developments aim at combining a martensitic matrix with retained austenite by employing a process called quenching & partitioning (Q&P) [52]. Here, austenite is immediately quenched to below the martensite-start temperature, yet cooling is interrupted before full martensite transformation. Fast reheating to a higher temperature enables partitioning of carbon from the initially formed martensite to enrich still existing austenite. That austenite, depending on the level of carbon enrichment, forms fresh martensite upon final cooling or remains as metastable retained austenite. This approach is principally limited to thin-gage strip products and requires specific adaptations of continuous annealing lines or galvanizing lines to allow fast reheating. Alloying concepts, including the benefits of molybdenum alloying, are similar to those for TBF steel [53]. Like martensitic steels, TBF as well as Q&P steels are sensitive to hydrogen embrittlement. Hence, the same beneficial effects of molybdenum alloying preferably in combination with niobium micro-alloying apply.

Recently such microstructural concepts have also been considered for production of ultra-high strength plate steel with heavier gage [54–57]. Yet, alloy concept and process have important differences compared to thin sheet steel. The relatively high carbon content of 0.2%–0.3% as practiced in TBF and Q&P steels is not desirable in plate products due to weldability and toughness concerns. While a TBF-like process would be possible in plate production, in-line Q&P processing is not. Instead, process variants with two inter-critical heat treatment steps and final

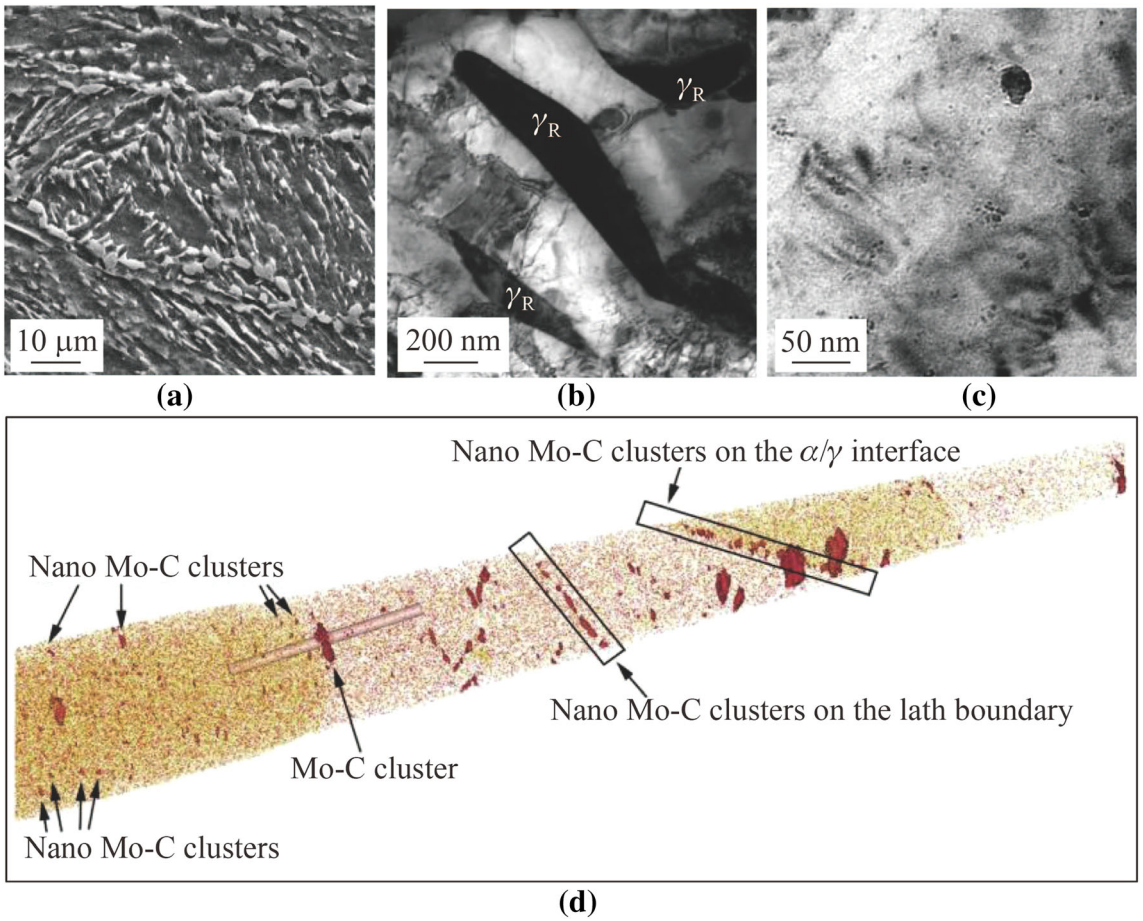

Fig. 23 Microstructural evolution during processing of steel according to the M^3 concept **a** carbon-enriched bainite/martensite islands dispersed in a ferritic matrix, **b** carbon-enriched reversed austenite (γ_R) formed after second inter-critical annealing stage, **c** nano-sized precipitates formed after final tempering cycle, **d** atom probe tomography of final microstructure showing molybdenum segregation at lath and phase boundaries and Mo-C clustering

Table 2 Mechanical properties of C-Si-Mn-Ni-Cu-Mo-Nb steel before and after M^3 heat treatment cycle

Condition	Y_S/MPa	T_S/MPa	A_{50}/%	A_U/%	CVN-40°C/J
As hot rolled	973	1 265	14.4	3.8	35
M^3 heat treated	977	1 037	20.4	9.0	66

tempering have been explored. The resulting microstructure, propagated in China as "M^3 concept", consists of meta-stable austenite in a multi-phase matrix strengthened by multi-scale precipitation (see Fig. 23) [58]. The first inter-critical annealing step forms a dual-phase microstructure consisting of carbon-enriched bainite/martensite islands dispersed in a ferritic matrix (see Fig. 23a), which is grain-size controlled by NbC precipitates. The second inter-critical treatment, executed at lower temperature, further enriches reversed austenite with carbon to become meta-stable at room temperature and induces co-precipitation of Nb, Cu and Mo (see Fig. 23b). The third step applies a sub-critical tempering treatment to this multi-phase microstructure to further enhance precipitation strengthening. Suitable alloy concepts limit carbon to the range of 0.1%–0.15%. Additions of 2%–3%Mn and 0.5%–1.0%Ni help stabilizing reversed austenite. Increased amounts of silicon and aluminum promote carbon partitioning and prevent cementite precipitation. Niobium, vanadium and copper additions provide precipitation on different scales for grain size control and strengthening. Molybdenum alloying in the range of 0.3%–0.4% deploys its versatile effects as discussed already before. A steel in that composition range contains approximately 22% retained austenite in the microstructure after the heat treatment sequence. The evolution of the mechanical properties by the heat treatment is detailed in Table 2 showing high ductility for a steel in the 1 000 MPa class.

5 Conclusions

The use of modern high-performance steels enables significant improvements in design of structures, efficiency of manufacturing, durability of equipment, safety, cost reduction and lifecycle sustainability. The production of such steels requires state-of-the-art steel rolling and heat treatment facilities in combination with suitable alloying concepts. Molybdenum was shown to be one of the most effective and versatile alloying elements by enabling robust processing of such steel grades as well as by providing superior application properties. Particularly the remarkable effect of molybdenum, ideally in synergy with niobium, in improving the resistance against hydrogen-induced cracking in ultra-high strength steels is an issue of intensive ongoing research activities.

References

1. Mohrbacher H (2013) Reverse metallurgical engineering towards sustainable manufacturing of vehicles using Nb and Mo alloyed high performance steels. Adv Manuf 1:28–41
2. Mohrbacher H, Spöttl M, Paegle J (2015) Innovative manufacturing technology enabling light weighting with steel in commercial vehicles. Adv Manuf 3:3–18
3. Isasti N, Jorge-Badiola D, Taheri ML et al (2014) Microstructural features controlling mechanical properties in Nb-Mo microalloyed steels. Part I: yield strength. Metall Mat Trans A 45:4960–4971
4. Isasti N, Jorge-Badiola D, Taheri ML et al (2014) Microstructural features controlling mechanical properties in Nb-Mo microalloyed steels. Part II: impact toughness. Metall Mat Trans A 45:4972–4982
5. Isasti N, Jorge-Badiola D, Taheri ML et al (2013) Phase transformation study in Nb-Mo microalloyed steels using dilatometry and EBSD quantification. Metall Mat Trans A 44:3552–3563
6. Pavlina EJ, Speer JG, van Tyne CJ (2012) Equilibrium solubility products of molybdenum carbide and tungsten carbide in iron. Script Mater 66(5):243–246
7. Hoerner M, Speer J, Eberhart M (2017) Comparison of Ab-initio solute-boundary binding energies and experimental recrystallization data in austenite for solute Nb and other elements. ISIJ Int 57(10):1847–1850
8. Hepburn DJ, MacLeod E, Ackland GJ (2014) Transition metal solute interactions with point defects in austenitic iron from first principles. Phys Rev B 92:014110
9. Li YJ, Ponge D, Choi P et al (2015) Segregation of boron at prior austenite grain boundaries in a quenched martensitic steel studied by atom probe tomography. Script Mater 96:13–16
10. Eckstein HJ, Fennert M, Ohser J (1993) Application of thermodynamic computations to the solution behaviour of niobium and vanadium carbonitrides. Steel Res 64(3):143–147

11. Lee SJ, Matlock D, van Tyne C (2011) An empirical model for carbon diffusion in austenite incorporating alloying element effects. ISIJ Int 51(11):1903–1911
12. Medina SF, Mancilla JE (1996) Influence of alloying elements in solution on static recrystallization kinetics of hot deformed steels. ISIJ Int 36(8):1063–1069
13. Akben MG, Bacroix B, Jonas JJ (1983) Effect of vanadium and molybdenum addition on high temperature recovery, recrystallization and precipitation behavior of niobium-based microalloyed steels. Acta Metall 31(1):161–174
14. Togashi F, Nishizawa T (1976) Effect of alloying elements on the mobility of ferrite/austenite interface. J Jpn Inst Metals 40(1):12–21
15. Tither G, Lavite M (1976) Beneficial stress-strain behavior of moly-columbium steel line pipe. JOM 27:15–23
16. Funakawa Y, Shiozaki T, Tomita K et al (2004) Development of high strength hot-rolled sheet steel consisting of ferrite and nanometer-sized carbides. ISIJ Int 44(11):1945–1951
17. Engberg G, Lissel L (2008) A physically based microstructure model for predicting the microstructural evolution of a C-Mn steel during and after hot deformation. Steel Res Int 79:47–58
18. Yen HW, Chen PY, Huang CY et al (2011) Interphase precipitation of nanometer-sized carbides in a titanium-molybdenum-bearing low-carbon steel. Acta Mater 59:6264–6274
19. Larzabal G, Isasti N, Rodriguez-Ibabe JM (2018) Precipitation strengthening by induction treatment in high strength low carbon microalloyed hot-rolled plates. Metall Mat Trans A 49:946–961
20. Huang BM, Yang JR, Yen HW et al (2014) Secondary hardened bainite. Mater Sci Technol 30(9):1014–1023
21. Belanger P, Hall J, Coryell J et al (2013) Automotive body press-hardened steel trends. In: Proceedings of the international symposium on the new developments of advanced high-strength steel, 23–27 June 2013, Vail, Colorado, USA, pp 239–250
22. Bian J, Mohrbacher H (2013) Novel alloying design for press hardening steels with better crash performance. In: Proceedings of the international symposium on the new developments of advanced high-strength steel, 23–27 June 2013, Vail, Colorado, USA, pp 251–262
23. Olsson R, Haglund N (1991) Cost effective fabrication of submarines and mobile cranes in high performance steels. Int J Join Mater 3:120–128
24. Shang C, Guo F (2018) The state of the art of long-distance gas pipeline in China. Gas Energy 1:24–29
25. Piette M, Dubrulle-Prat E, Perdrix C et al (2001) Effect of 0–0.1%Nb additions on mechanical properties of plates processed by thermomechanically controlled processing and accelerated cooling. Iron Mak Steelmak 28(2):175–179
26. Subramanian SV, Yang Y (2014) On austenite conditioning and recrystallization control of higher grade linepipe steels (X100) with niobium and molybdenum additions. In: Mohrbacher H (ed) Fundamentals and applications of Mo and Nb alloying in high performance steels, vol 1, TMS, pp 3–22
27. Bian J, Mohrbacher H, Zhang JS et al (2015) Application potential of high performance steels for weight reduction and efficiency increase in commercial vehicles. Adv Manuf 3:27–36
28. Kage I, Matsui K, Kawabata F (2005) Minimum maintenance steel plates and their application technologies for bridge—life cycle cost reduction technologies with environmental safeguards for preserving social infrastructure assets. JFE Tech Rep 5:37–44
29. Walp MS, Speer JG, Matlock DK (2004) Fire-resistant steels. Adv Mater Process 162:34–36
30. Mizutani Y, Ishibashi K, Yoshi K et al (2004) 590 MPa class fire-resistant steel for building structural use. Nippon Steel Tech Rep 90:45–52
31. Sugimoto K (2009) Fracture strength and toughness of ultra-high strength TRIP aided steels. Mater Sci Technol 25:1108–1117
32. Nagumo M (2001) Function of hydrogen in embrittlement of high-strength steels. ISIJ Int 41:590–598
33. Degenkolbe J, Mahn J, Muesgen B et al (1987) Experience gained in the accelerated cooling of plate directly after rolling. Thyssen Tech Rep 87(1):41–55
34. Takaki S, Ngo-Huynh KL, Nakada N et al (2012) Strengthening mechanism in ultra low carbon martensitic steel. ISIJ Int 52:710–716
35. Grossman MA (1942) Hardenability calculated from chemical composition. Trans Am Inst Min Metall Petrol Eng 150:227–259
36. Maki T, Tsuzaki K, Tamura I (1980) The morphology of the strengthening of lath martensite in steels. Trans Iron Steel Inst Jpn 20:207–215
37. Hannula J, Kömi J, Porter D et al (2017) Effect of boron on the strength and toughness of direct-quenched low-carbon niobium bearing ultra-high-strength martensitic steel. Metall Mat Trans A 48:5344–5356
38. Mohrbacher H (2018) Property optimization in as-quenched martensitic steel by molybdenum and niobium alloying. Metals 8:234. https://doi.org/10.3390/met8040234
39. Ohnuma M, Suzuki J, Wei FG et al (2008) Direct observation of hydrogen trapped by NbC in steel using small-angle neutron scattering. Script Mater 58:142–145
40. Mohrbacher H (2019) Metallurgical effects of niobium and molybdenum on heat-affected zone toughness in low-carbon steel. Appl Sci 9(9):1847. https://doi.org/10.3390/app9091847
41. Ahlblom B, Hansson P, Narström T (2007) Martensitic structural steels for increased strength and wear resistance. Mater Sci Forum 539(543):4515–4520
42. Ishikawa N, Ueda K, Mitao S et al (2011) High-performance abrasion-resistant steel plates with excellent low-temperature toughness. In: Proceedings of international symposium on the recent developments in plate steels. AIST, Winter Park, pp 81–91
43. Schmit F, Cobo S (2016) New press hardened steels and tailored blank applications. In: Materials in Car Body Engineering 2016, Bad Nauheim, Germany, 9–11 May 2016
44. Avtar R, Jha BK, Saxena A et al (1986) An as hot rolled approach to production of molybdenum and chromium microalloyed dual phase steels. Trans ISIJ 26:822–828
45. Coldren AP, Ellis GT (1980) Using CCT Diagrams to optimize the composition of an as-rolled dual-phase steel. J Metals 32(3):41–48
46. Geib MD, Matlock DK, Krauss G (1980) The effect of intercritical annealing temperature on the structure of niobium microalloyed dual- phase steel. Metall Trans A 11:1683–1689
47. Irie T, Satoh S, Hashiguchi K et al (1981) Metallurgical factors affecting the formability of cold-rolled high strength steel sheets. Trans ISIJ 21(11):793–801
48. Sugimoto K (2009) Fracture strength and toughness of ultra-high strength TRIP aided steels. Mater Sci Technol 25(9):1109–1117
49. Hashimoto S, Ikeda S, Sugimoto K et al (2004) Effects of Nb and Mo addition to 0.2%C-1.5%Si-1.5%Mn steel on mechanical properties of hot rolled TRIP-aided steel sheets. ISIJ Int 44(9):1590–1598
50. Sugimoto K, Murata M, Muramatsu M et al (2007) Formability of C-Si-Mn-Al-Nb-Mo ultra high-strength TRIP-aided sheet steels. ISIJ Int 47(9):1357–1362
51. Kobayashi J, Ina D, Yoshikawa N et al (2012) Effects of the addition of Cr, Mo and Ni on the microstructure and retained austenite characteristics of 0.2%C-Si-Mn-Nb ultrahigh-strength TRIP-aided bainitic ferrite steels. ISIJ Int 52(10):1894–1901
52. Speer JG, Matlock DK, de Cooman BC et al (2003) Carbon partitioning into austenite after martensite transformation. Acta Mater 51:2611–2622
53. Yan S, Liu X, Liang T et al (2019) Effect of micro-alloying elements on microstructure and mechanical properties in C-Mn-

Si quenching and partitioning (Q&P) steels. Steel Res Int 90:1800257. https://doi.org/10.1002/srin.201800257
54. Sun XJ, Li ZD, Yong QL et al (2012) Third generation high strength low alloy steels with improved toughness. Sci China Technol Sci 55(7):1797–1805
55. Yuan S, Shang C, Xie Z et al (2018) Impact of intercritical annealing on retained austenite and toughness of a 460 MPa grade multiphase heavy gauge plate steel. Steel Res Int 89:1800006. https://doi.org/10.1002/srin.201800006
56. Stewart RA, Speer JG, Thomas BG et al (2018) Process design for quenching and partitioning of plate steels. In: Proceedings of the 2nd international symposium on the recent developments in plate steels, Orlando, AIST, pp 469–475
57. Hernaut P, Ertzibengoa D, de Cooman BC et al (2018) Development of high-performance steel plates at NLMK clabecq. In: Proceedings of the 2nd international symposium on the recent developments in plate steels, Orlando, AIST, pp 139–149
58. Xie ZJ, Xiong L, Han G et al (2018) Thermal stability of retained austenite and properties of a multi-phase low alloy steel. Metals 8(10):807. https://doi.org/10.3390/met8100807

Pello Uranga is the Associate Director of the Materials and Manufacturing Division at CEIT and associate professor at Tecnun (University of Navarra). He got his PhD degree in Materials Engineering in 2002 from the University of Navarra. Currently, his research activity is mainly focused on the thermomechanical processing and the microstructural evolution modeling of steels. He has published over 100 technical papers in international journals and conferences, receiving five international awards. He is an active member of the AIST (Association of Iron and Steel Technology) and TMS (The Mineral, Metals and Materials Society) professional associations, as well as university program evaluator for ANECA (Spain) and ABET (USA).

Cheng-Jia Shang is the chief scientist and professor of the Collaborative Innovation Center of Steel Technology, University of Science and Technology Beijing. He was elected as Professional Fellow of the Institute of Materials, Minerals & Mining (FIMMM), UK, in 2017. His interest is in high-performance steels for marine engineering, oil and gas drilling, storage and transportation, bridge and other infrastructural applications. He is currently Executive Director of Council Member and Secretary-General of the Materials Science Branch of the Chinese Society for Metals, Deputy Director of the Foreign Affairs Committee of the Chinese Society for Metals, Deputy President of Corrosion and Degeneration Division, Society of Automotive Engineers of China Director of the Chinese Materials Research Society.

Takehide Senuma is a specially appointed professor of Okayama University in Japan. His major research field is the steel research. He graduated in 1975 with a degree in Mechanical Engineering from the Technical University of Aachen and received a Dr-Ing. degree from the same university. He worked for Nippon Steel as a researcher from 1981 to 1997 and as a general manager from 1998 to 2005. From 2005 to 2015, he was a professor at Okayama University.

Jer-Ren Yang received Ph.D. degree (Materials Science and Metallurgy) from University of Cambridge, England, UK in 1987. In February 1988, he joined the faculty of Department of Materials Science and Engineering, Taiwan University, where he has been a full Professor since August 1993. During the period of August 2007–July 2010, he was the head of the Department. Professor Yang's research interests include phase transformation of steels, crystal geometry and crystal defects. Professor Yang has published some 210 international SCI journal papers in the areas of materials science and engineering.

Ai-Min Guo is Chairman of CITIC Dameng Mining Industries Ltd and Vice General Manager/Chief Engineer of CITIC Metal Co., Ltd. He is a Phd in Metal Physical Engineering, Professor-Level Senior Engineer, specialist enjoying the Special Allowance of the State Council, National Candidate of New Century Talents Project, assessor of National Scientific and Technological Progress Award. Dr. Guo has been engaged in product development, production technology and application technology research for boiler and pressure vessels, bridges and buildings, ships, offshore platforms as well as other medium-thick and extra-thick steel plates for a long time. He focuses on researching advanced high-strength steel ductility mechanism, advanced medium and high-carbon steel micro-alloying technology, refinement, strengthening and toughening of structural steel materials and related welding technology. He also has a rich experience in steel structure engineering.

Hardy Mohrbacher specializes in materials and mechanical engineering including steel alloy design and processing, sheet metal forming and welding, automotive body design, non-destructive testing and materials characterization, plus the tribology of hard materials. He has written and co-authored over 200 scientific publication in the respective areas. He has held senior positions within, among others, Fraunhofer Institute for Nondestructive Testing (IZFP), Sidmar (ArcelorMittal Ghent) and ThyssenKrupp (TKTB). He is an Associate Professor at KU Leuven in Belgium and an Adjunct Professor at Shanghai University. Since 2007 he is owner and managing director of NiobelCon bvba, a consulting company focusing on steel alloy design, metallurgical processing and steel applications.

Adv. Manuf.
https://doi.org/10.1007/s40436-019-00282-1

Molybdenum alloying in cast iron and steel

Xiang-Ru Chen[1] · Qi-Jie Zhai[1] · Han Dong[1] · Bao-Hua Dai[2] · Hardy Mohrbacher[3,4]

Received: 29 June 2019 / Revised: 28 August 2019 / Accepted: 25 October 2019

Abstract Metal casting is an important manufacturing technology for efficiently producing massive components with complex shape. A large share of industrial castings is made from iron and steel alloys, combining attractive properties and low production cost. Upgrading of properties in cast iron and steel is mainly achieved by alloying and in fewer cases by heat treatment. Molybdenum is an important alloying element in that respect, increasing strength, hardness and toughness. It also facilitates particular heat treatments such as austempering. The paper describes the metallurgical functionality of molybdenum alloying in iron-based castings and demonstrates its effectiveness for applications in the automotive and mining industry.

Keywords Grey cast iron · Nodular iron · Pearlite · Austempering · Creep resistance · Wear resistant alloys · Hardness · Toughness · Mining industry · Automotive industry

✉ Xiang-Ru Chen
cxr16@shu.edu.cn

✉ Hardy Mohrbacher
hm@niobelcon.net

[1] School of Materials Science and Engineering, Shanghai University, Shanghai 200444, P.R. China

[2] CITIC Machinery Manufacturing Inc., Houma 043011, Shanxi, P.R. China

[3] Department of Materials Engineering, KU Leuven, 3001 Leuven, Belgium

[4] NiobelCon bvba, 2970 Schilde, Belgium

1 Introduction

Casting technology is very attractive for producing industrial components as well as everyday-life household items. Since castings are manufactured to near-net shape, intensive machining is not required resulting in cost-efficient production of complex-shaped items. The casting process requires specific alloy compositions allowing good form filling, a low defect level as well as achieving the desired target properties after solidification and down-cooling [1].

Cast iron is a material with long history and tradition. According to the binary iron-carbon diagram, cast irons are alloys having more than 2.0% carbon, thus solidifying in the eutectic range with low melting point. Cast irons usually solidify following the stable iron-carbon diagram, thus forming graphite during solidification. In technical alloys the addition of carbon and silicon is combined to a so-called carbon equivalent (CE = %C + 1/3%Si), which determines the range of cast irons according to Fig. 1 [2]. A CE of 4.3 represents a eutectic alloy while those with a lower CE and those with a higher CE are called hypo-eutectic and hyper-eutectic, respectively.

The family of cast irons comprises six classes of materials according to the characteristics of graphite and matrix microstructure: Grey irons with lamellar graphite—GJL (DIN EN 1561), ductile or nodular irons with spheroidal graphite—GJS (DIN EN 1563), vermicular irons with compacted graphite—GJV (ISO 16112), white cast irons—GJN (DIN EN 126113), malleable irons—GJMB/GJMW (DIN EN 1562), austenitic irons—GJLA-X/GJSA-X (DIN EN 13835).

Considering a global production volume of over 70 million metric tons per year, grey irons (64%) and ductile irons (35%), have the largest market share by far [3]. Molybdenum alloying is applied in both classes of iron,

Published online: 10 December 2019

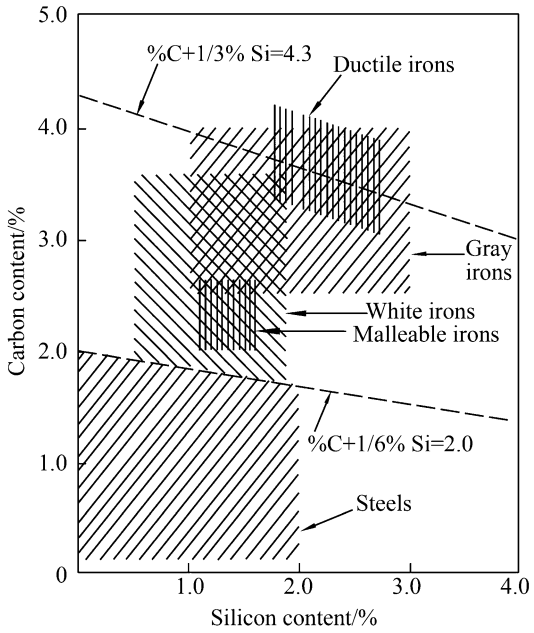

Fig. 1 Definition of cast iron alloys according to carbon and silicon contents [2]

typically for products with increased property demands. In particular cases, cast irons can be subjected to heat treatment after solidification for property improvement. The initial ferritic-pearlitic microstructure of the matrix is modified by so-called austempering to become bainitic with a high fraction of metastable retained austenite [4]. These irons are known as austempered ductile irons—ADI (DIN EN 1564) and austempered grey irons—AGI.

Cast steels are alloys where the combined addition of carbon and silicon (%C + 1/6%Si) is lower than 2% (see Fig. 1). Steel castings account for only about 1% of the global annual steel production. They are manufactured over a large variety of alloy compositions used in a multitude of applications. Thus, a high degree of specialization is involved with steel foundries. It can be stated that steel castings are preferred where manufacturing of a component starting from a wrought or rolled steel semi-product is too costly or too difficult. The different steel casting alloys can be distinguished according to the following application areas [5]: general applications (unalloyed C-Mn-Si steel), improved weldability and toughness for general purposes, high pressure purposes for use at low temperatures, high pressure purposes for use at room temperature and elevated temperatures, heat resistant steel castings, corrosion resistant steel castings, wear resistant steel castings.

Approximately half of the global annual castings output is produced by Chinese foundries [3]. The increasing demand for high-performance castings is driven by key industries such as the automotive, mechanical engineering and mineral processing sectors. The optimization of casting alloys typically involves a combination of properties to be considered. Applications in the automotive powertrain are demanding an improved combination of strength, heat conductivity and thermal fatigue resistance. In mineral processing optimized wear resistance is targeted, which is related to a suitable combination of hardness and toughness. The paper addresses the particular role of molybdenum alloying in this respect and highlights current alloy developments in China.

2 Effects of molybdenum alloying in cast iron

Molybdenum is known to act as carbide stabilizer in cast iron. At low addition level it has little effect on castability and chilling tendency. Free carbides are only formed at higher molybdenum addition. The amount and shape of graphite are not measurably affected by molybdenum additions below 0.5% [4, 5]. The main effect provoked by molybdenum alloying to cast iron is observed during solid state transformations. With increasing molybdenum alloy content, the pearlite phase field in the continuous cooling transformation (CCT) diagram is shifted towards longer times. Molybdenum addition up to around 0.5% acts a very powerful pearlite stabilizer and increases strength by refining pearlite [6, 7]. Higher molybdenum additions, preferably in conjunction with nickel or copper, promote the transformation from austenite into acicular ferrite. Such irons usually contain at least 0.8%Mo and more than 1.2%Ni [8]. The actual amount of alloy required depends upon the section thickness. The tensile strength of acicular irons is in the range of 400–500 MPa. They are more easily machinable at high levels of hardness (250–320 HB) than unalloyed irons due to the absence of free cementite.

Amongst the typical alloying elements, it is found that Mn and Ni coarsen the interlamellar spacing of pearlite, whereas an increasing content of Cr produces finer pearlite spacing. Si has only a slight influence on pearlite spacing. Molybdenum clearly has the strongest effect in decreasing the interlamellar spacing. The individual effect of these alloying elements on the pearlite interlamellar spacing, S_0, can be described as [9]

$$\log S_0 = -2.212 + 0.0514[\mathrm{Mn}] - 0.0396[\mathrm{Cr}] + 0.0967[\mathrm{Ni}] - 0.002[\mathrm{Si}] - 0.4812[\mathrm{Mo}] - \log(\Delta T/T_\mathrm{e}), \quad (1)$$

where S_0 is measured in μm; [Mn], [Cr], [Ni], [Si], [Mo] are the different alloy contents (mass fraction,%); and ΔT is the undercooling from the eutectoid temperature T_e. In pearlitic microstructures, the interfaces between ferrite and cementite act as barriers to dislocation movement [10]. The critical stress necessary to shift dislocations in ferrite lamellae is related to the macroscopic yield stress. That

critical stress rises with the refinement of the pearlitic microstructure, since a decrease of pearlite interlamellar spacing leads to an increase in the resistance to glide according to a Hall-Petch type relationship. Furthermore, finer pearlite microstructures comprising smaller colony size and shorter interlamellar spacing, show a more ductile fracture character. This one is represented by a larger number of dimples as well as a smaller share of ferrite/cementite lamellae in the fracture process zone [11].

2.1 Grey cast irons

Grey cast iron has limited strength and almost no ductility. Nevertheless, pearlitic grey cast iron is the preferred material for applications such as engine blocks, cylinder heads, flywheels or brake discs. This is reasoned by the low cost, good castability and favorable thermal conductivity of grey cast iron. Demands for higher thermal efficiency and weight reduction enabled by reducing component cross-sections require the development of high-performance grey cast iron with an improved combination of tensile strength and heat conductivity. However, those features promoting heat conductivity are typically detrimental to strength. The challenge is to find a suitable balance of microstructural design and hence alloy concept. The thermal conductivity of grey cast iron at ambient temperature ranges between 45 W/(m·K) and 55 W/(m·K), whereas it is clearly lower for vermicular graphite iron (32–42 W/(m·K)) and nodular iron (25–35 W/(m·K)). However, when the temperature increases towards 500 °C, the heat conductivity of grey cast iron declines while it remains nearly stable for vermicular and nodular iron [12]. Considering the matrix, ferrite has better heat conductivity than pearlite, yet the latter has higher strength. The heat conductivity of ferrite decreases with increasing alloy content. A higher volume share of graphite increases heat conductivity on expense of strength. A recent study indicated that the thermal conductivity was nearly independent of graphite flake length and aspect ratio above a threshold length of approximately 100 µm [13]. From an alloying point of view, it appears favorable reducing the level of solute elements for improving thermal conductivity. In this respect, silicon is the most critical element. The use of a carbide stabilizer with good solubility and rather large atomic size is considered to be favorable [14]. Molybdenum exactly fulfils these conditions. Based on various published results it can be estimated that 0.1% addition of Mo increases the tensile strength by approximately 10 MPa. In synergy with other alloying elements such as for instance chromium, vanadium or niobium, the strengthening effect can be even larger. At elevated operating temperature, Mo-alloyed grey cast iron better retains strength and has clearly improved creep resistance [6, 15].

Table 1 compares thermal conductivity and strength of various iron alloys [13, 16]. The grey iron alloys (GJL) have higher thermal conductivity and lower strength than vermicular graphite iron grades (GJV). However, an optimized near-eutectic grey iron grade (GJL-300 Mo HC) with reduced silicon content and 0.25%Mo addition combines a tensile strength of over 300 MPa with high heat conductivity. Raising the molybdenum content towards the earlier stated limit of 0.5% could further increase the strength [17].

Current grey iron grades according to typical automotive standards are represented in Fig. 2 showing that molybdenum alloying indeed provides superior strength in both hypo- and hyper-eutectic alloys. Niobium is a rather unconventional alloying element providing additional strength to grey cast iron. Unlike molybdenum, niobium affects the solidification structure and graphite morphology. Niobium additions up to around 0.3% were shown to refine the eutectic cell size as well as the pearlite interlamellar spacing (see Fig. 3) [18, 19]. This alloy concept is being used for the production of vehicle brake discs [18, 20]. Systematic alloy variations in laboratory trials have indicated that the tensile strength of grey cast iron can be most efficiently increased by simultaneously refining the eutectic cell size and the pearlite interlamellar spacing (see Fig. 4) [21]. In that respect, the combined alloying of molybdenum and niobium has a particularly high strengthening potential. In this combination, molybdenum is providing additional refinement of pearlite interlamellar spacing and promotes precipitation strengthening by niobium.

2.2 Nodular irons

Nodular iron, in contrast to grey iron, contains graphite in form of isolated spheroids within a matrix consisting of ferrite or pearlite. This results in higher strength, good elongation and increased toughness as compared to iron containing lamellar graphite. Nodular irons are particularly interesting for manufacturing complex-shaped components used for engine or machine parts subjected to high acceleration or impact loads as well as for pressure pipes and vessels. Like in grey cast irons, molybdenum is added to nodular iron for further enhancing strength and also here additions up to 0.5% do not harm the graphite morphology or nodule count. Molybdenum added to nodular irons particularly enhances tensile, creep, and stress-rupture strengths at elevated temperature [6, 7, 15]. This has led to the development of SiMo irons containing 4%–5% silicon and 0.5%–1.0% molybdenum which can be used for component temperatures up to 820 °C. Such alloys are typically used for turbocharger housings of diesel engines. Silicon and molybdenum are complementary alloying elements with silicon providing oxidation resistance and raising the ferrite-to-austenite transformation temperature

Table 1 Heat conductivity and tensile strength in grey iron (GJL) and vermicular graphite iron (GJV)

Grade	Alloy composition (mass fraction, %)	Heat conductivity/(W·(m·K)$^{-1}$) (@ 100 °C/400 °C)	Tensile strength/MPa (@ 20 °C)
GJL-250 CrCu	3.35 C, 1.8 Si, 0.5 Mn, 0.3 Cr, 0.5 Cu	42/38	260
GJL-300 Mo HC	3.6 C, 1.3 Si, 0.3 Mn, 0.25 Mo	50/43	310
GJV-350	3.5 C, 2.5 Si, 0.25 Mn	42/39	350
GJV-450	3.6 C, 2.2 Si, 0.4 Mn, 0.8 Cu, 0.06 Sn	38/36	450

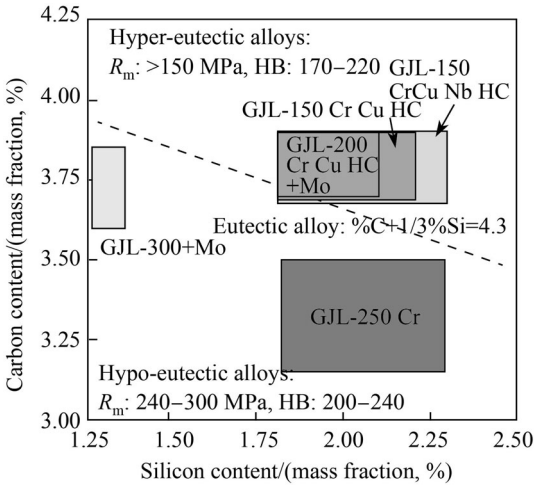

Fig. 2 Hypo- and hyper-eutectic alloy concepts of grey cast iron grades and specified mechanical properties according to European automotive standards

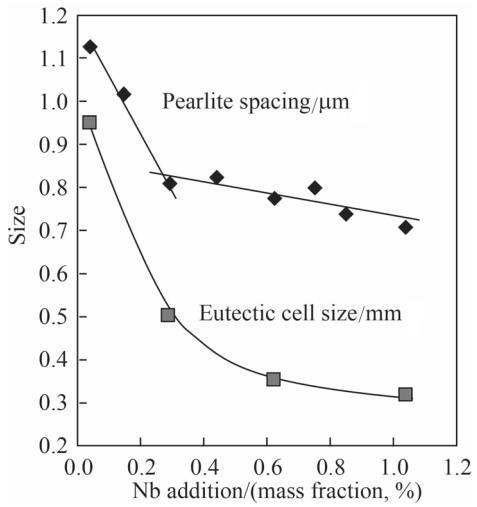

Fig. 3 Effect of niobium addition on microstructural refinement in grey cast iron [18]

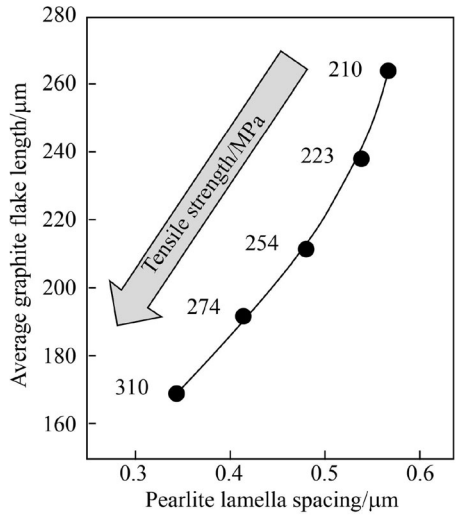

Fig. 4 Effect of microstructural refinement on tensile strength in grey cast iron based on laboratory results provided by Shanghai University [21]

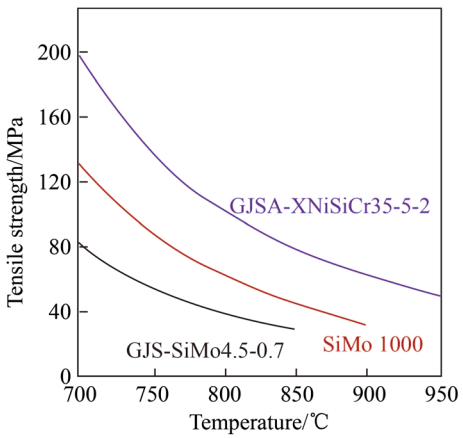

Fig. 5 Tensile strength at high temperature for SiMo iron alloys and austenitic cast iron Ni-resist D5S [22]

(A_1) while molybdenum increases the elevated temperature strength and creep resistance. Constrained thermal cycling tests of ferritic SiMo nodular iron demonstrated a strong beneficial effect of molybdenum [15]. A more recent variant of SiMo iron (SiMo1000) is alloyed with around 1% molybdenum and a high aluminum addition of around 3% while silicon is reduced to 2.5% [22]. This alloy allows raising the operating temperature limit further to 860 °C

(see Fig. 5). For even higher operating temperatures up to around 950 °C, austenitic cast irons such as GJSA-XNiSiCr35-5-2 also known as Ni-Resist D5S can be used [23]. It should be noted that molybdenum additions to such austenitic irons have similar effects as in ferritic SiMo alloys.

2.3 Austempered irons

Austempering designates a heat treatment in which the as-cast iron matrix is reheated into austenite upon which the iron is cooled in austenitic state to an isothermal holding temperature of around 300 °C [24]. The formation of pearlite during cooling must be avoided [25]. During austempering, an increasing fraction of bainite forms and carbon partitions to the remaining austenite phase. The highly carbon enriched austenite fraction remains metastable down to temperatures of −80 °C. The final microstructure of austempered ductile iron (ADI) consists of bainite and retained austenite (also called ausferrite) as well as spherical graphite resulting in very attractive properties. Figure 6 schematically indicates the evolution of mechanical properties by modifying graphite morphology and austempering of the matrix representing the transition from grey cast iron to ADI [26, 27]. ADI achieves similar strength as heat-treated steel at 10% lower material density, and has high noise damping capacity and self-lubricating properties in dry contacts. Toughness and elongation are better in ADI as compared to other cast iron materials at comparable strength. Accordingly, ADI is one of the most attractive construction materials for realizing weight reduction (see Fig. 7) [25]. The most significant use of ADI is found in vehicle and railway applications (see Fig. 8) [25, 26, 28, 29]. Some typical examples of truck and trailer components manufactured from ADI are shown in Fig. 9.

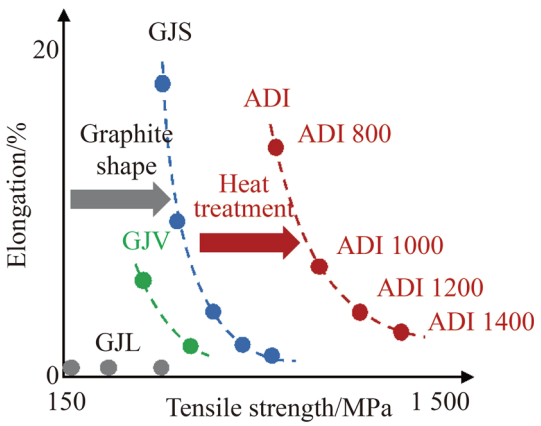

Fig. 6 Tensile characteristics of ADI in comparison to GJL, GJV and nodular iron (GJS) [26]

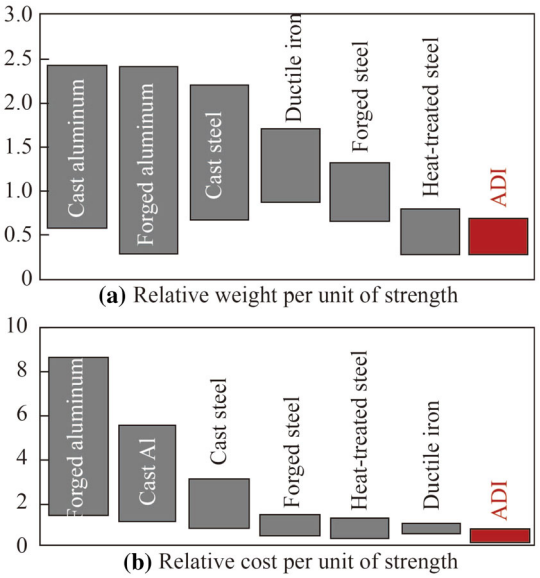

Fig. 7 Comparison of light weighting potential and cost for materials used for manufacturing of massive components [25, 26]

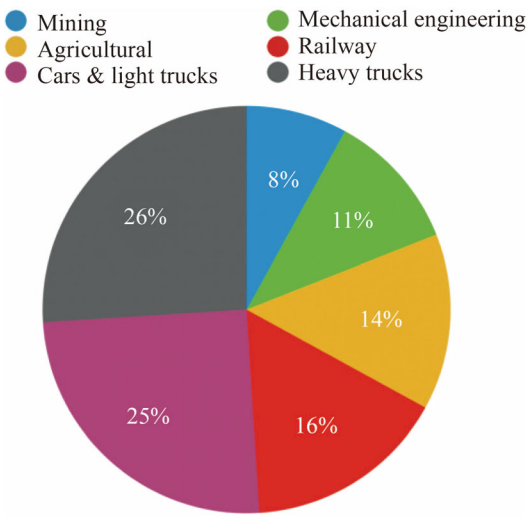

Fig. 8 Market share of major applications for ADI castings [29]

Molybdenum alloying is used to avoid pearlitic transformation during cooling to the austempering temperature avoiding the necessity for major capital investment in quenching facilities [30], especially when casting components with larger section size (see Fig. 10). Manganese is also an effective hardenability agent yet must be kept low (max. 0.3%) to develop maximum elongation and toughness in ADI. Larger additions of nickel or copper could supply the required hardenability, but combined nickel-molybdenum or copper-molybdenum alloying is more effective because of the synergetic effects of these elements on hardenability [31]. The inherently high silicon

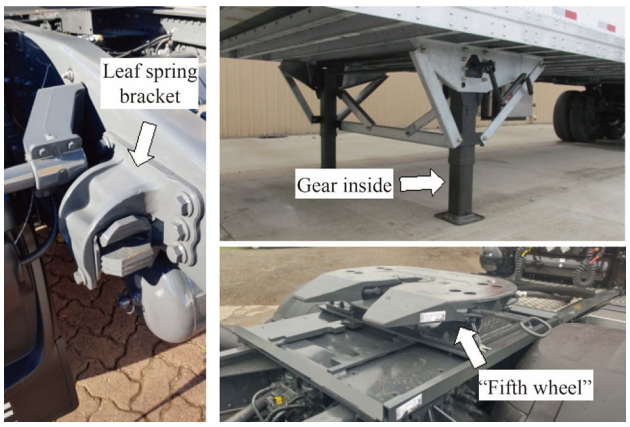

Fig. 9 Exemplary use of ADI components in trucks and semi-trailers

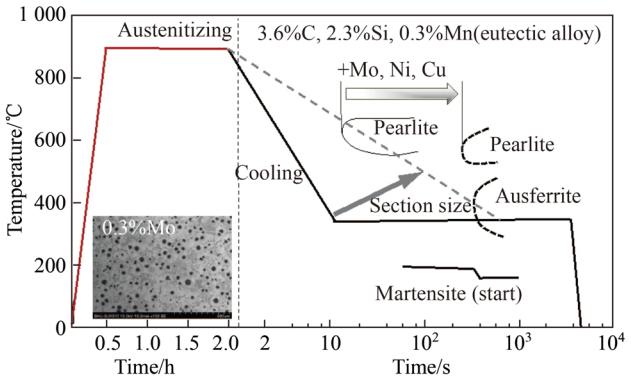

Fig. 10 Heat treatment cycle for austempering and effect of alloying elements on the matrix phase formation [25]

content inhibits carbide precipitation during austempering and thus helps stabilizing austenite.

Recent development activities at Shanghai University are focusing on further improving wear resistance of ADI. The approach intends reinforcing the ADI matrix with hard carbide particles. For this purpose, a Mo-alloyed base composition is co-alloyed with different levels of niobium. Niobium forms carbide particles, which precipitate already in the liquid phase when the concentration is larger than 0.2%. The combination of Mo and solute Nb produces a fine-grained ausferrite resulting in improved toughness. Niobium additions above 0.6%, however, deteriorate the graphite nodularity and reduce the nodule count [32]. The abrasion resistance was the highest for niobium addition in the range of 0.2%–0.6%. The microstructural features for achieving performance optimization are the share of ausferrite in the matrix and the presence of dispersed carbide particles (see Fig. 11). The carbide particles embedded in the matrix act as a barrier to the detrimental action of abrasive particles (see Fig. 12).

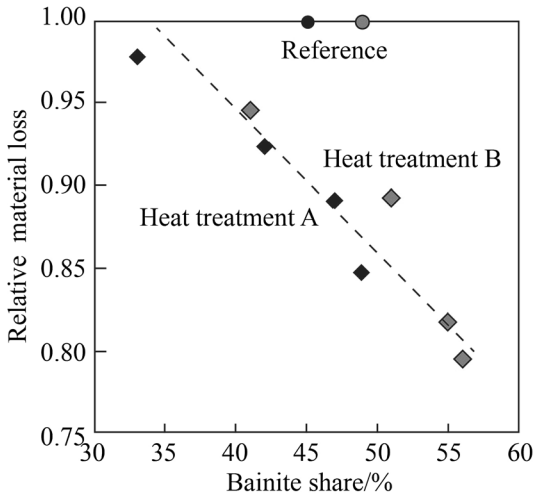

Fig. 11 Relative material loss of niobium alloyed material as a function of bainite share (the dashed line represents a linear fit of all samples with Nb addition (diamond symbol)) [32]

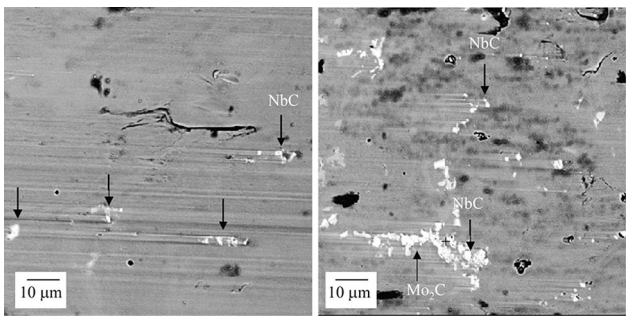

Fig. 12 Scanning electron micrographs of wear tracks in 0.55% Nb alloyed ADI indicating **a** the obstruction of ploughing by dispersed NbC particles and **b** large-sized eutectic carbides formed by molybdenum segregation in the intercellular region [32]

2.4 White cast iron

Wear-resistant alloyed irons also known as "white cast irons" have found widespread application in the mining industry for the manufacturing of crushers, mill liners, and slurry pumps as well as for sleeves of work rolls. Simple white cast irons are extremely brittle and nearly impossible to machine. Adding chrome in the range of 12%–28%, together with nickel and molybdenum, allows producing abrasion-resistant alloys that are tough and can be cast in large sizes to match the needs of the mining industry [33]. Eutectic carbides in the composition of M_7C_3 in combination with an austenitic, martensitic, or pearlitic matrix gives a full range of material design possibilities. Some of the components are cast with pearlitic matrix to allow machining and are subsequently heat treated to obtain an abrasion-resistant martensitic structure. The principal

effect of molybdenum as an alloy addition to white cast iron is increasing the hardenability or austenite stability of these alloys. Not necessarily all of the molybdenum added is effective for hardenability since it was found to also participate in alloy carbides formed in these materials. Molybdenum can form carbides by itself as Mo_2C if present in concentrations over 2%. At lower concentrations it is soluble in M_7C_3 and MC carbides. Mo_2C carbides have a hardness of 1 500–1 800 HB. Molybdenum is primarily used to stabilize the austenite during cooling after solidification and to prevent the formation of pearlite, similar as in the processing of ADI. Molybdenum has little effect on the martensite start (M_s) temperature, compared with other elements that tend to decrease the M_s temperature and over-stabilize the austenite phase [34]. Molybdenum additions less than about 1.0% have been found insufficient to suppress the formation of pearlite in heavy section castings, while amounts greater than 3.0% have no additional benefit in that respect. Molybdenum, if alloyed in conjunction with nickel, copper and manganese enhances the ability of suppressing pearlite. Combined alloying of molybdenum and niobium shows synergetic effects in delaying pearlite formation (see Fig. 13) and in increasing wear resistance [35].

White cast irons are the work horses of wear protection in the mining and cement industry, as well as in road construction where abrasion by mineral particles prevails. There are two main types of white irons. Ni-hard comes in 4 types covering hardness range from 200 HB to 600 HB, depending on the Mo addition ranging from 0 to 1%. The component thicknesses with such alloys is limited to up to 200 mm. Casting of thicker-walled components, however, is possible with high-chrome-molybdenum alloys. In chrome-molybdenum white irons a primary $(Cr,Fe)_7C_3$ carbide is being developed with a hardness of nearly twice that of quartz [27]. The $(Cr,Fe)_7C_3$ carbides in chrome-molybdenum white irons are embedded in an austenite/martensite matrix providing the higher toughness [36]. A prominent example is the proprietary alloy Climax 15-3 containing 20%–27%Cr and 0.5%–3.0%Mo [37]. This alloy is noticeably tougher and harder than Ni-hard iron grades. The linear abrasion rate of slurry pump impeller manufactured from Climax 15-3 exposed to a mixture of silica sand and water is multiple times lower than for a standard GG-25 grey iron alloy and still clearly superior to Ni-hard 4 (see Fig. 14) [38].

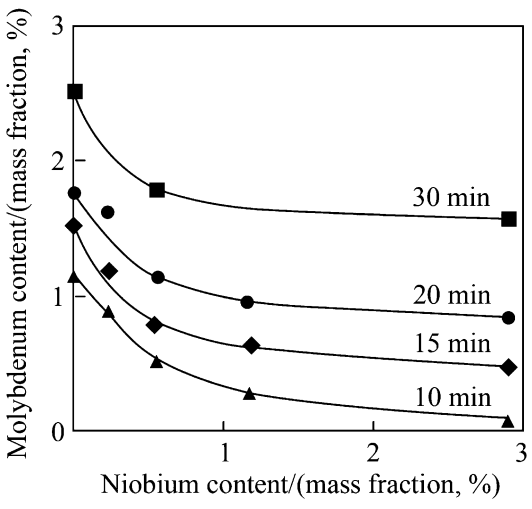

Fig. 13 Influence of Mo and Nb contents on the time for 5% pearlite transformation at 700 °C in 2.94%C-16.7%Cr-0.83%Mo-0.72%Cu white cast iron [35]

3 Cast steel alloys

The base composition of steel castings consists of carbon, manganese and silicon. Depending on the area of application, additional alloying elements such as Cr, Mo and Ni are required [39]. In contrast to rolled steel grades, cast steels cannot be thermo-mechanically processed and must fully rely on heat treatments for developing a suitable microstructure providing high-performance properties. Molybdenum is used at levels up to 0.4% to give additional solid solution strengthening and to particularly increase hardenability when heat treating heavy sections. Nickel is added for solid solution strengthening and when good low-temperature toughness is required. Chromium further increases hardenability. Microalloying elements such as Nb and V are typically added to control grain size and to provide precipitation strengthening [40]. The heat treatment of HSLA cast steels is often carried out in three stages being homogenization, austenitizing prior to normalizing or quenching and, finally, tempering or ageing. The homogenization treatment, usually done between 1 000 °C and 1 100 °C for holding times of up to 6 h, reduces segregation of alloying elements after initial solidification especially in heavy sections. Accelerated cooling from the

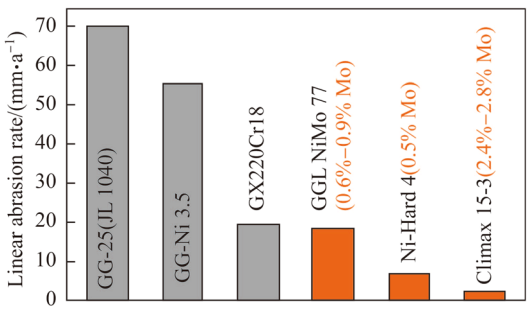

Fig. 14 Abrasion rates of various cast materials exposed to hydro-abrasive wear in a silica-based slurry [38]

Table 2 Materials used in the different stages of mineral ore processing [43]

Processing stage	Equipment	Component	Alloy type	Microstructure
Primary crushing	Primary crusher	Concaves and mantles	High-Mn steel	Austenitic
			Martensitic Cr-Mo steel (concaves)	Martensitic
Secondary and tertiary crushing	Cone crusher	Concaves and mantles	High-Mn steel	Austenitic
Grinding	SAG mill	Liners	Cr-Mo steel	Pearlitic
		Balls	Low alloy Cr steel	Martensitic
	Ball grinding mill	Liners	High Cr white iron	Martensitic
			Cr-Mo steel	Pearlitic
		Balls	Low alloy Cr steel	Martensitic

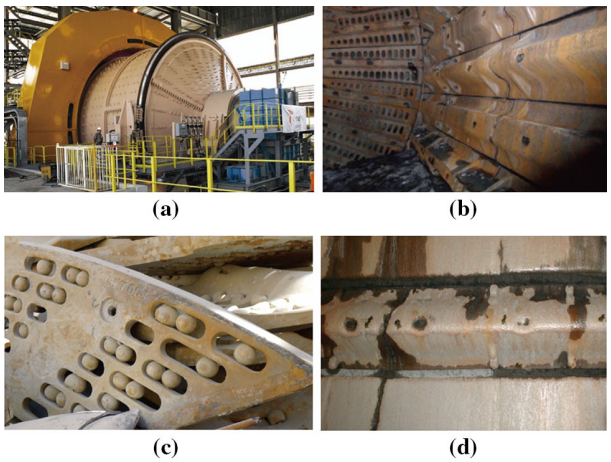

Fig. 15 **a** SAG mill with diameter of 12 m, **b** inside the SAG mill showing liners and exit grate, **c** clogging of exit grate by grinding balls, **d** wear appearance on liner

homogenization temperature promotes the refinement of the ferrite grain in the final microstructure. The tempering treatment optimizes toughness and allows precipitation of solute microalloying elements [40].

The market need for wear resistance castings in China amounts to approximately 5 million tons per year [41]. Major consuming sectors are the mining, cement and thermal power industries. Table 2 shows the typically used alloy types and material microstructures applied for various components in mineral ore processing stages. The equipment being most relevant to this consumption of casting components are ball mills (see Fig. 15). Approximately 55% of the material is used for breaker balls and 11% for liners. Any improvement in the performance, i.e., enhanced durability of these components results in a high economic benefit. In a large-size dressing plant processing 100 000 t of ore per day, the typical service life of liners is experienced to be less than 6 months. Thus, significant additional costs are due to maintenance and replacement of components in autogenous (AG) or semi-autogenous (SAG) grinding mills. As an example, a large ball mill processing 50 million tons of ore per year has a down-time cost of about 300 000 USD per hour [42, 43]. The typical average downtime for a maintenance term is about 20 h. For a SAG mill plant processing 50 million tons of ore annually, the benefit of a 10% extension of grinding ball lifespan causes only a 2.0% increase in alloy cost but saves over 1.5 million USD per year in reduced maintenance. The consumption of SAG mill liners is less than that of grinding balls; nevertheless, the estimated indirect benefit from a liner lifespan increase of 10%, is in the order of 1.7 million USD per year for an average SAG mill [43].

Ball grinding mill components can be manufactured by casting or by forging using rather similar steel alloys as shown in Table 3. In general, forged balls have a tempered martensite microstructure with retained austenite present throughout the entire section thickness. Cast grinding balls have a similar microstructure, yet with all of the characteristics of a cast section; chemical segregation and presence of discontinuities (pores, shrink holes, etc.). Thus, cast grinding ball have inferior mechanical properties making them unsuitable for use in SAG mills where failure by fracturing would occur due to high impact stresses. Ball consumption is mainly due to wear in ball grinding mills and also due to fracturing in SAG mills (approximately 10%) [44]. In large-size SAG mills (typically 38 – 40 feet diameter), ball fracturing can account for a higher percentage of consumption due to increased impact energies. In these cases, the ball quality becomes more important. Balls that are deformed can clog the exit grates of the SAG mill (see Fig. 15c), leading to unplanned maintenance. The chemical composition of the Cr-Mo steel used in liners does not adhere to any particular standard. However, the large majority of the suppliers manufacture their products in a composition range as shown in Table 4. It should be noted that there has been virtually no change in these types of alloys over the recent decades. Liners are subject to high impact loads produced mainly by grinding balls of up to 6 inches in diameter. Hence, steel used for liners must be sufficiently tough to avoid fracture under normal operating

Table 3 Alloys used for liners and grinding balls in a semi-autogenous ball mill [43]

	C/(mass fraction, %)	Mn/(mass fraction, %)	Cr/(mass fraction, %)	Si/(mass fraction, %)	Mo/(mass fraction, %)
Liners	0.50–0.75	0.75–1.00	2.00–2.50	0.40–0.60	0.30–0.45
Forged balls	0.55–0.90	0.70–1.25	0.37–1.20	0.18–0.70	0.00–0.20
Cast balls	0.75–0.95	0.40–1.10	0.20–1.10	0.30–0.60	Residual

Table 4 Alloy compositions and heat treatment conditions for laboratory optimization of liner steel [42]

Steel	C/(mass fraction, %)	Mn/(mass fraction, %)	Si/(mass fraction, %)	S/(mass fraction, %)	P/(mass fraction, %)	Cr/(mass fraction, %)	Mo/(mass fraction, %)	Nb/(mass fraction, %)	Heat treatment
1	0.84	0.81	0.42	0.038	0.027	2.04	0.26	–	880 °C/8 h
2	0.84	0.80	0.36	0.028	0.030	2.18	0.30	0.028	550 °C/20 h
3	0.86	0.77	0.38	0.032	0.029	2.17	0.29	–	920 °C/8 h
4	0.85	0.66	0.43	0.024	0.028	2.24	0.30	0.025	550 °C/20 h

conditions. Additionally, abrasive wear occurring inside the mill is significant; therefore, wear resistance is definitely a required property for these alloys. Accordingly, it is important finding a good balance between toughness and hardness balance in these castings, which can be achieved by refining the pearlitic microstructure.

Recent research activities at Shanghai University have been focusing on the improvement of liner castings by varying alloy compositions and heat treatment procedures of pearlitic steel (see Table 4) [42]. Niobium was micro-alloyed for providing additional microstructural refinement. The alloys were austenitized at two different temperature levels (880 °C and 920 °C) followed by air cooling to room temperature and subsequently tempered at 550 °C. The niobium added variants showed indeed a finer microstructure. This refinement of reduced lamellar spacing in the pearlite phase as well as an increased share of troostite and sorbite phases showed indeed better mechanical properties. It is also expected that niobium precipitates as ultra-fine NbC particles during the tempering treatment. As a result, the hardness increases from around 300 HB in steel 1 and 3–350 HB in the niobium added alloys (steels 2 and 4 in Table 4). Impact toughness is at around 50 J for all alloys whereas ductility (elongation, reduction of area) is improved in the niobium added materials. The hardness gain of around 16% is expected to improve the wear resistance in the same order of magnitude, which will result in a severe operating cost reduction for SAG mills, as was detailed before.

In another approach, a different alloy with lower carbon content and additional alloy content was designed as 0.4%C-0.7%Si-1.15%Mn-1.7%Cr-0.4%Mo-0.3%Ni-0.07%V-0.02%Nb [45]. Heat treatments of this alloy were performed as detailed in Table 5. These treatments result in microstructures consisting of either a bainitic or a martensitic matrix containing retained austenite. The amount of martensite is controlled by the cooling-stop temperature after re-austenitizing at 880–900 °C. The lowest cooling temperature produces the largest share of martensite resulting in the highest hardness, yet also in the lowest toughness (see Table 5). The differently treated steels were benchmarked in a grain-abrasion testing

Table 5 Mechanical properties and wear resistance (material loss) of 0.4%C-0.7%Si-1.15%Mn-1.7%Cr-0.4%Mo-0.3%Ni-0.07%V-0.02%Nb after different austempering treatments [45]

Heat treatment (austempering)	Toughness/(J·cm^{-2})	Hardness/HRC	Impact condition and material loss/g			
			10 000 × 1.5 J	20 000 × 1.5 J	30 000 × 1.5 J	10 000 × 2 J
880 °C/oil → 500 °C/air	71.5	45.3	0.093 8	0.232 1	0.355 4	0.121 4
880 °C/oil → 250 °C/furnace	46.5	52.3	0.083 3	0.180 3	0.238 9	0.085 6
900 °C/oil → 200 °C/furnace	35.3	53.6	0.083 6	0.210 3	0.246 4	0.095 0
880 °C/oil → 325 °C/air	62.9	50.6	0.083 2	0.206 4	0.231 9	0.090 5

machine (type MLD-10A) using impact energies of 1.5 J and 2 J as they typically occur in a large-size SAG mills. The material loss of the liner steel samples was monitored for a period of up to 30 000 impacts. The results in Table 5 show that the softest steel (45.3 HRC), despite its high toughness (71.5 J), has the lowest wear resistance. The other steels, with the hardness exceeding 50 HRC perform clearly better, having 25%–30% reduced material loss under the same test condition. It appears that the best balance between hardness (52.3 HRC) and toughness (46.5 J) results in superior performance. Compared to the pearlitic steels in Table 5, the austempered steels (see Table 5) have a much higher hardness at similar toughness and hence offer a significant optimization potential.

4 Conclusions

Molybdenum alloying to iron-based castings offers several benefits in terms of improving the product properties for demanding applications. In products with pearlitic microstructure, molybdenum refines the pearlite lamellar spacing, thus, increasing strength and improving toughness. Favorable combinations of heat conductivity and strength become possible in that way particularly in grey cast iron. The most prominent roles of molybdenum alloying in nodular irons are to enhance the creep resistance under high temperature conditions and to facilitate hardenability. The latter is required for austempering treatment of components with heavier wall gage. Molybdenum's hardenability effect is also favorable for producing white cast iron to increase the wear resistance of components. Molybdenum shows synergies with other alloying elements such as niobium, chromium, copper and nickel reflecting in improved hardenability. The Mo-Nb synergy particularly results in more efficient refinement of the microstructure and enhanced precipitation strengthening of niobium. Property improvement of castings results in significant savings of operating cost especially with components used in large-sized capital equipment. Better creep resistance and higher strength in vehicle components increase their durability and inherently contribute to improved fuel efficiency. The further development of casting alloys in this respect is of strategic importance for the progress of mining, power generation, transport and machine building industries in China.

References

1. Wang ZF, Yao M, Zhang XB et al (2013) Optimization control for solidification process of secondary cooling in continuous casting steel. Appl Mech Mater 263–266(3):822–827
2. Wayman ML (2003) Cast iron metallurgy. CASTI metals black book. 2nd edn. CASTI Publishing Inc, Edmonton, pp 67–132
3. WFO global foundry report 2018. World Foundry Organization 2018. www.foundrygate.com
4. Gundlach RB, Janowak FJ, Bechet S et al (1985) Mater Res Soc Symp Proc 14:399–409
5. Steel Founders's Society and ASM International (1995). In: Blair M, Stevens TL (eds) Steel castings handbook, 6th edn. https://doi.org/10.1361/schb1995p1-1
6. Gundlach RB (1978) Elevated-temperature properties of alloyed gray irons for diesel engine components. AFS Trans 86:55–64
7. Fairhurst W, Röhrig K (1974) Abrasion-resistant high-chromium white cast irons. Foundry Trade J 136:685–698
8. Angus HT (1976) Cast iron: physical and engineering properties. 2nd edn. Butterworths, London, pp 176–187
9. Capdevila C, Caballero FG, Garcia de Andres C (2005) Neural network model for isothermal pearlite transformation. Part I: interlamellar spacing. ISIJ Int 45(2):229–237
10. Dollar M, Bernstein IM, Thompson AW (1988) Influence of deformation substructure on flow and fracture of fully pearlitic steel. Acta Metall 36:311–320
11. Toribio J, González B, Matos JC et al (2016) Influence of microstructure on strength and ductility in fully pearlitic steels. Metals 6:318. https://doi.org/10.3390/met6120318
12. Holmgren D, Kallbom R, Svensson I (2007) Influences of graphite growth direction on the thermal conductivity of cast iron. Metall Mater Trans A 38(2):268–275
13. Liu YZ, Xing JD, Li YF et al (2018) Tomographical study of the effect of graphite on properties of cast iron. Steel Res Int. https://doi.org/10.1002/srin.201800086
14. Bertodo R (1970) Grey cast irons for thermal stress applications. J Strain Anal 5(2):98–109
15. Gundlach RB (1979) Thermal fatigue resistance of alloyed gray irons for diesel engine components. AFS Trans 87:551–560
16. Druschitz AP, Fitzgerald DC (2000) Lightweight iron and steel castings for automotive applications. In: Proceedings of SAE 2000 world congress, Detroit MI, paper 2000-01-0679
17. Turnbull GK, Wallace JF (1959) Molybdenum effect on gray iron elevated temperature properties. AFS Trans 67:35–46
18. Mohrbacher H, Zhai Q (2011) Niobium alloying in grey cast iron for vehicle brake discs. In: Materials science and technology (MS&T) 2011, processing, microstructure and properties of cast irons and cast and forged specialty steels, pp 434–445
19. Campomanes E, Goller R (1973) Effects of Cb addition on the properties and structure of gray iron. AFS Trans 81:122–125
20. Zhou W, Zhu H, Zheng D et al (2011) Niobium alloying effect in high carbon equivalent grey cast iron. China Foundry 8(1):36–40
21. Mohrbacher H (2018) On the metallurgical effects of niobium in cast iron alloys. In: WFO 2018 conference, Suzhou, China, pp 1–6
22. Kleiner S, Track K (2010) SiMo 1000—cast iron alloyed with aluminium for application at high temperatures. Giesserei Rundschau 11(12):229–234
23. Röhrig K (2004) Austenitische Gusseisen. konstruieren + giessen 29 Nr. 2:2–32
24. Tanaka Y, Kage H (1992) Development and application of austempered spheroidal graphite cast iron. Mater Trans 33:543–557
25. Harding RA (2007) The production, properties and automotive applications of austempered ductile iron. Kovove Mater 45:1–16

26. Keough JR, Hayrynen KL, Pioszak GL (2010) Designing with austempered ductile iron (ADI). In: AFS proceedings, paper 10-129, American Foundry Society, Schaumburg, IL USA
27. Berns H, Theisen W (2008) Eisenwerkstoffe—Stahl und Gusseisen, 4th edn. Springer, Berlin. https://doi.org/10.1007/978-3-540-79957-3
28. Keough JR, Hayrynen KL, Pioszak GL (2010) Designing with austempered ductile iron (ADI). In: AFS proceedings 2010. American Foundry Society, paper 10-129
29. Klöpper C, Bartels C, Schliephake U (2004) Strong benefits in weight reduction by the use of ADI. Konstruktion. VDI Verlag, Heft 7-8
30. Mi Y (1995) Effect of Cu, Mo, Si on the content of retained austenite of austempered ductile iron. Scr Metall 32:1313–1317
31. Semchysen M (1983) Recent developments on the role of molybdenum in irons and steels. In: Comins NR, Clark JB (eds) Specialty steels & hard materials. Pergamon Press, Oxford, pp 87–110
32. Chen X, Zhao L, Zhang W et al (2019) Effects of niobium alloying on microstructure, toughness and wear resistance of austempered ductile iron. Mater Sci Eng A 760:186–194
33. Fulcher JK, Kosel TH, Fiore NF (1983) The effect of carbide volume fraction on the low stress abrasion resistance of high Cr-Mo white cast irons. Wear 84:313–325
34. Vermeulen WG, Morris PF, De Weijer AP et al (1996) Prediction of martensite start temperature using artificial neural networks. Ironmak Steelmak 23(5):433–437
35. Guesser WL (1985) Niobium in high-chromium irons. Foundry Manag Technol 113(9):50–52
36. Loper CR, Baik HK (1989) Influence of molybdenum and titanium on the microstructures of Fe-C-Cr-Nb white cast irons. Trans AFS 97:1001–1008
37. Dougall JR (1974) An approach to mill liner materials for critical grinding service. In: Barr QE (ed) Proceedings of symposium materials for the mining industry. Climax Molybdenum Co., Greenwich, pp 169–172
38. KSB AG Company Brochure: cast materials from KSB, Pegnitz (Germany). www.ksb.com
39. Albright DL, Dunn DJ (1983) Wear behavior of iron and steel castings for the mining industry. JOM 35(11):23–29
40. Tither G (2001) Niobium in steel castings and forgings. In: Proceedings of the international symposium niobium 2001, Orlando, USA. TMS, pp 845–872
41. China Industry Research Institute (2018) Research and analysis of current situation and forecast of development trend of China's casting industry in 2019. China Industry Research Network, pp 35–36
42. Chen X, You M, Guo A et al (2018) Influence of niobium on the microstructure and properties of CrMo cast steel for liner plate. In: Mohrbacher H (ed) Proceedings of international symposium on wear resistant alloys for the mining and processing industry. TMS, pp 393–406
43. Pérez V, Villaseca D (2018) Opportunities for ferrous alloys used in copper mining. In: Mohrbacher H (ed) Proceedings of international symposium on wear resistant alloys for the mining and processing industry. TMS, pp 1–18
44. Sepúlveda JE (2006) Criteria for the selection, application and evaluation of grinding mill media. In: Paper presented at the first international ore processing meeting, Antofagasta, Chile, 26–28 July, 2006
45. Zhai CC (2018) Research on microstructure and properties of V-wear-resistant steel for lining board. Dissertation, Shanghai University

Xiang-Ru Chen is mainly engaged in research of high-performance cast steel materials using special alloying by niobium, vanadium, and rare earth elements. She has been involved in the development of wear-resistant steel, heat-resistant steel, low temperature steel, cast iron, aluminum alloys. She has supervised one project of the National Natural Science Foundation of China as well as several industrial projects. She published more than 40 papers in domestic and foreign journals. She won one provincial and local science and technology award and applied for 8 patents. She is member of the automotive materials branch of the Chinese Society of Automotive Engineering, the cryogenic steel branch of the Chinese Society of Metals, the wear-resistant materials branch of China, and the editorial board of Modern Cast Iron magazine.

Qi-Jie Zhai is the director of the Advanced Solidification Technology Center of Shanghai University, vice chairman of the China Foundry Society, director of the China Institute of Foundry Journal Workmen's Committee, and member of the World Foundry Organization (WFO) Ferrous Metals Technical Committee. He is editorial board member of 13 academic journals. 4 original technologies, including thermal simulation of metal solidification, homogenization of pulse magnetically induced oscillation, nucleation of double disturbances of temperature and composition, and engineering materials of solidification metastable phase and super performance, are proposed. 9 new foundry products, such as centrifugal casting double metal compound roll ring, are developed. 11 technical achievements have been put into application. He has supervised over 80 projects, filed 89 patent applications, published 466 academic papers, published 2 monographs. He was honored with 7 provincial science and technology awards and 1 national technical invention award.

Han Dong is Professor and Dean of the School of Materials Science and Engineering of Shanghai University. He also is Research fellow of the Central Iron & Steel Research Institute. He has been working in research of steel science and technology for over 30 years. He studied and proposed Deformation Induced Transformation (DIT) phenomenon and Multiphase, Metastable and Multiscale (M3) principal to control the microstructure evolution of steel and improve the performances. Novel steels, such as micron steel, medium manganese auto sheet steel, high toughness/ductility HSLA

steel plate, delayed fracture resistant steel, and fatigue failure resistant steel have been developed under his guidance. He was granted 58 patents, published 458 journal papers and two books and edited two special issues in journals.

Bao-Hua Dai is the Chief Engineer of CITIC Machinery Manufacturing Inc. where he has worked since 1982. He has long years of experience in practical production and casting process. During his career, he has held senior roles in many development and innovation projects, especially in recent years, like cast steel brake disc for high speed train, casting device of track shoe (obtain of 6 practical patents), performance test of casting material of node for marine use and structure design, preparation method of nodular cast iron and riser structure design of fixed casting mandrel under atmospheric pressure. He is a technical expert of Shanxi Foundry Society.

Hardy Mohrbacher specializes in materials and mechanical engineering including steel alloy design and processing, sheet metal forming and welding, automotive body design, non-destructive testing and materials characterization, plus the tribology of hard materials. He has written and co-authored over 200 scientific publication in the respective areas. He has held senior positions within, among others, Fraunhofer Institute for Nondestructive Testing (IZFP), Sidmar (ArcelorMittal Ghent) and ThyssenKrupp (TKTB). He is an Associate Professor at KU Leuven in Belgium and an Adjunct Professor at China's Shanghai University. Since 2007 he is owner and managing director of NiobelCon bvba, a consulting company focusing on steel alloy design, metallurgical processing and steel applications.

Adv. Manuf. (2016) 4:105–114
DOI 10.1007/s40436-016-0142-9

Metallurgical concepts for optimized processing and properties of carburizing steel

Hardy Mohrbacher[1]

Received: 29 February 2016 / Accepted: 5 May 2016 / Published online: 2 June 2016

Abstract Carburized steel grades are widely used in applications where high surface near hardness is required in combination with good core toughness as well as high strength and fatigue resistance. The process of carburizing lower to medium carbon containing steel can generally provide this combination of properties and has been practiced for several decades. Such steel is essential in the vehicle power-train, machines and power generation equipment. However, the increasing performance demands by such applications as well as economical considerations forced steel producers to develop better alloys and fabricators to design more efficient manufacturing processes. The present paper describes recent concepts for alloy design optimization of carburizing steel and demonstrates the forthcoming beneficial consequences with regard to manufacturing processes and final properties.

Keywords High temperature carburizing · Grain size control · Distortion control · Integrated manufacturing · Plasma nitriding · Micro pitting · Tooth root fatigue strength · Molybdenum steel · Niobium microalloying

1 Motivation for optimizing carburizing steel

Case carburizing steels (alternatively known as case hardening steels) are widely used in applications where high surface-near hardness is required in combination with good core toughness as well as high strength and fatigue resistance. These steels have been the material of choice for several decades to manufacture components like gears, shafts or bearings. Depending on the application and the component size the following alloy systems have been established:

(i) Chromium steels for smaller components when only low hardenability is required.
(ii) Manganese-chromium steels with medium hardenability for passenger vehicle components.
(iii) Chromium-molybdenum steels with medium/high hardenability for passenger and commercial vehicle components.
(iv) Chromium-nickel-molybdenum steels with high hardenability for severely loaded machinery and commercial vehicle components.
(v) Nickel-chromium steels with high hardenability for components with extraordinary toughness requirements.

Within these alloy systems, standardized steel grades are available in different major markets offering a guaranteed spectrum of mechanical properties. Case hardening steels have reached a high degree of technical maturity, which is due to the materials specification as well as a high standard in processing [1]. The manufacturing of a component involves a complex sequence of individual forming, machining and heat treatment operations including the actual case hardening treatment (see Fig. 1). During case carburizing the component is heated to a temperature in the austenite range in presence of a carbon containing gas atmosphere. Most of the established industrial processes limit this temperature to 950 °C. During extended holding under these conditions carbon diffuses into the surface-near layer. With the holding time increased, the diffusion depth increases. At the end of the diffusion time a concentration

✉ Hardy Mohrbacher
niobelcon@skynet.be

[1] NiobelCon bvba, 2970 Schilde, Belgium

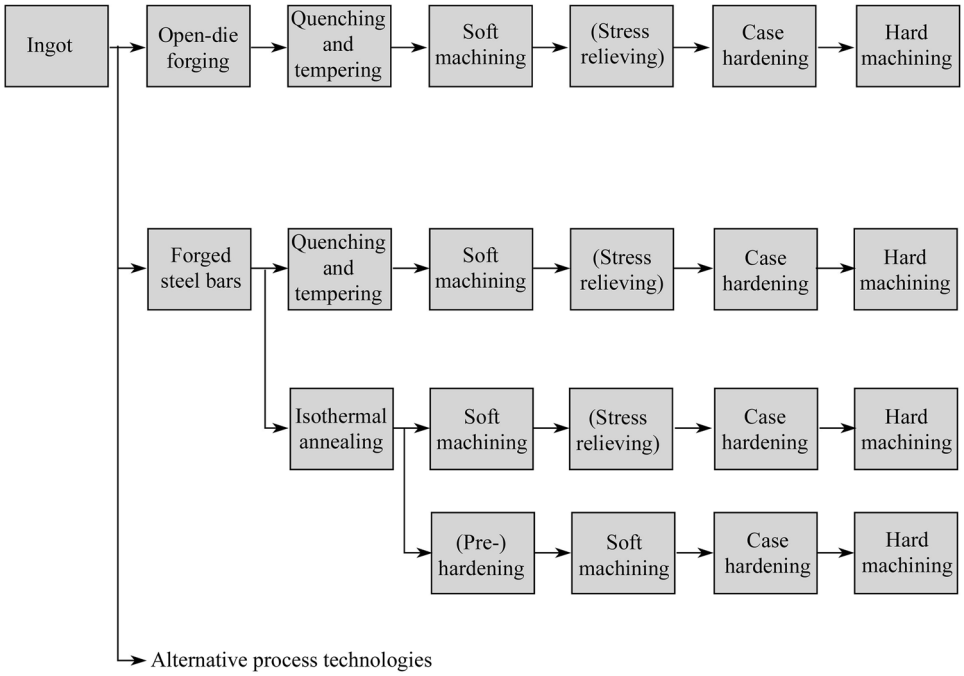

Fig. 1 Typical processing sequences for manufacturing of case carburized components

profile of carbon above that of the pre-existing carbon in the steel is established with the highest carbon level close to the surface. Subsequent quenching from austenite results in the formation of a hard surface layer with martensitic microstructure, especially in the carburized layer. Deeper inside the material bainitic or ferritic-pearlitic microstructure develops due to the lower carbon content as well as the reduced cooling rate. With regard to the carburizing treatment surface hardness, case depth and core hardness are characteristic criteria that are typically specified. After carburizing and quenching, annealing at moderate temperatures can be optionally applied facilitating hard machining such as grinding.

In recent years increasing application related demands towards case carburized components indicated some shortcomings of existing alloys [2]. For instance, large gear in high-power windmills regularly showed unexpected and early failure due to gear tooth breakage or pitting damage on gear flanges [3, 4]. Such catastrophic failure requires a complete exchange of the gearbox involving high replacement cost as well as loss of operational income due to downtime of the facility.

In the vehicle industry, several new challenges have arisen all with the aim of reducing fuel consumption and lowering emissions. Light weighting of passenger car bodies has a high priority in that respect but also weight reduction of powertrain components is increasingly being addressed. However, when a gearbox could be designed to smaller size, thus achieving lower weight, the specific operational load on the individual components will increase. Another fuel reducing trend is downsizing of the engine, which typically goes along with turbo charging. However, the characteristic of a turbo-charged engine is an instantly much higher torque applying over the entire window of operation as compared to a naturally aspirated engine that is building up torque more gradually. Consequently the specific load on gearbox components increases significantly with turbo-charged engines.

Gearboxes of commercial vehicles are standardly being exposed to high specific loads caused by input torque of up to 3 500 N·m. The competitive advantage of guaranteeing a longer lifetime of the gearbox has become a driving force for material improvement. Transmission producers have raised the lifetime guarantee in some cases to over 1.0×10^6 km. In addition, truck gearboxes can experience severely increased operational temperatures for short time periods when driving under high load with insufficient cooling [1]. The increased temperature can become high enough to cause softening of case carburized steel due to tempering effects. This softening lowers the load bearing capability of the gear and likely negatively alters the friction and wear properties at the surface. This same problem has been also observed as a cause of gearbox failure in windmills.

Any possible technical improvement, however, will always be judged against its cost. Considering the typical cost structure of an automotive gear unit (see Fig. 2), it is obvious that material and heat treatment has the largest

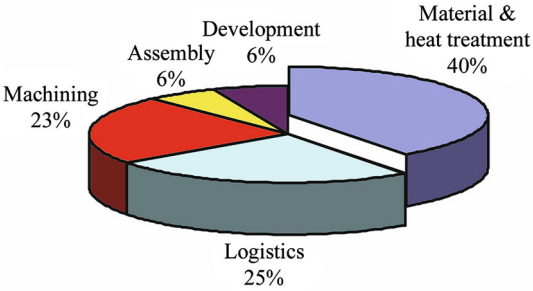

Fig. 2 Typical cost structure for manufacturing of a gear unit

impact. Besides those, machining also significantly contributes to the cost structure.

With regard to the material cost, the contribution of alloying elements is the most relevant. While manganese and chromium are relatively cheap, molybdenum and chromium are more costly. In general, the price of these alloying elements is not stable but subjected to volatility depending on the global supply-demand situation. There have been attempts to lower alloy cost of carburizing steels by replacing more expensive Cr-Mo or Cr-Mo-Ni steels by lower cost Cr-Mn steels. In some cases microalloying with boron has been applied to boost hardenability at comparably low cost. However, such alloy substitution always has to be checked against the service performance. It makes no sense saving alloy cost in first place when the result is a lower performance during service and forthcoming high repair and downtime cost exceeding the initial saving.

Considerable efficiency gains are possible by optimizing the carburizing heat treatment. When raising the carburizing temperature above the established upper limit of 950 °C, the diffusion speed of carbon increases and thus the treatment time to achieve the specified case depth decreases [5, 6]. Since carburizing is a batch process, more batches can be moved through a given furnace system per time unit, which ultimately can reduce the total number of heat treatment units required, and thus save capital investment. Table 1 indicates the efficiency gain for the carburizing treatment as well as the total heat treatment cycle in a vacuum carburization system. By raising the carburizing temperature from 930 °C to 1 030 °C, the diffusion time is reduced by 65% and the total cycle time is still 40% shorter [7]. It must be noted, however, that for raising the carburizing temperature to such higher level dedicated furnace equipment is needed. Furthermore, the steel subjected to the elevated temperature must resist excessive grain coarsening.

Another important cost-related aspect is due to quench distortion after carburizing. Such distortions need to be corrected by hard machining. This straightening operation requires additional processing time, rather expensive tooling and also removes part of the hard case.

2 Objectives for alloy improvement

According to the challenges outlined above, the present paper will indicate some recently achieved improvements of case carburizing steel alloys focusing on the following targets:

(i) Development of an innovative alloy providing a better service performance than that of the European premium grade 18CrNiMo7-6;
(ii) Development of a cost reduced alloy providing a similar service performance like that of the European premium grade 18CrNiMo7-6;
(iii) Development of alloy concepts allowing high temperature carburization;
(iv) Reduction of distortion after quenching;
(v) Possibility of additional plasma nitriding after case carburizing.

This approach involves detailed knowledge of metallurgical effects of the individual alloying elements always to be considered in relation to the processing conditions during manufacturing. Some principal aspects of alloying concepts will be summarized in the following.

3 Alloy concepts for high hardenability and tempering resistance

Hardenability of a case carburizing steel has a decisive influence on the properties related to manufacturing and machining of transmission components. High hardenability of the case carburizing steels results in more favorable shrinking behavior, leading again to a more uniform distortion during case hardening. This makes manufacturing more predictable and reproducible. Properties such as tooth root fatigue strength and tooth flank load capacity are determined by the surface hardness, case hardening depth, and core strength. Particularly the core strength of transmission components is directly related to hardenability, which again is controlled by the alloy concept.

Carbon is the most effective element with regard to hardenability (see Fig. 3). The increased carbon content in the carburized layer by itself provides good hardenability. However, the carbon level in the base steel is limited to allow for good impact toughness. Thus other alloying elements must be added for obtaining high core hardness (strength). Molybdenum, chromium and manganese are very powerful in providing increased hardenability. Manganese is used for less demanding applications due to its comparably low cost. Additions of chromium and molybdenum to carbon-manganese base steel offer the best hardenability and are used for more demanding

applications. Nickel alloying provides moderate increase in hardenability, yet the main reason for its addition is improving toughness. Higher additions of nickel can cause stabilization of retained austenite, especially in the carbon-enriched surface-near area, resulting in reduced strength and wear resistance.

For cost reduction reasons alloys using higher manganese and chromium additions, eventually combined with boron microalloying have been favored for many gear applications. However, such cost reduced alloy concepts, although providing good hardenability, have limitation in terms of toughness and tempering resistance. Besides, the prevention of intergranular oxidation requires Mn, Cr and also Si levels to be reduced. In the other extreme alloy producers have developed richly alloyed steels for those applications where transmission failure causes high replacement and outage costs. An example is 15NiMoCr10-4 (C:0.15%, Si:1.1%, Cr:1%, Mo:2% and Ni:2.5%), which is used in high-end applications, e.g., in aerospace or formula-1 gear. However, such steel requires special melting technology and is not widely available. Comparing this steel to another high-Ni steel (14NiCrMo13-4) the increase of the molybdenum content from 0.25% to 2.0% brings about a significant improvement of hardenability, surface hardness and also tempering resistance (see Fig. 4).

When the as-quenched microstructure after carburizing is exposed to elevated temperature, be it during service or during an additional heat treatment, the original hardness is rapidly reduced due to tempering effects (see Fig. 4). This loss of hardness is acceptable only within strict limits, as it will reduce fatigue endurance during service otherwise. Therefore the temperature window for tempering treatments in industrial manufacturing is typically set to 160–170 °C for a time period of approximately 2 h. When the temperature reaches higher values, for instance under uncontrolled service conditions, the surface hardness can drop to an unacceptably low level. In such cases steel with increased tempering resistance is required. Particularly higher molybdenum content results in a significant increase of tempering resistance and, thus, a significantly reduced hardness loss.

4 Alloy concepts for grain size control and high temperature carburizing

The carburizing treatment exposes steel to high temperature for long time. At carburizing temperature steel is in the austenitic phase allowing efficient in-diffusion of carbon from the surrounding atmosphere. However, with increasing time and temperature, austenite grains tend to grow in size. This grain growth has negative consequences with regard to the properties of the steel after quenching. Although quenching leads to phase transformation into martensite or bainite, the prior austenite grain size (PAGS) is still reflected in the transformed microstructure. Coarser PAGS results in lower yield strength, lower toughness, increased ductile-to-brittle transition temperature and larger residual stresses. Secondary negative consequences are reduced fatigue resistance and shape distortion after quenching requiring additional hard machining efforts. Particularly detrimental in this respect is a bi-modal grain size distribution comprising smaller and larger grains together. Current industry standards therefore impose restrictions to the size and volume share of large prior austenite grains.

The metallurgical approach to avoiding excessive austenite grain coarsening during carburizing treatments is to restrict austenite grain boundary motion by dispersing

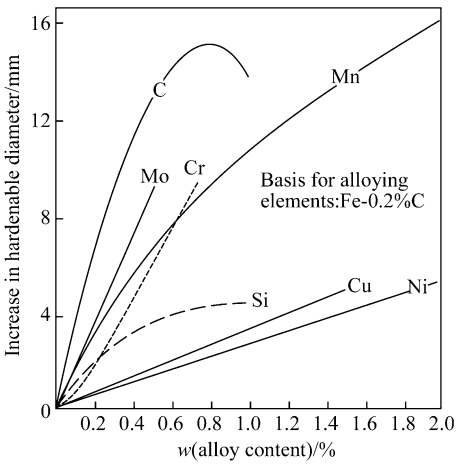

Fig. 3 Influence of single alloying elements on the increase of the hardenable diameter using Grange's technique [8]

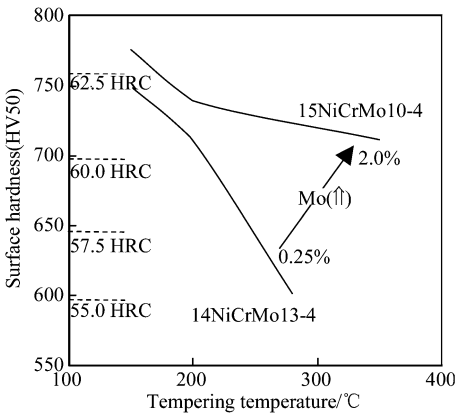

Fig. 4 Hardness loss of the carburized case after exposure (2 h) to elevated temperature in low-molybdenum and high-molybdenum alloyed steels [9]

small particles in the steel matrix [10–16]. These particles have the potential of pinning the austenite grain boundary. The size of the particles should be below 100 nm to have grain boundary pinning potential. Furthermore, the particles should not easily dissolve at carburizing temperature. In traditional carburizing steel, aluminum nitride (AlN) particles take this function. Aluminum and nitrogen are standardly present in steel as a result of steel making practices. The best grain coarsening resistance is achieved when both elements are present in the stoichiometric ratio of AlN, i.e., an Al:N weight ratio of 2:1. With this Al:N ratio and a sufficiently fine dispersion of these particles, which depends also on the processing history prior to carburizing, grain coarsening is obstructed up to 980 °C. For longer carburizing time this limit temperature is rather lower. The appropriate addition of stronger nitride and carbide forming elements such as titanium and niobium was found to raise the grain coarsening temperature considerably. With the addition of 0.025% Ti and preferably sub-stochiometric to nitrogen (Ti:N <3.4) the onset of grain coarsening occurs above 1 100 °C (see Fig. 5). However, targeting the titanium addition to the optimum range (maximum grain coarsening resistance) is difficult in day-to-day steelmaking practice. A similar effect is observed for an addition of 0.05% Nb. Much more stable high temperature resistance is yet obtained with a combined addition of Nb and Ti, which can raise the grain coarsening temperature to over 1 200 °C. As such long carburizing duration at a limit temperature of 1 050 °C offered by modern equipment becomes feasible. Co-addition of molybdenum is considered to further improve the dispersion of grain growth inhibiting nano-sized particles. Besides, larger atoms such as molybdenum and niobium when in solid solution segregate to the austenite grain boundary and exert strong solute drag. Hence Nb and Ti microalloyed carburizing steel allows taking advantage of the possibility of high temperature carburization and the forthcoming reduction of treatment cycle time (see Table 1). The cost savings, which can be realized by the shorter treatment cycle, clearly outweigh the alloy cost for Nb and Ti.

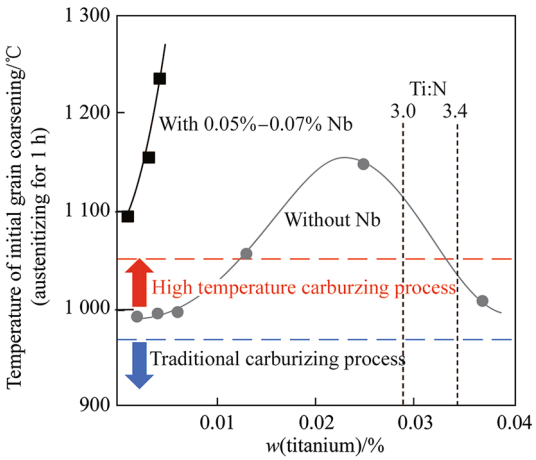

Fig. 5 Effect of microalloy additions on the temperature of initial grain coarsening in case carburizing steel grade 16MnCr105 [10]

5 Design of carburizing steel alloy variants for optimized properties and advanced processing

Based on the individual and synergetic effects of alloying elements described before, the intended processing route and the desired property profile, two modified alloy concepts have been designed (see Table 2) for a full scale production trial including gear running tests [17, 18]. One developed alloy design (variant V_1) is aiming for higher performance than that of 18CrNiMo7-6 at similar alloy cost. The content of carbon is increased for higher maximum hardness. The higher molybdenum content provides additional hardenability and tempering resistance. The nickel content is reduced for avoiding retained austenite formation and to reduce cost. The other developed alloy design (variant V_2) has a lower total alloy cost than 18CrNiMo7-6, yet aiming for similar performance. In both

Table 1 Influence of carburizing temperature on treatment time [7]

Vacuum carburization of 18CrNiMo7-6	Carburizing temperature/°C		
Case depth: 1.5 mm	930	980	1030
Loading/h	0.25	0.25	0.25
Heating/h	1.50	1.50	1.50
Diffusion time/h	8.50	5.00	3.00
Cooling to quenching temperature/h	0.75	1.00	1.25
Quenching and unloading/h	0.50	0.50	0.50
Overall/h	11.50	8.50	7.00
Reduction of overall cycle time (h) as compared to the reference of 11.5 h at 930 °C (%)	Reference	~3.00	~4.50
		~25	~40

Table 2 Chemical composition of developed case-carburizing steels

Steel grade	C	Si	Mn	Cr	Mo	Ni	Nb
Variant V_1	0.26	0.12	1.46	1.23	0.54	0.91	0.03
Variant V_2	0.21	0.25	1.17	1.15	0.21	0.22	0.04
18CrNiMo 7-6	0.15–0.21	≤0.40	0.50–0.90	1.50–1.80	0.25–0.35	1.40–1.70	–

concepts niobium microalloying is applied for austenite grain size control. The achieved mechanical properties of both developed case-carburizing steels obtained after heat treatment indeed correspond to the postulated expectations (see Fig. 6 and Table 3). The hardenability behavior of variant V_1 is superior to that of 18CrNiMo17-6, whereas that of variant V_2 is within the hardenability range of the reference. After an austenitizing treatment at 880 °C for 2 h followed by quenching in oil and holding at 180° for 2 h, variant V_1 shows clearly better tensile and fatigue strength while variant V_2 nearly exactly matches the strength of the reference grade. The toughness of both developed steels is, as expected, lower than that of 18CrNiMo7-6 in the first place due to the reduced nickel alloy content, yet remains still on a good level. The higher carbon content in variant V_1 leads to a further toughness reduction. Grain refinement by Nb microalloying on the contrary has the potential of improving toughness [19].

6 Suitability of alloy variants for advanced manufacturing processes

With regard to advanced manufacturing processes such as high temperature carburizing as well as additional plasma nitriding of the carburized steel, the austenite grain coarsening resistance and the anti softening resistance have been investigated. In several carburizing treatments, temperatures were varied up to 1 050 °C and treatment time up to 25 h was applied. The steels were FP treated before carburizing. The efficiency of the microalloying concept against grain coarsening becomes evident for an exemplary treatment condition of 1 030 °C and 25 h (see Fig. 7). Under this demanding condition the standard 18CrNiMo7-6 develops a bimodal grain size distribution with a fraction of very coarse grains below ASTM3, which is not permissible according to standards. On the contrary, the microalloyed variant exhibits no grains coarser than

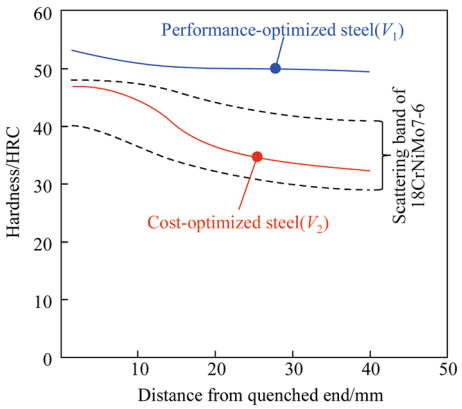

Fig. 6 Blind hardening behavior by Jominy method for the two modified steel grades in comparison to the standard high hardenability grade 18CrNiMo7-6

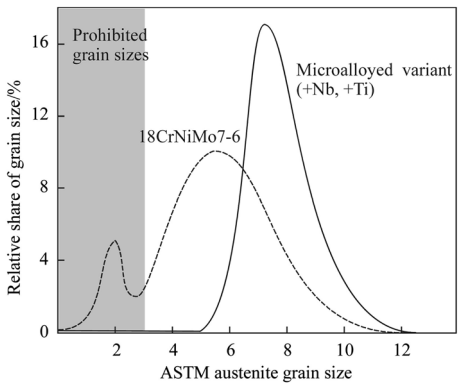

Fig. 7 Prior austenite grain size distribution in standard 18CrNiMo7-6 steel and a microalloyed variant after carburizing treatment at 1 030 °C for 25 h

Table 3 Mechanical properties of developed case-carburizing steels (austenitized at 880 °C/2 h then quenched in oil at 180 °C/2 h)

Property	Variant V_1	Variant V_2	18CrNiMo7-6
Tensile strength R_m/MPa	1 758	1 182	1 182
Impact energy A_v/J	47	55	80
Rotating fatigue limit $\sigma_{(50\%)}$@N=10^7/MPa	722	491	510
Hardenability@11 mm (HRC)	51	44	41
Hardenability@25 mm (HRC)	50	36	36

ASTM5 and an in general much finer average grain size as well as narrower grain size scatter. Thus the microalloyed variant is suitable for high temperature carburizing.

This suitability is also demonstrated by the cumulative frequency of prior austenite grain sizes in a microalloyed variant treated at temperature up to 1 050 °C (see Fig. 8). There is virtually no difference in the size distribution between standard conditions (950 °C) and high temperature carburizing. The grain size being in the range of ASTM 7–9 can be considered as particularly fine and the scattering range is small. A small grain size scattering range also results in more limited quench distortion and hence reduced straightening effort [20].

In pulsed plasma nitriding the sputtering of nitrogen atoms into the surface-near area leads to an additional hardness boost and introduces compressive stresses. The processing temperature for plasma nitriding can range between 350 °C and 570 °C depending on the material. The duration of the process ranges from 10 min to 70 h. The typical layer thicknesses are between 0.1 mm and 0.7 mm. Applying this technology to already carburized steel requires that the softening under the conditions of plasma nitriding remains limited. On the current variants V_1 and V_2 the possibility of plasma nitriding was tested at treatment temperatures of 400 °C and 440 °C for the duration of 10 h (see Table 4). The steels were carburized at 1 030 °C before plasma nitriding. Variant V_1 was cooled at −70 °C for 2 h after quenching (180 °C/oil) to convert retained austenite into martensite. Both steel variants were tempered at 200 °C for 2 h. The surface hardness after quenching is similar in the two variants. However, the core hardness is considerably higher in variant V_1. Tempering results in a loss of surface hardness in both variants as expected. The core hardness of variant V_1 is also reduced while that of variant V_2 is slightly increased, which can be explained by a bake-hardening effect that occurs in steels with carbon content up to around 0.2%. The plasma nitriding treatment results in a very high surface hardness in variant V_1 for both nitriding temperatures reaching around 1000HV1. However, a significant hardness drop is observed in the high-carbon layer immediately below the nitride zone due to tempering effects (see Fig. 9). Towards the core, hardness difference between the two treatments becomes smaller. The depth at which the hardness drops below 550HV1 is reduced by around 50% after nitriding at 400 °C and becomes definitely too small after treatment at 440 °C. Thus, it can be concluded that variant V_1 is suitable for combined carburizing and plasma nitriding process with a temperature limit of 400 °C. A further increased addition of molybdenum above the current level of 0.5%

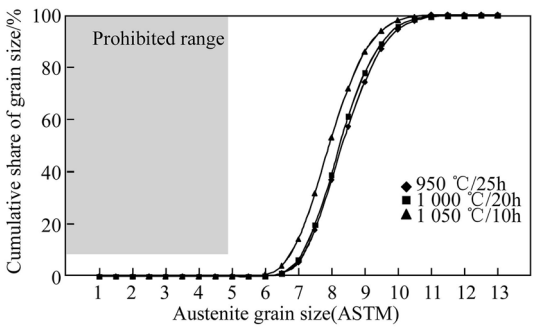

Fig. 8 Prior austenite grain size distribution in a microalloyed variant of 18CrNiMo7-6 steel after different carburizing conditions

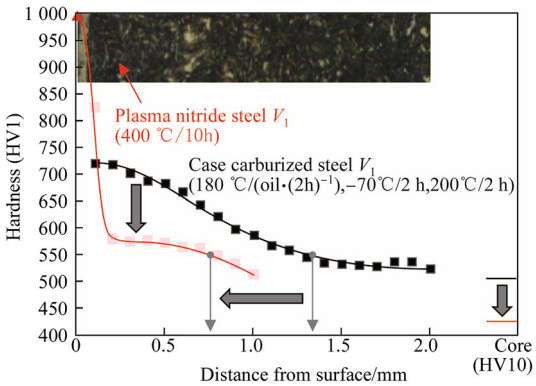

Fig. 9 Hardness depth scans of steel variant V_1 after the standard carburizing treatment and after additional plasma nitriding treatment (microstructure of the plasma nitriding sample)

Table 4 Hardness data (average values of 3 samples) after individual heat treatment steps

Treatment after carburizing at 1 030 °C	Variant V_1			Variant V_2		
	Surface (HV1)	Core (HV10)	550HV1 depth/mm	Surface (HV1)	Core (HV10)	550HV1 depth/mm
As-quenched (180 °C/(oil 2 h))	769	544	2.0	786	408	1.3
Cooling −70 °C/2 h, tempering 200 °C/2 h	717	505	1.5	–	–	–
Tempering 200 °C/2 h	–	–	–	672	430	1.2
Plasma nitriding at 400 °C/10 h	994	432	0.8	707	416	0.3
Plasma nitriding at 440 °C/10 h	1 009	422	0.4	570	395	0.1

would certainly increase the suitability for the combined carburizing and plasma nitriding process of this alloy. In variant V_2 surface hardness is increased only slightly after nitriding at 400 °C and even drastically reduced after performing the treatment at 440 °C. This alloy is hence clearly not suitable for the combined carburizing and plasma nitriding process.

7 Performance of alloy variants under operating conditions

Operational performance of the developed steel variants V_1 and V_2 was tested and benchmarked at FZG TU Munich, Germany using a standard method as described in Refs. [21, 22]. The tooth root load-carrying capacity was tested in a pulsator rig. Investigations on the flank load carrying capacity were performed by running tests on a back-to-back gear test rig according to DIN ISO 14635-1. The test gears for these investigations were case hardened at 1 030 °C after gear milling. Subsequent to case carburizing, the test gears were mechanically cleaned by shot blasting. The flanks as well as the tooth roots of the test gears for the investigations on the tooth root bending strength were not ground. For the running tests, gear wheels with a module of 5 mm and a gear ratio of 17/18 were used. This test gear is typical for the examination of the pitting load capacity. The tooth root load-carrying capacity is one of the determining factors in gear design. Besides the strength of the material itself, the existing state of stress (load induced stresses and residual stresses) significantly influences the tooth root load-carrying capacity. The mechanical cleaning procedure by shot blasting as used in this test program introduces compressive stresses in the sub-surface zone and is beneficial to fatigue resistance [21].

A performance benchmark of both developed concepts against the established case carburizing alloys is shown in Fig. 10. In this graphy the grey shaded area indicates the typical performance range of state-of-the-art carburizing grades [23]. Alloy variant V_1 ranks on top (quality level ME) of the property field of established alloys according to DIN3990 [5] and is performing better than many higher alloyed steel grades including the reference grade 18CrNiMo7-6. Alloy variant V_2 compares well with the state-of-the-art alloys, achieving quality level MQ.

The performed gear running tests allowed determining the flank pitting load capacity limits for the two developed steel variants. A benchmark comparison of these data against established case carburizing grades is done in Fig. 11. Alloy variant V_1 exhibits a very high pitting endurance limit and clearly outperforms even the best currently available alloys of quality level ME. The pitting endurance limit of alloy variant V_2 is situated in the upper

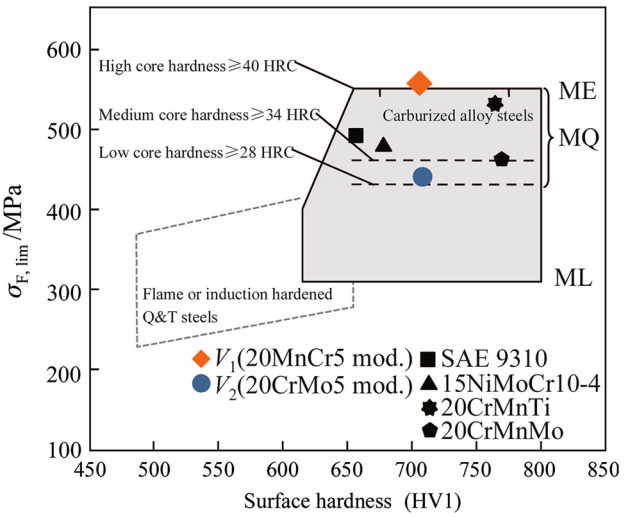

Fig. 10 Benchmarking of gear tooth root fatigue strength ($\sigma_{F,lim}$) of developed case-carburizing steel variants versus established alloys (DIN3990)

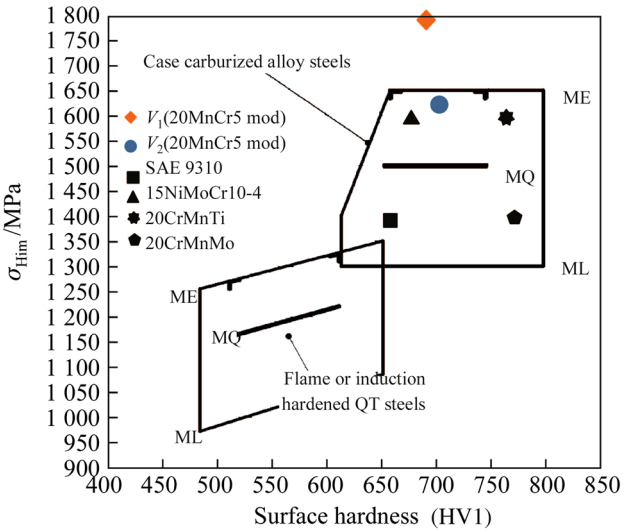

Fig. 11 Benchmarking of gear tooth flank micropitting strength ($\sigma_{H,lim}$) of developed case-carburizing steel variants versus established alloys (DIN3990)

region of the established contact stress field for case hardened steels, reaching quality level ME.

The current results suggest that alloy variant V_1 has the potential of providing an economically viable solution for highly loaded gear in heavy machinery and vehicles. Its use in vehicle transmission could enable downsizing of components, leading to the reduction of weight. In larger transmissions such as those used in trucks and heavy machinery, its use can help avoiding unexpected failure and extending warranty periods. The results of alloy variant V_2 indeed position it as a cost attractive alternative to the established premium grade 18CrNiMo7-6.

8 Enhanced manufacturing opportunities

The fact that high temperature carburizing is possible with such optimized alloy variants not only implicates timesaving for the carburizing process as such but also allows far-going reorganization of the entire manufacturing philosophy. For instance, car producer Volkswagen qualified case hardening of gear components on a production basis at 1 050 °C for 2.5 h instead of at 980 °C for 4 h using case hardening steel VW 4521 (20NiMoCr6-5) with successful completion after 21 months [24]. The steel, which was modified by the addition of 0.03%Nb, proved to have good fine grain stability and was superior to standard steel. In production, the furnace throughput could be increased by about 50%, reducing capital investment into equipment for treating the required production volume. Measurements indicated that dimensional variations and distortion were significantly reduced, resulting in less rework efforts. Experience at transmission producer ZF indicated that increasing the carburization temperature in mass production requires an in-depth approval of processing and application properties of transmission components [25]. For carburizing at 1 050 °C, Nb and Ti microalloyed steels are necessary to prevent grain growth. Gears and shafts require extreme consistency and minimum scatter in dimensional and shape changes. Thus, the distortion characteristics of components and possible consequences for soft and hard machining have to be considered. Furthermore, a fine-grained microstructure of case-hardened parts has to be ensured for good fatigue strength. An even greater economic potential lies in the complete reorganization of the production philosophy as outlined by Heuer et al. [26]. Traditional gear production separates soft machining, heat treatment and hard machining into dedicated areas without continuous material flow. The individual processing operations occur in batches, requiring intermediate buffer zones for storage and transport. An advanced production philosophy relies on the continuous flow of individual gear pieces and grouping the processing steps into an integrated production cell. However, this approach requires the synchronization between the rather different processing times with carburizing being the bottleneck. The carburizing cycle can be accelerated drastically by application of the innovative "high-temperature low-pressure carburizing" process including high pressure gas quenching using advanced multi-zone furnace equipment. For a given case depth of 0.65 mm, the cycle time is reduced from 180 min to 40 min when the temperature is raised from 960 °C to 1 050 °C. By this process time reduction, it becomes possible to integrate the heat treatment operation into the gear manufacturing line and to synchronize heat treatment with gear machining allowing individual part cycle time of 10–30 s.

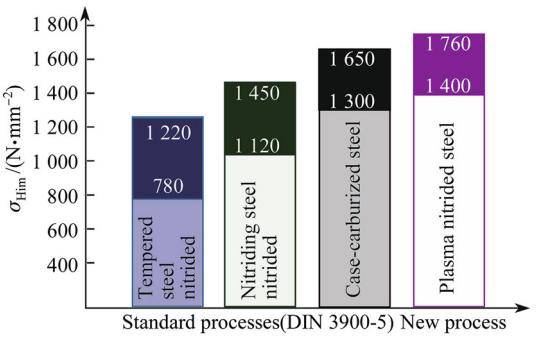

Fig. 12 Comparison of established surface hardening processes versus novel plasma nitriding process with regard to achievable gear tooth flank micropitting strength ($\sigma_{H,lim}$)

Plasma nitriding has been indicated as an alternative process to case carburizing for producing highly loaded gear components. Especially the extremely high surface hardness and compressive residual stress in the layer promise a high resistance against micropitting. In comparative gear running tests (the same as those in this study) various standardized heat treatment methods (DIN 3990-5) were compared to the pulsed plasma nitriding process [27]. The results shown in Fig. 12 indicate that the gear tooth flank micropitting strength could reach values above level ME (see Fig. 11). However, the gear tooth flank micropitting strength of steel variant V_1 after case carburizing performs already better than plasma nitriding steel. Therefore, plasma nitriding would be rather interesting as an additional treatment after case carburizing for gear operating under extreme conditions. As demonstrated by the current study, the steel needs high tempering resistance for providing sufficient core hardness and hardening depth (550HV). Metallurgical measures to achieve this are an increased molybdenum content (>0.5%), secondary precipitation hardening by vanadium microalloying and increased silicon alloying obstructing cementite formation. These measures can apply individually or in combination.

9 Conclusions

Incremental optimization of processing as well as alloy design has been enabling successive improvements in the cost, quality and performance of case carburized gear components. However, quantum leaps in this respect are possible when alloy design and processing are optimized in a synergistic way. This approach implies a sound knowledge of underlying metallurgical effects particularly with respect to the processing conditions along the manufacturing chain.

The current study has clearly demonstrated that by this approach great improvement with regard to performance under gear running conditions could be achieved without significant alloy cost increase. Dedicated alloying with molybdenum and niobium plays a key role in this approach.

Acknowledgement The experimental benchmarking tests on both alloy variants were financially supported by the International Molybdenum Association, London (www.imoa.info). The Gear Research Centre (FZG) of the Technical University of Munich is gratefully acknowledged for executing the experimental tests. Dr. Frank Hippenstiel of BGH Siegen kindly provided the tested steel materials.

References

1. Hock S, Mallener H, Sauter J et al (1994) Leistungsfähigkeit von Einsatzstählen und ihre Beeinflussung durch Anlassen. Härterei Technische Mitteilungen HTM 49(2):130–133
2. Dehner E, Weber F (2007, July) Experience with large, high speed load gears. Gear Technology, July, pp 42–52
3. Musial W, Butterfield S, McNiff B (2007) Improving wind turbine gearbox reliability. In: Proceeding of European wind energy annual conference, EWEA 2007, 7–10 May, Milan
4. Hau E (2006) Wind turbines, technologies, application, economics, 2nd edn. Springer, Berlin, pp 305–383
5. Löser K (2005) Innovative heat treating technologies in the automotive industry. In: Proceedings of steel in cars and trucks 2005. Verlag Stahleisen, Berlin, pp 237–244
6. Hock S, Kleff J, Kellermann I (2005) Temperature—the key to optimize cost and result in carburizing vehicle driveline parts. In: Proceedings of steel in cars and trucks 2005. Verlag Stahleisen, Berlin, pp 245–255
7. Hiller G (2014) Advantages of low pressure carburising and high pressure gas quenching technology in manufacturing. Int Heat Treat Surf Eng 8(1):35–41
8. Grange RA (1973) Estimating the hardenability of carbon steels. Metall Trans 4(10):2231–2244
9. Gay G (2009) Special steels for new energy sources. European conference on heat treatment, Strasbourg (France)
10. Huchtemann B, Schüler V (1993) Influencing the austenite grain size of special engineering steels. Thyssen Technische Berichte Heft 1(93):97
11. Kubota M, Ochi T (2007) Development of anti-coarsening steel for carburizing. Mater Sci Forum 539–543:4855
12. Leap MJ, Brown EL (2002) Effects of composition and processing on development of grain coarsening resistance in cold forged and carburized steel. Mater Sci Technol 18:945
13. Kimura T, Kurebayashi Y (2001) Niobium in microalloyed engineering steels, wire rods and case carburized products. In: Proceedings of the international symposium niobium TMS, p 801
14. Hippenstiel F (2007) Tailored solutions in microalloyed engineering steels for the power transmission industry. Mater Sci Forum 539–543:4131
15. Alogab KA, Matlock DK, Speer JG et al (2007) The influence of niobium microalloying on austenite grain coarsening behavior of Ti-modified SAE 8620 steel. ISIJ Int 47(2):307
16. Alogab KA, Matlock DK, Speer JG et al (2007) The effects of heating rate on austenite graingrowth in a Ti-modified SAE 8620 steel with controlled niobium additions. ISIJ Int 47(7):1034
17. Hippenstiel F, Mohrbacher H (2011) Optimization of molybdenum alloyed carburizing steels by Nb microalloying for large gear applications. In: Proceedings of materials science and technology (MS&T), pp 446–453
18. Mohrbacher H (2015) Improved gear performance by niobium microalloying of molybdenum-based carburizing steels. In: International conference on advances in metallurgy of long and forged products, pp 59–69
19. Wang CF, Wang MQ, Shi J et al (2007) Effect of microstructure refinement on the strength and toughness of low alloy martensitic steel. J Mater Sci Technol 23(5):659–664
20. Randak A, Eberbach R (1969) Einfluß der Austenitkorngrösse auf einige Eigenschaften des Stahles 16MnCr5. HTM Härtereitechnische Mitteilungen 24(3):201
21. Bretl N, Schurer S, Tobie T et al (2014) Investigations on tooth root bending strength of case hardened gears in the range of high cycle fatigue. Thermal Processing for Gear Solutions, Fall/Winter, p 52
22. Höhn BR, Stahl K, Schudy J et al (2012) FZG rig-based testing of flank load-carrying capacity internal gears. Gear Technology, June/July, pp 60–69
23. McVittie D (1999) ISO 6336-5: strength and quality of materials. Gear Technology, January/February, pp 20–23
24. Klenke K, Kohlmann R, Reinhold P et al (2008) Grain growth behaviour of the case hardening steel 20NiMoCr6-5 + Nb (VW 4521 + Nb) for gear components during high temperature carburization. HTM J Heat Treat Mater 63(5):265–275
25. Kleff J, Hock S, Kellermann I et al (2005) High temperature carburization-influences on distortion behavior of heavy-duty transmission components. In: Proceedings of the 1st international conference on distortion engineering, Germany, pp 227–234
26. Heuer V, Löser K, Schmitt G et al (2011) Integration of case hardening into the manufacturing-line: one piece flow. American Gear Manufacturers Association Technical Paper, 11FTM24, October 2011, pp 1–12. ISBN: 978-1-61481-023-0
27. Strobl V, Gebeshuber A, Müller T et al (2010) New advances and applications in pulsed-plasma nitriding of gear and power train systems. Elektrowärme International 3:221–226

Adv. Manuf.
https://doi.org/10.1007/s40436-019-00270-5

Editorial: Industrial relevance of molybdenum in China

Tim Outteridge[1] · Nicole Kinsman[1] · Gaetano Ronchi[1] · Hardy Mohrbacher[2,3]

Received: 27 June 2019 / Revised: 5 July 2019 / Accepted: 5 July 2019

Abstract About 80% of all molybdenum mined in the world (not including units recovered via recycling) is used as an alloying element in iron and steel. In general, the intensity of molybdenum use in China is still lower than in more highly developed regions such as the USA and Europe. This difference is manifest in both carbon steels and stainless steels, suggesting a significant opportunity for more widespread use of molybdenum in the future as China follows its self-reliance policy, calling for more sophisticated materials. Active market development, as being pursued by the International Molybdenum Association (IMOA), is a key asset in that respect. This article summarizes some key facts on molybdenum mining, use and market development in China.

Keywords China molybdenum industry · Global molybdenum reserves · Molybdenum applications · End-user markets · Molybdenum alloying · Market development

1 Global molybdenum reserves

According to the United States Geological Survey (USGS), almost half the world's reserves of molybdenum are located in Chinese territory [1]. Other significant reserves, accounting for 40% of the total, are found in North and South America (see Fig. 1). In the opinion of the USGS ''...resources of molybdenum are adequate to supply world needs for the foreseeable future''. Figure 2 indicates the major regions of primary production, i.e., freshly mined molybdenum production. The total production volume of around 259 000 t is quite well balanced over three major mining hubs, China, South America and North America, although China is by far the largest single producing country. Figure 3 reveals that China is also the largest user of molybdenum in the world, yet, it does not dominate the international molybdenum market in terms of supply, nor demand for products, as it is largely self-sufficient. East/West trade represents only a small percentage of its output and use. Whereas imports are predominantly raw materials, exports are mainly in the form of downstream value-added products, so in this respect, the trade of molybdenum follows a familiar pattern.

2 Molybdenum miners and products in China

In 2018, China's use of molybdenum reached a record level of over 97 000 t [2] whilst it produced almost 92 000 t of molybdenum. Accordingly, the country was a net-importer of molybdenum. The majority (nearly 85%) of molybdenum production in China originates from primary mines, where molybdenum is the sole mineral target, while the remainder comes as a byproduct of copper mining. The key producers Jinduicheng, China Moly, Yichun Luming and Manzhouli China Gold represent a large proportion of Chinese concentrate production. Some major producers have integrated downstream capacity to manufacture value added molybdenum products, supplying users directly. However, there is a large segment of the mining industry that produces molybdenum concentrates only, relying on independent converters and downstream manufacturers, to

✉ Tim Outteridge
toutteridge@imoa.info

[1] International Molybdenum Association, London, UK

[2] Department of MTM, KU Leuven, Leuven, Belgium

[3] NiobelCon bvba, Schilde, Belgium

Published online: 10 September 2019

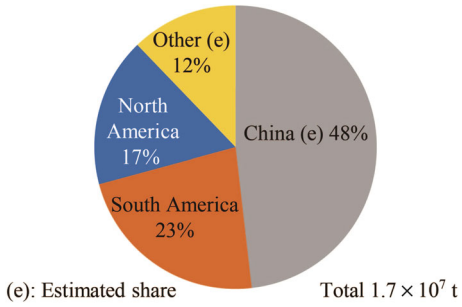

Fig. 1 Global distribution of known molybdenum reserves [1]

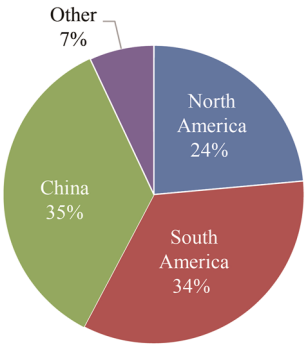

Fig. 2 Regional share of worldwide molybdenum production (basis 259 000 t) for the year 2018, excl. scrap (Source: IMOA)

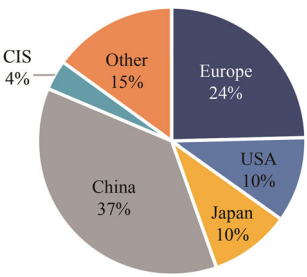

Fig. 3 Regional share of worldwide molybdenum use (264 000 t) for the year 2018, excl. scrap (Source: SMR [2])

make metallurgical and chemical products, for their markets. The dramatic growth of the Chinese steel industry, which now exceeds 50% of global production as well as the limited availability of local scrap mean that primary raw

Table 1 Ferromolybdenum (FeMo) and molybdate (MoO_4^{2-}) production in China from 2016 to 2018 (Sources: Comelan and International Molybdenum Association)

Year	Output/t			Share/%		
	FeMo	Molybdate	Total	FeMo	Molybdate	Total
2016	60 701	20 170	80 871	75	25	100
2017	70 469	20 323	90 753	78	22	100
2018	74 447	17 123	91 570	81	19	100

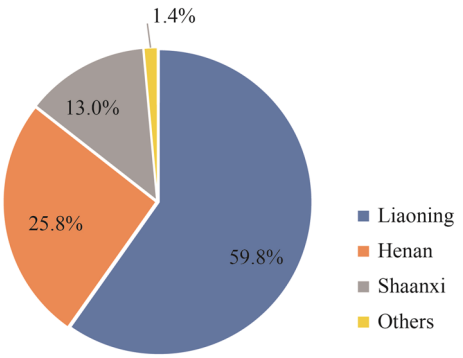

Fig. 4 Chinese FeMo production share by province in 2018 relative to a total output of 74 400 t

materials such as ferromolybdenum (FeMo), continue to be in high demand. The share of FeMo has been steadily growing in the last three years and in 2018 it exceeded 80% of the total Chinese molybdenum production while the output of molybdate diminished over the same period (see Table 1).

Ferromolybdenum production in China is geographically localized in the three provinces Liaoning, Henan and Shaanxi. FeMo production in Shaanxi and Henan is highly concentrated, with Jinduicheng and China Moly being the dominant players in these provinces, whereas the production in Liaoning province is fragmented with nearly 20 producers being active. The top three companies in that province, China New Dragon, Huludao Wanfeng and Chaoyang Jinda, produce close to half of the regional FeMo output (see Fig. 4).

3 First- and end-uses of molybdenum in China

China uses around 30% of the world's molybdenum including that recurring via scrap recycling. The first-uses of molybdenum in China are detailed in Fig. 5 and compared to those in the rest of the world. Alloy steels and stainless steels dominate the first uses of molybdenum. In comparison with other markets, China uses a smaller share of molybdenum in super alloys, stainless steels and alloy steels, and a higher share in tool and high-speed steels, molybdenum metal, castings and chemicals.

The main end-uses and major relevant application sectors of molybdenum are identified in Fig. 6. Here, some significant differences between China and the rest of the world become apparent. In particular, a much smaller share of molybdenum is used in the oil & gas sector. This is partially due to the fact that China is not a major oil producing country. Furthermore, the production of pipe steel, which depends highly on active pipeline construction projects, was relatively low in the period considered

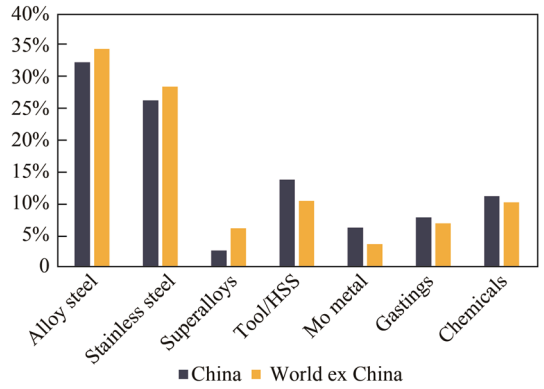

Fig. 5 First-uses of molybdenum in China and the rest of the world (excluding scrap recurrence) in the year 2017 (Source: SMR [2])

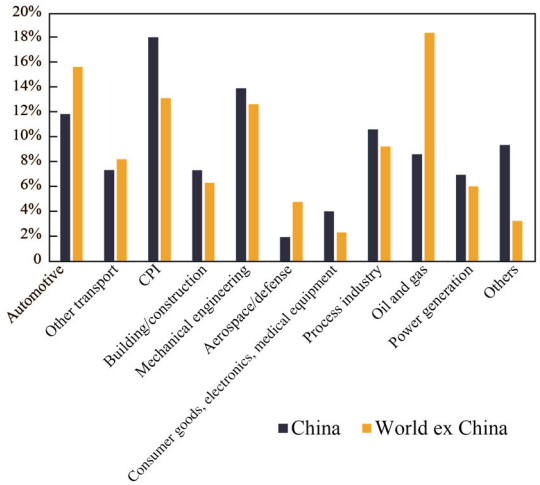

Fig. 6 End-uses of molybdenum in China and the rest of the world (including scrap recurrence) in the year 2017 (Source: SMR [2])

(2017), but consumed a large amount of molybdenum in other years. The recent West-to-East gas pipeline strings, for instance, used in the order of 10 000 t of molybdenum each for alloying the typically applied X80 grade steel (0.2%–0.3% (mass fraction) Mo) as well as in welding consumables used for pipe manufacturing and installation. Comparably smaller also, are the uses of molybdenum in the automotive and aerospace/defense sectors. Despite being the country with the largest vehicle production worldwide, less molybdenum is used in engineering steels for power train applications and also, turbochargers requiring molybdenum-containing heat-resistant alloys are less prevalent in China. The lower use of molybdenum in the aerospace/defense sector is mainly related to the fact that there is no domestic production of aircraft turbines in China, yet. On the contrary, China uses relatively more molybdenum in sectors such as chemical process industries (CPI), building and construction, mechanical engineering, consumer goods, electronics and medical equipment, non-

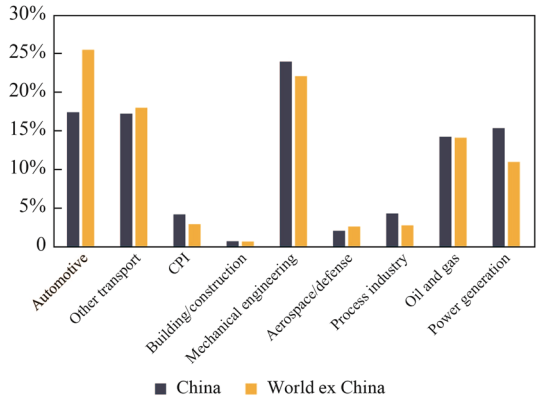

Fig. 7 End use application sectors for alloy steels in China and the world ex China (Source: SMR report [2])

chemical process industries, power generation and others. This is related to significant investments in these areas as a consequence of general economic growth as well as the specific target of producing increasingly higher-value added and internationally competitive products.

4 Molybdenum market development activities in China

Similar to other regions, the largest share of molybdenum use in China is found in alloyed engineering steels, followed by stainless steel [2]. However, even though China nowadays produces 52% of all carbon steel and 53% of all stainless steel globally, the specific use of molybdenum as an alloying element is still smaller than in other markets. In the carbon steel sector, the specific use of molybdenum (including the units recovered form scrap) currently reaches approximately 55 g/t compared to the average of 133 g/t in other major steel producing countries [3]. The corresponding figures for stainless steel are 1.1 kg/t in China versus 2.9 kg/t in other major stainless steel producing countries. Consequently, there is a significant potential to increase the use of molybdenum in the Chinese steel industry by adopting alloy design solutions from other regions and by deploying local product development activities. The comparison of end uses for alloy steels shown in Fig. 7 suggests that steel development for automotive applications should be a priority for molybdenum market development since the gap between China and the highly developed markets is the largest in this area. Furthermore, the automotive industry is highly globalized and requires local supplies of alloys in major production countries according to the material standards established at the home base. Other sectors relevant to market development are the machine building industry, and the production of heavy-duty transport equipment.

Chinese steel companies have made major investments in steel production facilities over the last two decades. Consequently, they have at their disposal some of the most modern and capable equipments, principally allowing the processing of leading-edge steel products. In many such products molybdenum can be a decisive alloying element, where the benefits of its use to improve steel properties go far beyond just increasing strength and hardness. The lesser-known metallurgical benefits of molybdenum alloying often make it the ideal alloying element for today's advanced manufacturing techniques and high-end applications. In that respect, it is necessary to demonstrate and communicate the full metallurgical potential of molybdenum alloying. Additionally, it is of key importance to explain that the obtained benefits of molybdenum containing steels outweigh the additional alloy cost [4].

IMOA's market development program is fully dedicated to communicating the known benefits of molybdenum alloying, demonstrating cost-benefit analyses and discovering new advantageous metallurgical effects. The practical implementation of that program consists of three major activities being knowledge dissemination, alloy implementation and knowledge generation. Knowledge dissemination relies on regular visits to steelmakers and end users often combined with in-house seminars. On occasions, symposia have been organized bringing a larger number of experts together, typically representing all relevant players in the area of interest. In selected cases of significant urgency, alloy implementation is assisted by direct consulting and support actions. Due to the prominent size of China's metallurgical industry, academic research activities in alloy related topics are higher than elsewhere in the world. IMOA interacts with Chinese research facilities via academic lectures or by funding R&D projects. In that way, existing knowledge is passed on to the next generation of metallurgists and new scientific understanding is created. For all IMOA market development activities, the topical focus has always been closely aligned with China's economic and industrial development priorities. In the different phases of the IMOA market development program, the focus was initially on steel for infrastructural applications including high strength pipeline steel. Later, the development of ultra-high strength steel for light-weighting of passenger and commercial vehicles became a dominant area of activities. Currently, two important initiatives are underway. A knowledge generating project investigating the effects of molybdenum alloying in cast iron components has been established at Shanghai University. An alloy implementation support activity aims to develop new high-performance gear steel with leading Chinese producers of special steels as well as major domestic manufacturers of automotive and large machinery gears.

References

1. United States Geological Survey (USGS)—National Minerals Information Center (2019). Accessed 09 May 2019
2. Moll M (2018) Molybdenum end use analysis 2018, Steel & Metals Market Research GmbH (SMR), Reutte, Austria
3. IMOA estimate based on data from Worldsteel, ISSF and SMR
4. Mohrbacher H (2013) Reverse metallurgical engineering towards sustainable manufacturing of vehicles using Nb and Mo alloyed high performance steels. Adv Manuf 1:28–41

Tim Outteridge is the Secretary-General of the International Molybdenum Association (IMOA). He graduated in 1978 with a degree in Metallurgy from the University of Sheffield and started his career in the molybdenum industry at Noranda Sales Corporation in London. From 1990 he held responsibility for the global molybdenum business at Noranda and later took on the same role in Rio Tinto, at Kennecott Utah Copper. He joined IMOA in 2008.

Nicole Kinsman is IMOA's Technical Director. She is a mechanical engineer with a PhD in metallurgy from the Swiss Federal Institute of Technology and an MBA from Carnegie Mellon University. Before joining IMOA she was a Market Development Manager at TMR, a stainless steel consulting firm in Pittsburgh, PA. She has specialized in stainless steel technical market development for over twenty years.

Gaetano Ronchi is IMOA's Senior Consultant in Asia since 2013. He has a PhD in electromechanical engineering from Politecnico Milano; is a certified as a welding engineer by the Italian Welding Institute and has an MBA from Stockholm School of Economics. He has over 45 years' experience in metals welding with a particular focus on stainless steel and advanced corrosion resistant grades. During his career, Gaetano has held many senior roles including Managing Director of a Sandvik Steel subsidiary, CEO and Sales and Marketing VP for Acciai Speciali Terni and Managing Director of Avesta (now Outokumpu).

Hardy Mohrbacher specializes in materials and mechanical engineering including steel alloy design and processing, sheet metal forming and welding, automotive body design, non-destructive testing and materials characterization, plus the tribology of hard materials. He has held senior roles within, among others, Fraunhofer Institute for Nondestructive Testing (IZFP), Sidmar (ArcelorMittal Ghent) and ThyssenKrupp (TKTB). He is an Associate Professor at KU Leuven in Belgium and an Adjunct Professor at China's Shanghai University.